UNIVERSITY OF KENT

DOCTORAL THESIS

Fermions coupled to solitons on low-dimensional spheres

Author:

Jack MCKENNA

Supervisor:

Dr. Steffen KRUSCH

A thesis submitted in fulfillment of the requirements

for the degree of Doctor of Philosophy in

Mathematics

School of Mathematics, Statistics and Actuarial Science

University of Kent

September 16, 2022

Between my finger and my thumb
The squat pen rests; snug as a gun.

Under my window, a clean rasping sound
When the spade sinks into gravelly ground:
My father, digging. I look down

Till his straining rump among the flowerbeds
Bends low, comes up twenty years away
Stooping in rhythm through potato drills
Where he was digging.

The coarse boot nestled on the lug, the shaft
Against the inside knee was levered firmly.
He rooted out tall tops, buried the bright edge deep
To scatter new potatoes that we picked,
Loving their cool hardness in our hands.

By God, the old man could handle a spade.
Just like his old man.

My grandfather cut more turf in a day
Than any other man on Toner's bog.
Once I carried him milk in a bottle
Corked sloppily with paper. He straightened up
To drink it, then fell to right away
Nicking and slicing neatly, heaving sods
Over his shoulder, going down and down
For the good turf. Digging.

The cold smell of potato mould, the squelch and slap
Of soggy peat, the curt cuts of an edge
Through living roots awaken in my head.
But I've no spade to follow men like them.

Between my finger and my thumb
The squat pen rests.
I'll dig with it.

Seamus Heaney, "Digging", *Death of a Naturalist* [26].

UNIVERSITY OF KENT

Abstract

School of Mathematics, Statistics and Actuarial Science

Doctor of Philosophy

Fermions coupled to solitons on low-dimensional spheres

by Jack McKenna

We examine models of Dirac fermions coupled to topological solitons on the circle S^1 and the sphere S^2. The fermion is coupled to a pseudoscalar kink in the (1+1)-dimensional model, and to an isovector modelling a baby Skyrmion in the (2+1)-dimensional model. In each case, we solve the spectrum of the fermionic Hamiltonian exactly when the soliton field is kept fixed as a background field, and the fermion dynamics do not cause any back-reaction on the soliton field. In the (1+1)-dimensional model, we then bring the kink field out of the background, fully coupling it to the fermion field. After a change of coordinates to a set of bosonic coordinates constructed out of bispinors, we demonstrate that solutions to the bosonic dynamical system can be understood analytically via the framework of elliptic functions. We show that for a particular class of solutions with no axial charge, we can recover the underlying fermion field from the bispinor solution. In the (2+1)-dimensional model we specialise to the case of the background soliton of topological degree 1 and exploit an $SU(2)$ symmetry to describe the fermion spectrum.

Covid-19 Impact Statement

I have lived in London since the start of my Ph.D. Pre-COVID, I commuted by public transport to Canterbury three to four days a week, and required little to work from home the rest of the week. COVID was a disruption to this as my ability to commute was restricted even beyond the initial campus closure. I did not have space in my home at first to efficiently work from home indefinitely. In May 2021 my partner and I moved to a larger flat with a home office, which was an essential relief, but in turn I was no longer able to afford to commute to Canterbury as frequently.

I live with chronic depression and anxiety disorders since my teens, generally well managed medically and therapeutically. However, the stress during the pandemic had a significant toll on me, especially the protracted social isolation. I have occasionally needed to take time off to recuperate and generally have not been able to work at my fullest capacity over the past year.

Steffen has been supportive and we have had an excellent routine of (at least) weekly remote meetings. Nonetheless, some goals of our research into the kink-fermion coupling discussed in Chapter 3 have lapsed and had to be made more modest this past year. These are outlined in Section 3.9.

Signed (Author):

_____

Date:

_____

Signed (Supervisor):

_____

Date:

_____

Acknowledgements

There are many people to whom I am grateful for pointing me on the journey that has brought me here. I am particularly indebted to my 8th grade mathematics teacher Jeff Ratliff, who recognised in me a hunger for understanding before I was possibly even aware of it myself. Without a doubt, he was the single most important factor in the realisation of a vocation. Another teacher to whom I am grateful is Colette Henry, my Leaving Certificate mathematics teacher, who would not abide for me to remain bored in class. She pushed me onto the IMO track, leading to two years of experiences which encouraged me to pursue my undergraduate studies in mathematics.

I would have had a much worse time at Cambridge if it were not for the kindness and compassion of Jonathan Evans, Ed Brambley and the late Jan Saxl. They went above and beyond in their pastoral care for me while I was going through one of the worst periods of my life.

I would not have had the confidence to aim for the goal of pursuing a Ph.D. if it were not for the friends, colleagues and mentors I met during the period of 2015-2018 while enrolled in King's College London for my Graduate Diploma and Masters degrees. I am thankful to Neil Lambert in particular for his mentoring during that time. I am also very grateful to Gerard Watts, who was a sure source of advice and perspective while I was applying to Ph.D. programmes.

My relationship with Steffen Krusch has been everything I could ask for in a supervisor. He has been a guide, a lifeline, and a constant source of encouragement. I am honoured to call him a colleague and friend.

Many people in the University of Kent have been a great support in recent years. David Brown is a good friend and has often provided essential stress relief. Andy Hone and Tom Winyard have been excellent colleagues and I am grateful to their insights on the ideas contained in this thesis. In

each of their tenures as my secondary supervisor, Clélia Pech and Jing Ping Wang were eager sounding boards and gave crucial advice on administrative matters. I can't do justice in words to my appreciation for Claire Carter as an administrator, a pastoral carer and a friend.

I've been very thankful to be part of the Solitons at Work community since its inception, both as a research community and as a social group, particularly over the COVID-19 pandemic. I would like to thank Chris Halcrow, Calum Ross and Bruno Barton-Singer both for their friendship and for their mathematical insights. My research has also benefited from stimulating conversations with Nick Manton and Derek Harland.

I cherish my friends whose love has given me the confidence to face the challenges of recent years. In no particular order, I extend the deepest loving gratitude to Chris McCarthy, Bearaigh O'Halloran, Iain Gillett, Shrish Parmeshwar, Phil Hughes, Jess Sim, Lena Nicolai and Mark Popinchalk.

My brother Luke and my parents Barney and Rosaire have provided the material and emotional support upon which this entire endeavour has been founded. When I could not envision reaching this point, they were able to imagine it for me, and transfer that vision to me.

Above all else, I am thankful for the support, love, sacrifices and companionship of my cherished partner, Laura Hardman. None of this would have been possible without her.

Contents

List of Figures

List of Tables

Chapter 1

Introduction

1.1 A personal introduction

"Geometry"—William Thurston is alleged to have said—"is the user interface of mathematics". We might allege a similar claim for theoretical physics; however, in order for that statement to be taken seriously, the author should confess that I am firmly a *mathematical* physicist. As it is a little early in the thesis to be making such wild conjectures, I will attempt to clarify my feelings on the matter before we proceed any further.

I have always been fascinated by the geometric foundation of classical mechanics since I first took a course in Lagrangian and Hamiltonian dynamics. It was a revelation that Poisson manifolds are the natural environment to understand conservation laws from a Hamiltonian perspective. Wanting to understand the role of Lie groups and Lie algebras led me to discover the riches of both representation theory and differential geometry. This was complemented by the glimpses of differential geometry I had previously seen in undergraduate electrodynamics courses, with the terminology of two-forms and covariant derivatives. The power of differential geometry in classical field theory is beautifully demonstrated in electrodynamics, with the seemingly straightforward question of "why isn't there a *magnetic* monopole?"

Following this thread led to Dirac's construction of a magnetic monopole [20], and then Wu and Yang's construction in the language of fibre bundles

[72]. I wrote my graduate diploma dissertation on the rigorous construction of gauge theories in terms of connections on principal bundles, and described the 't Hooft-Polyakov monopole [27, 54] as my final worked example. This gave me my first introduction to the power of Bogomol'nyi's equations [11], and the power of Prasad and Sommerfeld's solutions [55].

These BPS equations demonstrate that topological solitons can take on remarkably simple solutions which are, in a sense, a multiple of the identity function. This applies to both $\mathrm{SU}(2)$ instantons on $\mathbb{R}^4$ [see e.g. 48, Chapter 10], and particularly BPS $B = 1$ Skyrmions on S^3 [23, 37, 40]. This motivates my particular examination of similar fermion-(baby) Skyrmion models on S^1 and S^2. Nonetheless, the famous BPS trick is not just an incredible tool for calculation or for finding solutions, but it opens the door to moduli spaces and encourages us to explore their rich geometric structure.

The contemporary field of topological soliton research forges deep links between applied physics and pure mathematics. The Skyrme theory has application to topics such as nuclear matter [see e.g. 5, 14, 25, for some varieties] and condensed matter physics [examples include 19, 22, 34, 49, 60] but is founded in the power of differential geometry and algebraic topology, and connects to deep results such as the index theorem and spectral flow [12, 31]. A self-confessed mathematical physicist could hardly find a better playground in which to conduct research.

1.2 Contents of the thesis

In Chapter 2, we give a brief overview of the field of topological solitons, and discuss some contemporary research relevant to our models. We briefly outline a couple of examples of kinks, as well as mentioning some features of the Skyrme model. We highlight treatment in the literature regarding the coupling of fermions to kinks in a number of models and the connection

to our approach. This will motivate and the choices of Lagrangians, given below, which define the dynamics we will study.

Our main results are contained in Chapters 3 and 4. Chapter 3 contains our main results on fermions coupled to kinks. Here we examine in detail a simple theory of fermion coupling to a pseudoscalar field modelling a periodic topological kink. We start by considering the stationary state dynamics of the fermion $\psi(t,\theta)$ when the scalar field is considered to be in the background, so there is no back-reaction onto the kink arising from the coupling with the fermion. This will be modelled by the Lagrangian

$$\mathcal{L}_f = \overline{\psi}\left(\mathrm{i}\hbar\partial\!\!\!/ - g\mathrm{e}^{\mathrm{i}\gamma^3 n\theta}\right)\psi. \tag{1.1}$$

We identify a translation symmetry which permits us to use a basis of momentum eigenstates to solve the linear Dirac equation, and we can describe the energy spectrum of the fermion analytically. This is an example of a treatment used in many similar models of fermion-soliton coupling to find the solutions and energy spectra of the fermions in the absence of back-reaction, made particularly simple by our choice of coupling term and low-dimensional spacetime.

We introduce the back-reaction of the kink to our consideration by adding an appropriate dynamical term for the scalar field to our Lagrangian, changing it to

$$\mathcal{L} = \frac{M^2}{2}\partial_\mu\phi\,\partial^\mu\phi + \overline{\psi}\left(\mathrm{i}\hbar\partial\!\!\!/ - g\mathrm{e}^{\mathrm{i}\gamma^3\phi}\right)\psi. \tag{1.2}$$

where $\phi(t,\theta)$ is the dynamical kink field. We examine the equations of motion, and the symmetries, of the altered model. In particular, we see that the previous translation symmetry no longer exists in a particularly helpful manner for finding solutions, but is instead in a manner of speaking replaced by an internal symmetry shared by the kink and the fermion. We will argue that such an internal symmetry is important quite generally for understanding

why the fermion would localise onto the kink field, as has been observed in previous treatments of fermion-soliton coupling.

We model the system as a boundary value problem for an ansatz of stationary state fermion, and static kink, solutions, and we compute some solutions numerically, which are consistent with the symmetry predictions of the model. In particular, we generate new, "non-trivial" solutions which are not explained by the simpler model without back-reaction.

We demonstrate that, with a suitable change of variables, the equations of motion for the fermion-kink system including back-reaction can be reduced to a dynamical system with several interesting features. The explicit fermionic fields all combine into a set of bosonic coordinates formed from bispinors of the original system; for this reason, we refer to the reduced dynamical system as the bispinor picture. Within the bispinor picture, the internal symmetry which we argue is important for localisation gives an even stronger implication: the equations of motion for the fermion bispinors do not depend on the kink, while conversely the solution to the equation of motion for the kink is determined by a solution to the bispinor equations. In a sense, this bispinor perspective demonstrates that the kink is subordinate to the fermion in our model, at least within our ansatz. Nonetheless, perhaps the strongest implication of the bispinor picture is that the bosonic dynamical system can be solved in terms of elliptic functions. Thus, although we may not be able to write bosonic solutions explicitly in terms of elementary functions, the technology of the Jacobi elliptic functions allows us to express these solutions in terms of well-understood special functions, and to make strong qualitative and quantitative statements about their features in terms of certain parameters of the model.

The bispinor system is strictly weaker than the original system of fermions and the scalar kink, and thus we would not expect that *every* solution of the bispinor picture extends to a solution of our original system. Nonetheless,

we show that in the case we focus on, we can satisfy a consistency condition arising from the relevant Dirac equations to solve for explicit fermion components given a solution to the bispinor system. We discuss a systematic approach for numerically exploring the configuration space of solutions to the bispinor system in order to obtain corresponding solutions to the full fermion-kink system.

In Chapter 4 we look at coupling fermions to a non-linear sigma field which models baby Skyrmions on a spherical spatial manifold, via a coupling term analogous to how we previously coupled fermions and kinks, while necessarily including isospin. Our starting point will be the Lagrangian

$$\mathcal{L}_f = \overline{\Psi}(\mathrm{i}\hbar\hat{\not{D}} - g\boldsymbol{\tau}\cdot\boldsymbol{\phi})\Psi, \tag{1.3}$$

where $\Psi(t,\theta,\phi)$ represents the fermion which now carries isospin, and $\boldsymbol{\phi}(t,\theta,\phi)$ is the isovector triplet of scalar fields comprising the baby Skyrmion. This treatment is highly motivated by a quite analogous system of fermions on a background $B = 1$ BPS Skyrmion on S^3, as developed by Goatham and Krusch [23]. Preserving some of the geometry of the sphere in our solutions, such as taking an ansatz of axial symmetry, makes them resemble suitably nice topological solitons in Skyrme models (or in instanton models). We therefore assume a suitably simple and symmetric background configuration of the soliton fields, and as in the previous chapter first examine fermion dynamics in the absence of back-reaction. Once again, we construct the problem of finding Hamiltonian eigenstates for stationary state solutions of the Dirac equation. There is again a symmetry of the space manifold which we can use to identify a conserved angular momentum. With two spatial dimensions, however, this is not enough to give a full decomposition of Hamiltonian eigenstates: we need an additional mutually conserved "quantum number" to serve as a label.

Separating variables according to our ansatz of axial symmetry, we find that the differential equation for the remaining unknown profile function is of Fuchsian type when extended to the complex plane. We can therefore consider Frobenius series solutions around its regular singularities (which are its only singularities). Moreover, we find that the Fuchsian behaviour of the pole at complex infinity gives us a condition on the energy spectrum of solutions. We will focus on the case where the baby Skyrmion just has topological charge 1. We observe that in this case, the fermion lives in a representation of $\mathrm{SU}(2)$. Constructing the Casimir operator for this representation gives us the second quantum number needed for a full decomposition of the Hamiltonian eigenstates. We obtain the explicit energy eigenvalues of Hamiltonian eigenstates, and outline the constructive approach to deriving explicit component expressions for the eigenstates.

We conclude with Chapter 5. We recap our results and outline some directions for future work. In particular we discuss the role of the axial symmetry of the kink-fermion model in Chapter 3, and outline some possible extensions of the model with a focus on this symmetry. We also discuss broader contexts for investigating coupling between fermions and solitons on spheres.

We include two appendices. In Appendix A we explicitly work through some differential geometry to derive the spin connection and the change of basis transformations for fermions on S^2, which we have used in Chapter 4. Appendix B contains some Maple worksheets which implement some lengthy algebraic manipulations, and perform the subsequent Fuchsian analysis, for Chapter 4. It also contains a worksheet very briefly demonstrating some established results for the spectrum of fermions on S^2 as previously treated by Abrikosov [1].

Chapter 2

Background

2.1 A quick introduction to topological solitons

A topological soliton is a minimal-energy configuration in a non-trivial topological sector of a field theory. They are typically localised in some sense and so can be modelled in a particle-like way. The simplest examples are kinks in (1+1) dimensions, such as the celebrated ϕ^4 and sine-Gordon models [43, 54, 64]. The ϕ^4 kink arises from a Lagrangian which, in natural units where $c = 1 = \hbar$, may be expressed as

$$\mathcal{L} = \frac{1}{2}\partial_\mu\phi\partial^\mu\phi - \lambda\left(m^2 - \phi^2\right)^2. \tag{2.1}$$

A static solution localised at position a to the equation of motion obtained by varying (2.1) is

$$\phi(x) = m\tanh\left(\sqrt{2\lambda}m\,(x-a)\right), \tag{2.2}$$

and a Lorentz boost gives the moving kink with velocity v,

$$\phi(t,x) = m\tanh\left(\sqrt{2\lambda}m\frac{x-vt-a}{\sqrt{1-v^2}}\right). \tag{2.3}$$

The sine-Gordon model has Lagrangian density

$$\frac{1}{2}\partial_\mu\partial^\mu\phi - (1-\cos\phi). \tag{2.4}$$

A static solution localised at position a is

$$\phi(x) = 4\tan^{-1} e^{x-a}, \tag{2.5}$$

and a Lorentz-boosted moving kink is

$$\phi(t,x) = 4\tan^{-1} e^{\frac{x-vt-a}{\sqrt{1-v^2}}}. \tag{2.6}$$

In each case, the kink interpolates between distinct topological vacua at $x = \pm\infty$ and thus cannot dynamically decay.

Even such apparently simple models can lead to complex behaviour. An old question of kink-antikink scattering is still a contemporary area of research exhibiting extremely rich physics such as multi-bounce resonance windows and spectral walls [3, 4, 6, 15, 42]. Not all of the study of kinks is classical: the quantum sine-Gordon model gives rise to the deep notion of bosonisation in (1+1)-dimensional quantum field theory [17].

The Skyrme model is a non-linear (3+1)-dimensional $SU(2)$ sigma model [63, 65]. It is an effective field theory of QCD, becoming exact in the limit $N \to \infty$, where N is the number of colour charges [69, 70]. It has topological soliton solutions which can be interpreted as baryons. There is an analogous "baby Skyrme" model in $(2+1)$ dimensions which is a significant simplification but also admits topological solitons [53], which have applications to condensed matter physics [see e.g. 66]. More recently a model of "magnetic Skyrmions" has been developed in $(2+1)$ dimensions [10], particularly in models of chiral magnets [8]. Magnetic skyrmions have been experimentally observed in condensed matter systems [22], and have potential applications to low-energy data storage as a framework for "racetrack memory" [19, 47].

2.2 Topological solitons, spheres, and fermions in low dimensions

The dynamics of fermions coupled to topological solitons have been examined in various low-dimensional models, where the coupling term is motivated by analogy to "chiral bag" models of nucleon and fermion fields [see e.g. 16, 28]. When the nucleon is modeled by a topological soliton, the fermion typically also carries isospin, and couples to the isovector soliton via a bispinor term. Spacetime is typically chosen to be either flat Minkowski space, or such that a canonical spatial slice is taken to be an n-sphere, perhaps by compactification of an originally flat spacetime. Often, it is easiest to consider the soliton to be an independent background field for the fermion, so there is no back-reaction of the fermion on the soliton and the fermion can be (numerically or analytically) solved for a choice of a known soliton solution. Occasionally the soliton is instead fully coupled to the fermion and solutions of the full combined system are obtained. A numerical approach is generally necessary; when the fermions can be solved analytically, the symmetries of the model usually aid classification of the solutions, and these solutions may sometimes be expressed in terms of hypergeometric functions (or indeed well-known subfamilies of "the" hypergeometric function). A typically observed phenomenon is localisation of the fermion by the soliton. Such models also sometimes feature *spectral flow*, where the fermionic energy eigenvalues, which depend on the physical parameters of the system, can sometimes pass through the value 0 and change sign as we evolve the physical parameters. The existence of such fermionic zero modes is predicted by the index theorem for the relevant Dirac operator.

In $(1+1)$ dimensions, fermions have been added to scalar field models that admit topological solutions on the real line, such as ϕ^4 theory and sine-Gordon theory. In one space dimension, the soliton is modelled using a scalar

(or pseudoscalar) field, such that the model admits solutions where this field interpolates between topologically distinct vacua; as particles or localised excitations, the solitons are precisely these topologically non-trivial solutions. Fermions on a background ϕ^4 kink solution modelled with a very simple chiral coupling term have been modelled by Shahkarami, Mohammadi, and Gousheh [62], using a Lagrangian of the schematic form

$$\mathcal{L} = \overline{\psi}\left(\mathrm{i}\gamma^\mu\partial_\mu - g\mathrm{e}^{\mathrm{i}\phi\gamma^5}\right)\psi. \tag{2.7}$$

Here ψ is the fermion, ϕ is the fixed pseudoscalar kink, γ^5 is the chiral Dirac matrix, and g is a coupling constant.[1] This system has been solved numerically [24, 62], giving insight into scattering coefficients as well as the role of the topological winding number and and an interpretation that the fermionic zero modes contribute to the system's Casimir energy. Numerical solutions have also been found when the pseudoscalar kink is taken out of the background and allowed to react to the fermion [61]; that system is modelled by the addition of the terms of the typical ϕ^4 Lagrangian (2.1) to (2.7).

On a background sine-Gordon kink, a fermion can be added with a coupling term motivated by the chiral bag model by interpreting the kink as an isovector and promoting the fermion to an isospinor representation. Loginov [39] has modelled this coupling by using a Lagrangian for the fermion of the form

$$\mathcal{L}_f = \mathrm{i}\overline{\psi}\gamma^\mu\partial_\mu\psi - g\boldsymbol{\phi}\cdot\overline{\psi}\boldsymbol{\tau}_\perp\psi, \tag{2.8}$$

where $\boldsymbol{\phi}$ is the background isovector corresponding to the sine-Gordon kink, and $\boldsymbol{\tau}_\perp$ denotes the "isovector of isospin matrices", in the same sense that

[1] In [62], the authors use the notation M instead of g for the coupling constant, and explicitly interpret this as a fermionic mass parameter. However, in Chapter 3, we will use M to denote a different parameter, so to avoid confusion we take the liberty of renaming their coupling constant to the nomenclature that we will use.

we typically write γ^μ to denote the vector of spin matrices. Fermion scattering states then have wavefunctions that can be expressed in terms of Heun functions. The dependence of the transmission and reflection coefficients on physical parameters such as the fermion mass is investigated numerically, and it is observed that fermionic zero modes polarise the vacuum.

The examples of fermion-kink coupling in the Lagrangians (2.7) and (2.8) provide the general prototype of models we will consider. We consider them to have a similar "flavour", and interpret the chiral coupling in (2.7) to be an isospin-less analogue of the spin-isospin coupling in (2.8), the latter of which directly generalises to models of higher-dimensional solitons. However, we note that these are not the only coupling terms between fermions and kinks which have been studied. Dirac fermions coupled to kinks is also an active area of contemporary research linked to the questions of kink-antikink collisions [9] and kink quasi-normal modes [13]. Those models employ coupling terms of the generic form $G(\phi)\overline{\psi}\psi$ for a function G of the kink field ϕ. The simplest case where G is constant gives standard Yukawa coupling, but cases such as $G(\phi) = \sin\phi$ are also considered. Although these are outside the scope of our treatment, they demonstrate the breadth of activity in this field.

In $(2+1)$ dimensions, fermions have been added to models which admit solitons in the plane, such as those known as baby skyrmions [51] where the soliton is stabilised by a Skyrme term, and magnetic skyrmions [52] where the soliton is stabilised by a Dzyaloshinskii-Moriya interaction, or DMI, term. A typical Lagrangian in such models contains terms for the isospin-carrying fermion Ψ in the form

$$\mathcal{L}_f = \mathrm{i}\overline{\Psi}\gamma^\mu\partial_\mu\Psi - g\overline{\Psi}\left(\boldsymbol{\phi}\cdot\boldsymbol{\tau}\right)\Psi, \tag{2.9}$$

where $\boldsymbol{\phi}$ is the isovector field modelling the soliton and again $\boldsymbol{\tau}$ comprises the isospin matrices. The direct analogy to (2.8) is clear. In flat space, a mass term

$-m\overline{\Psi}\Psi$ may be added to the fermion, and in the case of magnetic Skyrmions the derivative term is augmented by the presence of an external magnetic field.

In the absence of back-reaction in such models, there is typically a combined rotation-isorotation symmetry of the fermion fields, corresponding to a generalised angular momentum generator; the conserved eigenvalue of this operator aids classification of the fermion solutions. When back-reaction is considered in the baby Skyrmion model, it is numerically observed that a strongly coupled fermion deforms the soliton. One zero-crossing fermion mode is observed under spectral flow. In the case of the magnetic Skyrmion model, the introduction of the fermion leads to new physics, as it allows for a multi-soliton bound state which cannot arise in its absence. Recently, Barsanti and Tallarita [7] have also studied a model of fermions coupled to baby Skyrmions on a cylinder and determined an analytic sector.

In $(3+1)$ dimensions, the Skyrme model on a spatial 3-sphere exhibits a particularly straightforward BPS solution for topological degree $B = 1$ [40]. This solution has been used as a background for spin-isospin fermions [23, 37] with analogous coupling to that at (2.8) and (2.9):

$$\mathcal{L}_f = \mathrm{i}\overline{\Psi}\gamma^\mu D_\mu \Psi - g\overline{\Psi}\left(\boldsymbol{\phi}\cdot\boldsymbol{\tau}\right)\Psi. \tag{2.10}$$

In this case, the covariant derivative D_μ contains a contribution from the non-trivial spin connection on the curved space S^3. Similarly to the baby Skyrmion model in $(2+1)$ dimensions, there is a generalised angular momentum of the fermion around the background Skyrmion, the eigenvalue of which provides a quantum number. A full description of fermion solutions is possible with some analytical tools by observing that part of the energy

eigenvalue problem is expressed as a Fuchsian differential equation. A family of solutions can be expressed in terms of a basis of spinorial eigenfunctions of the Dirac operator, similar to the role of so-called "spinor harmonics" or "monopole harmonics" on the 2-sphere [1, 21]. This model of fermions on a $B = 1$ Skyrmion on S^3 as studied by Goatham and Krusch [23] particularly motivated our investigation of fermions on a background baby Skyrmion on S^2. Our treatment of fermions and background baby Skyrmion on S^2 will start from a Lagrangian which is exactly analogous to (2.10). We hope that similar techniques will allow us to classify our fermion solutions. Moreover, we are interested in seeing whether, when the spatial sphere is made large, our model becomes similar to the results obtained by Perapechka, Sawado, and Shnir [51] for fermions on a background baby Skyrmion in flat space.

In general, there is ample evidence that zero modes of Dirac operators play a significant role in models of topological solitons, both physically and geometrically. Aside from the mentioned physical qualities of zero-mode fermions in coupled fermion-soliton systems, for example, Ross and Schroers have shown that vortices on S^2 are linked to magnetic zero modes of Dirac operators in three dimensions by Cartan geometry [57]. Manton and Schroers have shown that a vector bundle of Dirac zero modes over a moduli space of BPS monopoles can be used to explore the quantum interaction of monopoles and fermions [41].

Chapter 3

Fermion-kink coupling on $\mathrm{S}^1 \times \mathbb{R}$

In this chapter, we present a $(1+1)$-dimensional model of a (classical) Dirac fermion coupled to a scalar field as an idealised model of a fermion in the presence of a topological kink. Our spacetime manifold is $\mathbb{R} \times \mathrm{S}^1$, with an unbounded time direction and a periodic space direction. Although the model is Lorentz-invariant, we break the relativistic symmetry to work in a privileged frame, and consider static solutions for the kink and steady state solutions for the fermion in this non-relativistic perspective, seeking to solve the energy eigenvalue problem for the fermion. We first consider the case where the kink is fixed with an idealised uniform winding in the background, so there is no back-reaction from the fermion on the kink. In this case, the problem is linear, and a symmetry of the coupling term allows us to define an appropriate "generalised angular momentum" operator, the square of whose eigenvalue is a conserved quantum number and permits the organisation of the fermion solutions by energy levels. The energy levels are typically degenerate of dimension 2, and there are two useful bases for such energy levels: a (signed) angular momentum basis, and a parity basis. There is a conserved Noether charge W, the axial charge of the fermion, which can be understood as a measure of how badly the discrete parity symmetry is broken for any fermion solution: it vanishes for parity eigensolutions, but is maximised, in an exact sense, for angular momentum eigensolutions.

Next, we take the kink "out of the background" by introducing a Dirichlet

term for the kink into the action, weighted by a parameter we call the *activity*, which resists the back-reaction from the fermion on the kink. In the limit of infinite activity, the kink is restored to the background and the problem reduces to the previous special case. In general, the problem with the fully coupled kink is non-linear. Moreover, the symmetries of the system are altered in such a way that the generalised angular momentum of the previous case decomposes into two separate symmetries: the usual space translation of the fields in the Poincaré group, and a new continuous internal symmetry combining a target space rotation of the kink with an axial spin transformation of the fermion. There is no longer an immediately clear quantum number corresponding to the previous role of angular momentum. The angular momentum eigensolutions of the fermion, with a uniform kink, do remain as solutions of the general model. However, the parity eigensolutions of the special case do not remain solutions of the general case, as they violate the new internal symmetry.

We investigate the system numerically by making suitable ansätze so that the equations of motion form a boundary value problem. We find solutions where the kink is not simply uniform, as it would be in the absence of back-reaction, and where the fermion components appear by inspection to form parity eigenspinors. To excellent numerical accuracy, these new solutions do satisfy the conservation equation for the internal symmetry, and have vanishing axial charge. We therefore interpret these as the appropriate parity eigenstates of the system when back-reaction is permitted.

By considering the Lorentz-invariant bispinors of the model, we observe that under the ansatz of a static kink and a stationary state fermion, the behaviour of the kink is fully determined by the density profile $|\psi|^2$ of the fermion field ψ, which itself obeys a non-linear differential equation that admits solutions in terms of elliptic functions. We employ the theory of the

Jacobi elliptic functions to describe a specific class of analytical solutions, exhibiting fermionic states of definite parity, and describe how in this picture one could try to find physical solutions to the kink-fermion system by hunting for the intersection points of a pair of transcendental curves. We can again observe the role of the axial Noether charge W in "interpolating" between definite-parity solutions and the preserved "angular momentum" solutions. Finally, we demonstrate that, at least for the definite parity solutions, no information is lost by moving from the original fermionic coordinates to the picture with just the bispinor coordinates: we can always reconstruct the underlying fermion field from a solution to the bispinor system.

3.1 Conventions and representations

Throughout, we specifically retain the reduced Planck's constant $\hbar$, and the length scale ρ giving the radius of S^1, so that we can examine limiting behaviour of these parameters in the future. We set $c = 1$, and take the spacetime metric

$$g = \mathrm{d}t \otimes \mathrm{d}t - \rho^2 \, \mathrm{d}\theta \otimes \mathrm{d}\theta. \tag{3.1}$$

We take a local orthonormal frame to be ${e_\alpha}^\mu = \mathrm{diag}(1, -\frac{1}{\rho})$. We denote the matrix inverse to the frame matrix ${e_\alpha}^\mu$ to be ${e^\alpha}_\mu$, such that

$${e^\alpha}_\mu {e_\alpha}^\nu = \delta^\nu_\mu, \quad {e^\alpha}_\mu {e_\beta}^\mu = \delta^\alpha_\beta. \tag{3.2}$$

With our choice of frame, the local tangent vector basis is given by

$$\hat{e}_0 = \frac{\partial}{\partial t}, \quad \hat{e}_1 = -\frac{1}{\rho}\frac{\partial}{\partial \theta}, \tag{3.3}$$

and the local dual basis is

$$\hat{\vartheta}^0 = \mathrm{d}t, \quad \hat{\vartheta}^1 = -\rho\, \mathrm{d}\theta. \tag{3.4}$$

With respect to this frame, $g(\hat{e}_\alpha, \hat{e}_\beta) = \eta_{\alpha\beta} = \mathrm{diag}(1, -1)$.

For the spin representation, we take the chiral representation of matrices γ^α satisfying $\{\gamma^\alpha, \gamma^\beta\} = 2\eta^{\alpha\beta}$:

$$\gamma^0 = \begin{pmatrix} 0 & 1 \\ 1 & 0 \end{pmatrix}, \quad \gamma^1 = \begin{pmatrix} 0 & -1 \\ 1 & 0 \end{pmatrix}. \tag{3.5}$$

Given a Clifford algebra $\mathrm{Cl}(V)$ on a vector space V, we can construct the corresponding spin group $\mathrm{Spin}(V)$. Thus, a representation of the generators of the Clifford algebra extends to define a representation of the spin group. On an even-dimensional space, this representation (3.5) of the spin group is not irreducible. It decomposes into two *chiral* or *Weyl* components, each of half the dimension of the overall Dirac representation. Here our Dirac representation has two complex dimensions, and the Weyl representations are of complex dimension one. Our choice of representation decomposes as a direct sum; that is, each of the components of a spinor belongs to a different Weyl subrepresentation. Correspondingly, there is a chiral γ matrix whose eigenspaces are the Weyl subrepresentations. It is found here simply as the product of the γ matrices for the local vector basis elements. It is conventional to refer to it as γ^{n+1} on a Lorentzian manifold of dimension n, as it is equivalent to the corresponding Dirac matrix for a truly Riemannian (i.e. not pseudo-Riemannian) manifold of dimension $n + 1$, which would be labelled starting from 1 instead of 0. We therefore have the additional γ matrix,

$$\gamma^3 = \gamma^0\gamma^1 = \begin{pmatrix} 1 & 0 \\ 0 & -1 \end{pmatrix}. \tag{3.6}$$

Note that the anti-commutation relations of the gamma matrices give us the equivalent expressions $\gamma^3 = -\gamma^1\gamma^0$ and $\gamma^3 = \frac{1}{2}\left(\gamma^0\gamma^1 - \gamma^1\gamma^0\right)$. It is also evident that $\left(\gamma^3\right)^2 = 1$.

We use the frame to construct spacetime gamma matrices γ^μ from the local gamma matrices γ^α by defining

$$\gamma^\mu = e_\alpha{}^\mu \gamma^\alpha. \tag{3.7}$$

In particular, while $\gamma^t = \gamma^0$, $\gamma^\theta = -\frac{1}{\rho}\gamma^1$. It is useful to introduce an overall energy scale,

$$a = \frac{\hbar}{\rho}. \tag{3.8}$$

Adopting this notation, the Dirac operator can be expressed quite simply in terms of the familiar local gamma matrices γ^0, γ^1 as

$$\mathrm{i}\hbar\not{\partial} = \mathrm{i}\hbar\gamma^0\frac{\partial}{\partial t} - \mathrm{i}a\gamma^1\frac{\partial}{\partial\theta}. \tag{3.9}$$

(Note that in two dimensions, there is no non-trivial contribution from the spin connection to the Dirac operator.)

We conventionally view all transformations as active: under a (say, Lorentz) transformation Λ of spacetime coordinate,

$$x \mapsto \Lambda x, \tag{3.10}$$

a generic field $\phi(x)$ on spacetime transforms as

$$\phi'(x) = R_\Lambda \phi(\Lambda^{-1}x), \tag{3.11}$$

where R_Λ is the appropriate representation of the transformation Λ on the field ϕ.

In the local basis, define the Lorentz invariant and alternating tensor $\hat{\varepsilon}_{\alpha\beta}$ according to

$$\hat{\varepsilon}_{01} = 1 = -\hat{\varepsilon}_{10}, \tag{3.12}$$

the indices of which we can raise with the local Minkowski metric $\eta^{\alpha\beta}$. Then we have the following useful identities in the local Clifford algebra:

(i) $\gamma^3 = \frac{1}{2}\hat{\varepsilon}_{\alpha\beta}\gamma^\alpha\gamma^\beta$,

(ii) $\gamma^\alpha\gamma^\beta = \eta^{\alpha\beta} - \hat{\varepsilon}^{\alpha\beta}\gamma^3$,

(iii) $\gamma^\alpha\gamma^3 = \hat{\varepsilon}^\alpha{}_\beta\gamma^\beta$.

We can contract with the frame to define a Lorentz invariant, alternating tensor in the spacetime basis, $\hat{\varepsilon}_{\mu\nu} = \hat{\varepsilon}_{\alpha\beta}e^\alpha{}_\mu e^\beta{}_\nu$. Explicitly, the non-zero components are easily seen to be

$$\hat{\varepsilon}_{t\theta} = -\rho = -\hat{\varepsilon}_{\theta t}. \tag{3.13}$$

(We see the utility of the hat on $\hat{\varepsilon}_{\alpha\beta}$: it serves as a reminder that the corresponding spacetime basis tensor $\hat{\varepsilon}_{\mu\nu}$ is scaled differently to the usual Levi-Civita symbol.)

3.2 Overview of the Lagrangian: parameters and dimensions

Let us introduce, and perform some dimensional analysis upon, the most general Lagrangian that we will study for this model of fermion-kink coupling. When we admit full coupling between the fermion and the kink, we will use the Lagrangian density

$$\mathcal{L} = \frac{M^2}{2}\partial_\mu\phi\,\partial^\mu\phi + \overline{\psi}\left(\mathrm{i}\hbar\partial\!\!\!/ - g\mathrm{e}^{\mathrm{i}\gamma^3\phi}\right)\psi. \tag{3.14}$$

The dynamical fields are the scalar field $\phi(t,\theta)$ used to model the kink, and the Dirac spinor field $\psi(t,\theta)$. We have chosen a chiral coupling term like the model studied by Shahkarami, Mohammadi, and Gousheh [62]; the fermionic terms are the same as those we saw at (2.7), but we denote the chiral Dirac matrix now by γ^3. We have included a Dirichlet term for the scalar field, but we do not include a potential term for scalar field independent of its interaction with the fermion. The action corresponding to this Lagrangian is

$$S = \int_{\mathbb{R}\times\mathrm{S}^1} \left[\frac{M^2}{2} \partial_\mu \phi \, \partial^\mu \phi + \overline{\psi} \left(\mathrm{i}\hbar \not{\partial} - g \mathrm{e}^{\mathrm{i}\gamma^3 \phi} \right) \psi \right] \rho \, \mathrm{d}t \, \mathrm{d}\theta. \tag{3.15}$$

Having taken $c = 1$, there are two basic dimensions we should consider: energy, which we denote $[E]$, and distance, which we denote $[L]$. Note that although the time coordinate t is dimensionful, with $[t] = [L]$, the angular coordinate θ is dimensionless, i.e. $[\theta] = 1$, and so we must be careful to include factors of the length scale ρ arising from the metric where necessary. In particular, this implies that we need to be careful with the dimension of derivative operators, depending on coordinate and whether the derivative has covariant or contravariant indices. We have $[\partial_t] = [\partial^t] = [L]^{-1}$ as usual, but $[\partial_\theta] = 1$ whereas

$$\partial^\theta = -\frac{1}{\rho^2} \frac{\partial}{\partial \theta} \quad \Rightarrow \quad [\partial^\theta] = [L]^{-2}. \tag{3.16}$$

The product of ∂_μ and ∂^μ, either on distinct operands such as in the Dirichlet term or forming the d'Alembertian on a single operand, satisfies $[\partial_\mu][\partial^\mu] = [L]^{-2}$. Similarly, the local gamma matrices γ^0, γ^1 and γ^3 are dimensionless, but the spacetime gamma matrices defined at (3.7) have dimensions $\left[\gamma^t\right] = 1$ but $\left[\gamma^\theta\right] = [L]^{-1}$. This implies that the Dirac operator $\not{\partial}$ does have the dimension of a spatial derivative:

$$[\not{\partial}] = \left[\gamma^\mu \partial_\mu\right] = [L]^{-1}. \tag{3.17}$$

Overall, the action S should have dimension $[S] = [E][L]$, so in our case with two spacetime dimensions, we see that the Lagrangian (density) should satisfy $[\mathcal{L}] = [E][L]^{-1}$. Planck's constant (reduced or not) conventionally has units of action, so $[\hbar] = [E][L]$ also. This lets us determine a consistent set of dimensions for the remaining parameters and fields. From the Dirac term, we find the dimension of the fermion field:

$$\left[\mathrm{i}\hbar\overline{\psi}\partial\!\!\!/\psi\right] = [\hbar][\partial\!\!\!/]\,[\psi]^2 = [E][\psi]^2 \quad \Rightarrow \quad [\psi] = [L]^{-\frac{1}{2}}. \tag{3.18}$$

The scalar field ϕ should be explicitly dimensionless in order for us to exponentiate it in the coupling term. Therefore, the dimensionful coefficient M^2 must be included in the Dirichlet term for consistency. We find in particular the following:

$$\left[\frac{M^2}{2}\partial_\mu\phi\,\partial^\mu\phi\right] = [M^2][L]^{-2} \quad \Rightarrow \quad [M^2] = [E][L]. \tag{3.19}$$

We will refer to the nonnegative real coefficient M of dimension $[E]^{\frac{1}{2}}[L]^{\frac{1}{2}}$ as the *activity* of the scalar field ϕ, since its role is to enforce dimensional consistency with the action.

Finally, we quickly observe that the coupling constant g in the interaction term must have dimension of energy:

$$\left[g\overline{\psi}\mathrm{e}^{\mathrm{i}\gamma^3\phi}\psi\right] = [g][L]^{-1} \quad \Rightarrow \quad [g] = [E]. \tag{3.20}$$

We observe three dimensionless combinations of the physical parameters. There is a quantity $\tilde{g}$ defined by

$$\tilde{g} = \frac{g}{a} = \frac{\rho g}{\hbar}, \tag{3.21}$$

describing the strength of the coupling relative to the energy scale set by the

size of the system. There is also a dimensionless measure $\tilde{M}^2$ of the scalar field activity,

$$\tilde{M}^2 = \frac{M^2}{\hbar}. \tag{3.22}$$

We will see that the quotient of these quantities,

$$\frac{\tilde{M}^2}{\tilde{g}} = \frac{M^2}{\rho g}, \tag{3.23}$$

gives a measure of the relative inertia of the kink to back-reaction effects caused by the fermion. In practice, we will mostly be working in units of the energy scale a, and so will effectively think of this by comparing $\frac{M^2}{\rho}$ to g. However, from around Section 3.6 to the end of this chapter when we discuss the role of elliptic functions in the fully coupled model, we will usually rescale to work with dimensionless quantities.

3.3 The prescribed kink

3.3.1 Lagrangian and symmetries

We will first consider the case where the kink is fixed in the background and experiences no back-reaction owing to the presence of the fermion. As discussed in Section 2.2, previous treatments have fixed the kink to take the form of a known soliton solution in a scalar field theory. Since our most general Lagrangian (3.14) does not include a potential term for the scalar field, the background solution should be appropriate to the theory of a free scalar field on the circle (i.e. a massless Klein-Gordon field). For maximal simplicity, we choose to prescribe the background kink to be static and uniform with winding number $n \in \mathbb{Z}$, i.e.

$$\phi(t, \theta) = n\theta. \tag{3.24}$$

We note that this solution is always the lowest-energy solution within the homotopy class specified by n, so we consider it to be a sensible profile for the scalar field about which to later test the back-reaction from the fermion.

To consider the dynamics of the fermion chirally coupled to this background kink, we choose to work with a model of a Dirac fermion $\psi(t,\theta)$ with Lagrangian density

$$\mathcal{L}_f = \overline{\psi}\left(\mathrm{i}\hbar\partial\!\!\!/ - g\mathrm{e}^{\mathrm{i}\gamma^3 n\theta}\right)\psi. \tag{3.25}$$

The kink is totally absent except for influencing the form of the coupling term. The Dirac fermion $\psi(t,\theta)$ is the only dynamical field in this treatment. We apply the variational principle directly to this Lagrangian. The Dirac equations are

$$\left(\mathrm{i}\hbar\partial\!\!\!/ - g\mathrm{e}^{\mathrm{i}\gamma^3 n\theta}\right)\psi = 0 \tag{3.26}$$

and the spinorial conjugate equation.

The Lagrangian is manifestly time-invariant, leading to a conserved Noether charge corresponding to the total energy,

$$\mathrm{E}_{\mathrm{tot}} = \int_0^{2\pi} \psi^\dagger\gamma^0\left(\mathrm{i}a\gamma^1\frac{\partial}{\partial\theta} + g\mathrm{e}^{\mathrm{i}\gamma^3 n\theta}\right)\psi\,\rho\,\mathrm{d}\theta = \int_0^{2\pi}\psi^\dagger\hat{H}\psi\,\rho\,\mathrm{d}\theta, \tag{3.27}$$

with $\frac{\partial \mathrm{E}_{\mathrm{tot}}}{\partial t} = 0$. We use the above expression to define the self-adjoint Hamiltonian operator $\hat{H}$. The equation of motion (3.26) can be written as a Schrödinger-type equation,

$$\mathrm{i}\hbar\frac{\partial\psi}{\partial t} = \hat{H}\psi. \tag{3.28}$$

We will seek in particular *steady state* solutions, of the form

$$\psi(t,\theta) = \mathrm{e}^{-\frac{\mathrm{i}}{\hbar}E_f t}\psi(\theta), \tag{3.29}$$

where the fermionic energy density E_f must therefore be a (real, constant) eigenvalue of $\hat{H}$.

The fermion has a global $\mathrm{U}(1)$ phase symmetry under the transformation

$$\psi(t,\theta) \mapsto \mathrm{e}^{\mathrm{i}\alpha}\psi(t,\theta), \tag{3.30}$$

and there is a corresponding conserved $\mathrm{U}(1)$ charge T which we choose to define as

$$T = \int_0^{2\pi} \psi^\dagger \psi \, \rho \, \mathrm{d}\theta. \tag{3.31}$$

Observe that with this definition, T is dimensionless. It therefore effectively sets a normalisation of the fermion field, and so we will typically refer to the local quantity $|\psi|^2 = \psi^\dagger\psi$ just as the "density" of the fermion, without labouring the point that it is a $\mathrm{U}(1)$ Noether charge density.

We will see that while the kink is in the background, the value of T does not play a role in the physics, so it is convenient to simply take $T = 1$ until we move to the fully coupled model. This convention identifies the fermionic energy density eigenvalue E_f with the total energy $\mathrm{E}_{\mathrm{tot}}$; we will generally ignore the distinction, and refer to E_f just as the energy of the fermion.

When we have thus prescribed the kink in the background, and are only free to transform the fermion field, we observe a continuous symmetry under which

$$\psi(t,\theta) \mapsto \mathrm{e}^{-\mathrm{i}\alpha\frac{n}{2}\gamma^3}\psi(t,\theta-\alpha), \tag{3.32}$$

with conserved charge (by Noether's theorem)

$$Q_L = \int_{S^1} \left(-\frac{\partial \mathcal{L}_f}{\partial(\partial_t\psi)} \left(\mathrm{i}\gamma^3\frac{n}{2}\right) + \vartheta^t{}_\theta \right) \mathrm{d}\theta \tag{3.33}$$

(where $\vartheta^{\mu}{}_{\nu}$ is the energy-momentum tensor)

$$= \int_{\mathrm{S}^1} \psi^\dagger \left(-i\hbar \frac{\partial}{\partial \theta} + \hbar \frac{n}{2} \gamma^3 \right) \psi \, \mathrm{d}\theta = \int_{\mathrm{S}^1} \psi^\dagger \hat{L} \psi \, \mathrm{d}\theta. \tag{3.34}$$

We define the self-adjoint *generalised angular momentum* operator $\hat{L}$ according to the above:

$$\hat{L} = \hbar \left(-\mathrm{i} \frac{\partial}{\partial \theta} + \frac{n}{2} \gamma^3 \right). \tag{3.35}$$

The absence of ρ from the integral at (3.33) is of no consequence: in practice we only work with the operator $\hat{L}$ rather than the quantity Q_L. It is easily checked that

$$[\hat{L}, \hat{H}] = 0, \tag{3.36}$$

so we can seek a joint eigenbasis of static solutions for both energy and this angular momentum. There is also a discrete parity symmetry,

$$\psi(t, \theta) \mapsto \gamma^0 \psi(t, 2\pi - \theta). \tag{3.37}$$

We should comment that strictly, what we are calling (generalised) angular momentum is really just (generalised) momentum for this (1+1)-dimensional system, and in particular it is a Lorentz vector quantity which transforms as a vector under parity, rather than a pseudovector picking up an extra minus sign relative to vector quantities, which would be the typical characteristic of an angular momentum in an odd number of space dimensions. However, we will still consistently refer to it as angular momentum by virtue of its analogy to Fourier modes in higher dimensions.

3.3.2 Solutions in angular momentum and parity bases

Our aim is to solve the eigenvalue equation for a static fermion,

$$\hat{H}\psi(\theta) = E\psi(\theta). \tag{3.38}$$

We first derive the eigenspinors $\psi_l(\theta)$ of the operator $\hat{L}$ defined above at (3.35), satisfying

$$\hat{L}\psi_l(\theta) = \hbar l \psi_l(\theta). \tag{3.39}$$

In the chiral basis, we write the fermion as

$$\psi = \begin{pmatrix} \psi_R \\ \psi_L \end{pmatrix}, \tag{3.40}$$

where the subscripts R and L refer respectively to the right- and left-handed chiral (Weyl) components. In this basis, equation (3.39) is expressed

$$\hbar \begin{pmatrix} -\mathrm{i}\frac{\partial}{\partial\theta} + \frac{n}{2} & 0 \\ 0 & -\mathrm{i}\frac{\partial}{\partial\theta} - \frac{n}{2} \end{pmatrix} \begin{pmatrix} \psi_l^R \\ \psi_l^L \end{pmatrix} = \hbar l \begin{pmatrix} \psi_l^R \\ \psi_l^L \end{pmatrix}. \tag{3.41}$$

Thus the angular momentum eigenspinors are

$$\psi_l(\theta) = \begin{pmatrix} A\mathrm{e}^{\mathrm{i}(l-\frac{n}{2})\theta} \\ B\mathrm{e}^{\mathrm{i}(l+\frac{n}{2})\theta} \end{pmatrix}, \tag{3.42}$$

where A, B are complex coefficients and $l \pm \frac{n}{2}$ must be an integer.

Susbstituting the above expression for an angular momentum eigenspinor into the energy eigenvalue equation (3.38), we observe that the energy eigenvalue problem reduces to the finite-dimensional eigenvalue problem

$$\det(H_{\mathrm{alg}} - E\mathbb{I}) = 0, \tag{3.43}$$

where we define H_{alg} to be the *algebraic Hamiltonian* for angular momentum eigenvalue l:

$$H_{\text{alg}} = \begin{pmatrix} -a(l-\frac{n}{2}) & g \\ g & a(l+\frac{n}{2}) \end{pmatrix}. \tag{3.44}$$

The algebraic eigenvalue problem (3.43) gives a quadratic equation in the energy E,

$$\left(E - a\left(l+\frac{n}{2}\right)\right)\left(E + a\left(l-\frac{n}{2}\right)\right) - g^2 = 0. \tag{3.45}$$

The solutions give the energy spectrum in terms of n, l and g:

$$E = \frac{an}{2} \pm \sqrt{a^2l^2 + g^2}. \tag{3.46}$$

Thinking of the spectrum as dependent on the coupling constant g, we see that there are two branches for each choice of n and l. On the upper branch, taking $E = E^+ = \frac{an}{2} + \sqrt{a^2l^2+g^2}$, the eigenvector condition on the coefficients A, B becomes

$$\frac{B}{A} = \frac{al + \sqrt{a^2l^2+g^2}}{g}. \tag{3.47}$$

Thus an explicit (not normalised) solution on the upper energy branch is

$$\psi_{l,E^+}(t,\theta) = \mathrm{e}^{-\frac{\mathrm{i}}{\hbar}\left(\frac{an}{2}+\sqrt{a^2l^2+g^2}\right)t} \begin{pmatrix} g\mathrm{e}^{\mathrm{i}(l-\frac{n}{2})\theta} \\ (al+\sqrt{a^2l^2+g^2})\mathrm{e}^{\mathrm{i}(l+\frac{n}{2})\theta} \end{pmatrix}. \tag{3.48}$$

On the lower energy branch, taking $E = E^- = \frac{an}{2} - \sqrt{a^2l^2+g^2}$, the condition on the coefficients is

$$\frac{B}{A} = \frac{al - \sqrt{a^2l^2+g^2}}{g}, \tag{3.49}$$

and an explicit solution on the lower branch is

$$\psi_{l,E^-}(t,\theta) = \mathrm{e}^{-\frac{\mathrm{i}}{\hbar}\left(\frac{an}{2}-\sqrt{a^2l^2+g^2}\right)t} \begin{pmatrix} g\mathrm{e}^{\mathrm{i}(l-\frac{n}{2})\theta} \\ (al-\sqrt{a^2l^2+g^2})\mathrm{e}^{\mathrm{i}(l+\frac{n}{2})\theta} \end{pmatrix}. \tag{3.50}$$

Consider the behaviour of these solutions as g tends to 0. Evaluating the limit carefully and noting, for example, that

$$\frac{al - \sqrt{a^2l^2 + g^2}}{g} = \frac{-g}{al + \sqrt{a^2l^2 + g^2}}, \tag{3.51}$$

we see that the solution on the upper branch becomes a left-handed Weyl spinor, while the solution on the lower branch becomes a right-handed Weyl spinor:

$$\lim_{g\to 0} \psi_{l,E^+}(\theta) = \begin{pmatrix} 0 \\ 2al\mathrm{e}^{\mathrm{i}(l+\frac{n}{2})\theta} \end{pmatrix}, \tag{3.52}$$

$$\lim_{g\to 0} \psi_{l,E^-}(\theta) = \begin{pmatrix} 2al\mathrm{e}^{\mathrm{i}(l-\frac{n}{2})\theta} \\ 0 \end{pmatrix}. \tag{3.53}$$

The parity operation $\hat{P}\psi(t,\theta) = \gamma^0\psi(t, 2\pi - \theta)$ commutes with the Hamiltonian, but not with the angular momentum operator $\hat{L}$; parity exchanges an eigenstate of angular momentum l with the corresponding eigenstate of angular momentum $-l$. We define an energy eigenstate $\psi^P_{|l|^\pm} = \psi^P_{|l|,E^\pm}$ of definite parity $P = \pm 1$ to be a state satisfying

$$\gamma^0\psi^P_{|l|,E^\pm}(t, 2\pi - \theta) = P\psi^P_{|l|,E^\pm}(t,\theta). \tag{3.54}$$

Since the parity operation changes the sign of angular momentum, we expect that over the angular momentum basis, states of definite parity can be constructed as (without loss of generality choosing $l \geq 0$):

$$\psi^{+1}_{|l|} = \frac{1}{\sqrt{2}}\left(\psi_l + \psi_{-l}\right), \tag{3.55}$$

$$\psi^{-1}_{|l|} = \frac{1}{\sqrt{2}}\left(\psi_l - \psi_{-l}\right). \tag{3.56}$$

This is valid when the angular momentum eigenstates $\psi_{\pm l}$ have a consistent

normalisation, so that $|\psi_l|$ equals a fixed constant independent of the value of l.

Explicit coordinate expressions for the parity eigenstates are made compact by adopting the following shorthand: let us define

$$\alpha_l^{\pm} = \sqrt{g^2 + \left(-al \pm \sqrt{a^2 l^2 + g^2}\right)^2}, \tag{3.57}$$

$$\beta_l^{\pm} = \sqrt{g^2 + \left(al \pm \sqrt{a^2 l^2 + g^2}\right)^2}. \tag{3.58}$$

Then, in terms of the above expressions, the parity eigenstates may be written as the following:

$$\psi^{+}_{|l|^{\pm}}(\theta) = \frac{1}{4\sqrt{\pi(a^2 l^2 + g^2)}} \begin{pmatrix} \mathrm{e}^{-\mathrm{i}\frac{n}{2}\theta}\left[\left(\alpha_l^{\pm} + \beta_l^{\pm}\right)\cos(l\theta) \right. \\ \left. \quad + \mathrm{i}\left(\alpha_l^{\pm} - \beta_l^{\pm}\right)\sin(l\theta)\right] \\ \mathrm{e}^{\mathrm{i}\frac{n}{2}\theta}\left[\left(\beta_l^{\pm} + \alpha_l^{\pm}\right)\cos(l\theta) \right. \\ \left. \quad + \mathrm{i}\left(\beta_l^{\pm} - \alpha_l^{\pm}\right)\sin(l\theta)\right] \end{pmatrix}, \tag{3.59}$$

$$\psi^{-}_{|l|^{\pm}}(\theta) = \frac{1}{4\sqrt{\pi(a^2 l^2 + g^2)}} \begin{pmatrix} \mathrm{e}^{-\mathrm{i}\frac{n}{2}\theta}\left[\left(\alpha_l^{\pm} - \beta_l^{\pm}\right)\cos(l\theta) \right. \\ \left. \quad + \mathrm{i}\left(\alpha_l^{\pm} + \beta_l^{\pm}\right)\sin(l\theta)\right] \\ \mathrm{e}^{\mathrm{i}\frac{n}{2}\theta}\left[\left(\beta_l^{\pm} - \alpha_l^{\pm}\right)\cos(l\theta) \right. \\ \left. \quad + \mathrm{i}\left(\beta_l^{\pm} + \alpha_l^{\pm}\right)\sin(l\theta)\right] \end{pmatrix}. \tag{3.60}$$

We present some plots at Figures 3.1 and 3.2 of the energy spectra $E(g)$ as functions of g for some small non-negative values of n and l. In all cases we have set the energy scale at $a = 1$.

We defined the normalisation constant T at (3.30-3.31) as a total Noether charge with reference to the typical fermionic $\mathrm{U}(1)$ current, $J^{\mu} \propto \overline{\psi}\gamma^{\mu}\psi$. In the context of parity, let us consider this entire current proper. Since the time component is the fermion density $\psi^{\dagger}\psi$ which is time-independent for stationary states, the space component $\psi^{\dagger}\gamma^3\psi$ is independent of θ and proportional

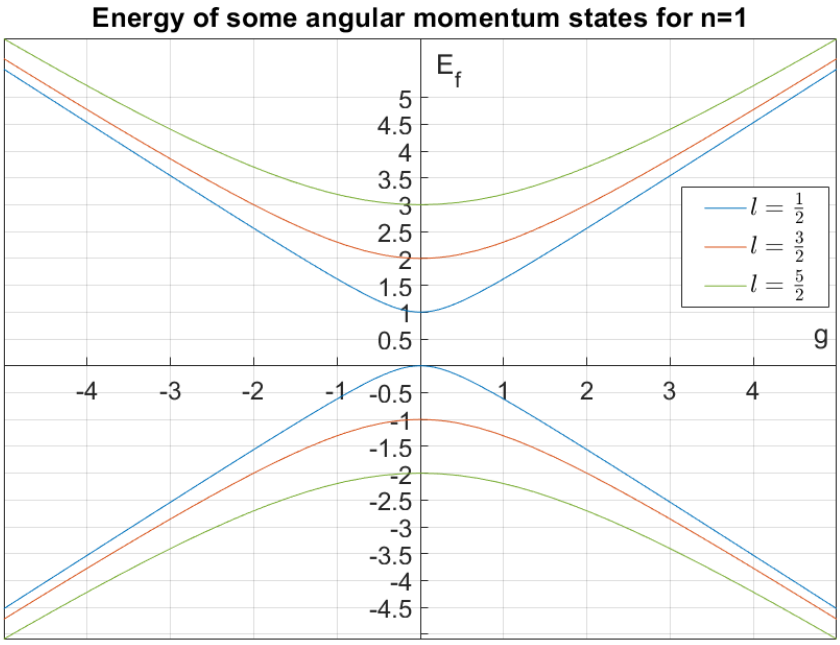

FIGURE 3.1: Plots of the fermion energy spectra $E(g)$ on the $n = 1$ kink for small non-negative values of l. ($a = 1$)

to $|\psi_R|^2 - |\psi_L|^2$. It is convenient to define

$$W = \psi^\dagger \gamma^3 \psi \propto J^\theta, \tag{3.61}$$

and call this the axial charge density of the fermion. Note that for parity solutions, $W = 0$. For angular momentum solutions $\psi_{l,E^\pm}$, we find

$$W = \mp \frac{al}{\sqrt{a^2 l^2 + g^2}} \frac{T}{2\pi\rho}. \tag{3.62}$$

We will later show that this strictly maximises the possible value of W^2 within the given energy level.

Having determined the general dependence of the energy spectrum on n and l, we can comment on the existence of zero-crossing modes. We solve

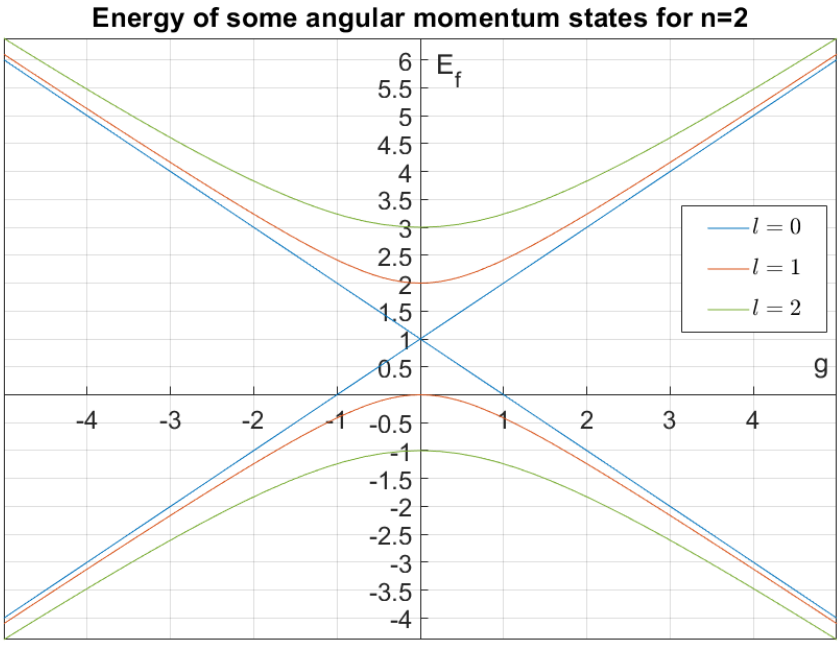

FIGURE 3.2: Plots of the fermion energy spectra $E(g)$ on the $n = 2$ kink for small non-negative values of l. ($a = 1$)

the energy spectrum (3.46) for $E = 0$, obtaining

$$g_*^2 = \frac{a^2 n^2}{4} - a^2 l^2, \tag{3.63}$$

where g_* is the value of the coupling constant which admits a zero-energy solution for the given n and l. Since we require the coupling constant to be real, we see that the existence of zero-crossing modes is controlled by the inequality

$$|2l| \leq |n|. \tag{3.64}$$

When this inequality is strictly satisfied, the fermion solution exhibits zero energy at non-trivial values of the coupling constant, whereas when it is saturated, the fermion goes to zero energy when the coupling constant goes to zero. We observe that zero-crossing modes can only exist if the angular momentum of the fermion is sufficiently low in comparison to the winding

number of the kink.

3.3.3 A numerical perspective

It will be useful to numerically explore soliton-fermion systems where the determination of the spectrum is not so analytically straightforward. To this end, we can also demonstrate numerical solutions to the stationary state equation (3.28) of this model. We use the MATLAB package `bvp4c` which can handle ordinary differential equation boundary value problems with unknown parameters (such as, in our case, the energy eigenvalue $E = E_f$). In order to implement this package, it is necessary to re-write the system in terms of real first order ODEs. We express ψ as

$$\psi = \begin{pmatrix} y_1 + \mathrm{i}y_2 \\ y_3 + \mathrm{i}y_4 \end{pmatrix}, \tag{3.65}$$

with equations of motion:

$$y_1' = \frac{E}{a}y_2 - \frac{g}{a}y_4\cos(n\theta) + \frac{g}{a}y_3\sin(n\theta), \tag{3.66}$$

$$y_2' = -\frac{E}{a}y_1 + \frac{g}{a}y_3\cos(n\theta) + \frac{g}{a}y_4\sin(n\theta), \tag{3.67}$$

$$y_3' = -\frac{E}{a}y_4 + \frac{g}{a}y_2\cos(n\theta) + \frac{g}{a}y_1\sin(n\theta), \tag{3.68}$$

$$y_4' = \frac{E}{a}y_3 - \frac{g}{a}y_1\cos(n\theta) + \frac{g}{a}y_2\sin(n\theta). \tag{3.69}$$

E is treated as a further unknown which `bvp4c` will also attempt to determine, so in total there are five unknown functions. We will need five appropriate boundary conditions on the vector $\boldsymbol{y}(\theta)$, as well as an initial guess of the solution.

This system of ODEs is linear, and the normalisation of the fermion is in principle unimportant. As we have alluded to, however, we will see in the

fully-coupled regime that the choice of normalisation will be physically relevant, and mathematically relevant to solving the equations of motion. It is useful therefore to also numerically implement the normalisation condition now. For simplicity we will set $\rho = 1$ for the entirety of our numerical treatment, so we wish to enforce the integral condition that, for some chosen real constant T,

$$\int_0^{2\pi} \psi^\dagger \psi \, \mathrm{d}\theta = T. \tag{3.70}$$

We achieve this by introducing one more a priori unknown function, y_5, representing the cumulative global fermionic density (formally, a $\mathrm{U}(1)$ charge),

$$y_5(\theta) = \int_0^{\theta} |\psi(\theta')|^2 \, \mathrm{d}\theta'. \tag{3.71}$$

Thus, to the above equations, we add

$$y_5' = y_1^2 + y_2^2 + y_3^2 + y_4^2, \tag{3.72}$$

with the boundary conditions $y_5(0) = 0$ and $y_5(2\pi) = T$. Even though this introduces a further unknown, it provides two natural boundary conditions on the system, so we only require four further boundary conditions; it is natural to impose periodicity of each real component of the fermion in order to provide the correct number. (As above, since E is *a priori* unknown, `bvp4c` requires a sixth boundary condition in addition to one for each ODE.)

For our initial guess to an eigensolution for chosen n and $l^{\pm}$, we use our knowledge of the analytic solutions to choose an approximate energy, and

give a 'solution' which has the correct Fourier modes of the fermion components active, but scaled uniformly,

$$y_1 = \sqrt{\frac{T}{4\pi}} \cos\left(\left(l - \frac{n}{2}\right)\theta\right), \tag{3.73}$$

$$y_2 = \sqrt{\frac{T}{4\pi}} \sin\left(\left(l - \frac{n}{2}\right)\theta\right), \tag{3.74}$$

$$y_3 = \sqrt{\frac{T}{4\pi}} \cos\left(\left(l + \frac{n}{2}\right)\theta\right), \tag{3.75}$$

$$y_4 = \sqrt{\frac{T}{4\pi}} \sin\left(\left(l + \frac{n}{2}\right)\theta\right), \tag{3.76}$$

and uniform charge density for y_5,

$$y_5 = \frac{T\theta}{2\pi}. \tag{3.77}$$

As long as the initial guess of the energy eigenvalue is not too far from the true value, `bvp4c` will typically converge fairly quickly to the correct eigensolution. We display some numerically obtained angular momentum solutions at Figures 3.3 and 3.4; typically, the calculated energy eigenvalue is accurate to approximately one part in 10^9. In Figures 3.5 and 3.6, we plot some numerically determined parity eigenstates along with their local densities, which are non-constant for parity solutions, unlike for angular momentum solutions.

As a numerical tool to explore the structure of the energy spectrum for varying g (which, again, will be useful in more complicated models), we can iterate this process, by using a numerical solution computed at one value of g as the initial guess for the code run at a slightly different value of g. Once again, provided the initial guess of the energy eigenvalue is good, we can iteratively reproduce the analytic spectra to good accuracy; some results are plotted at Figure 3.7.

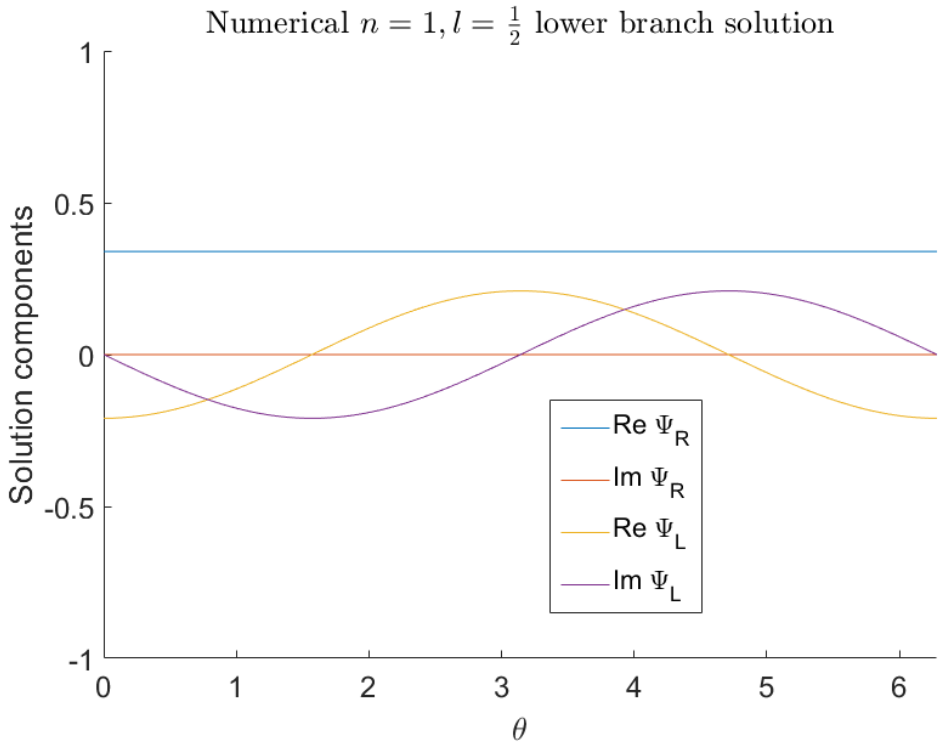

FIGURE 3.3: Numerical solution for the $l = \frac{1}{2}$ eigenfermion of the uniform $n = 1$ kink at $g = 1$. ($T = 1$).

3.4 The fully coupled model

3.4.1 Adding kink dynamics

To introduce kink dynamics to the model, we restore the Dirichlet energy term for the kink into the Lagrangian density, and so now work with the full expression which we previously stated at (3.14):

$$\mathcal{L} = \frac{M^2}{2}\partial_\mu\phi\,\partial^\mu\phi + \overline{\psi}\left(i\hbar\partial\!\!\!/ - ge^{i\gamma^3\phi}\right)\psi. \tag{3.78}$$

The Euler-Lagrange equations for this Lagrangian are the Dirac equation for the fermion,

$$\left(i\hbar\partial\!\!\!/ - ge^{i\gamma^3\phi}\right)\psi = 0, \tag{3.79}$$

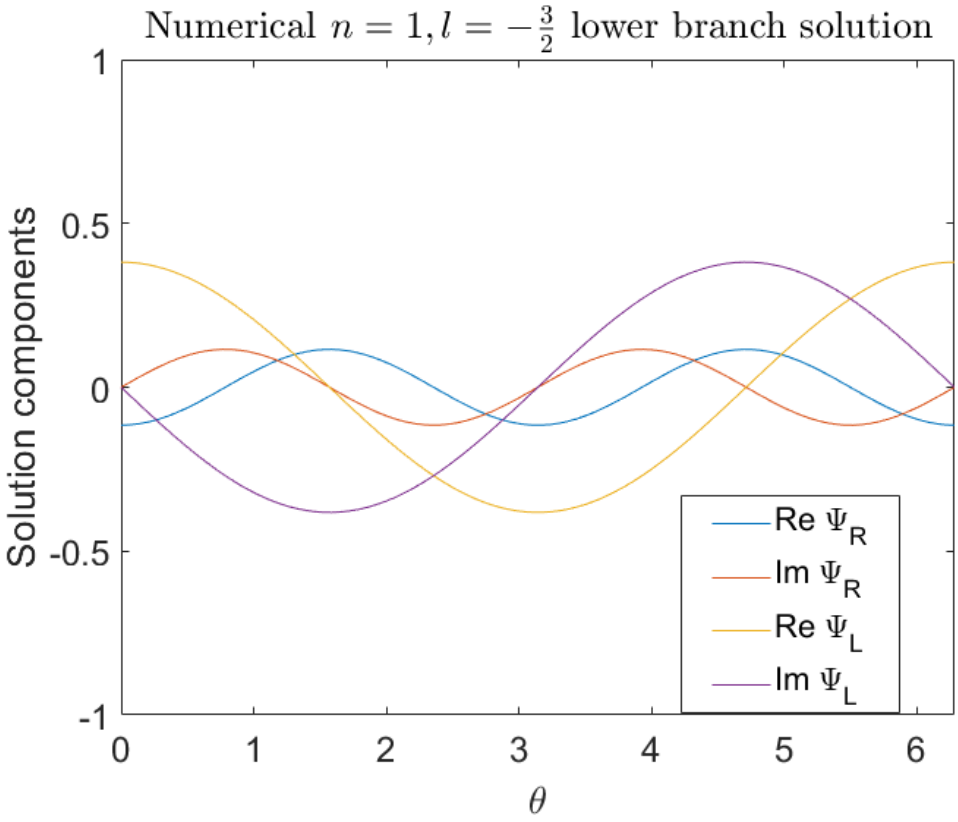

FIGURE 3.4: Numerical solution for the $l = -\frac{3}{2}$ eigenfermion of the uniform $n = 1$ kink at $g = 1$. ($T = 1$).

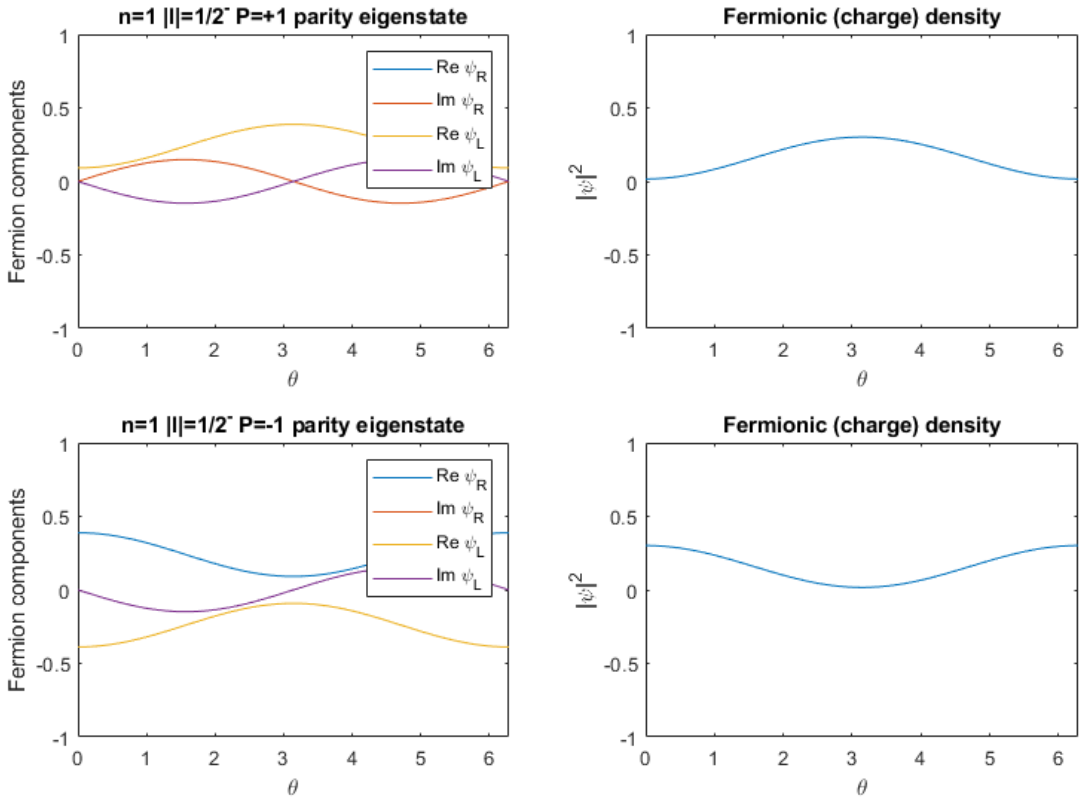

FIGURE 3.5: $|l|^{\pm} = \frac{1}{2}^{-}$ parity eigenstates

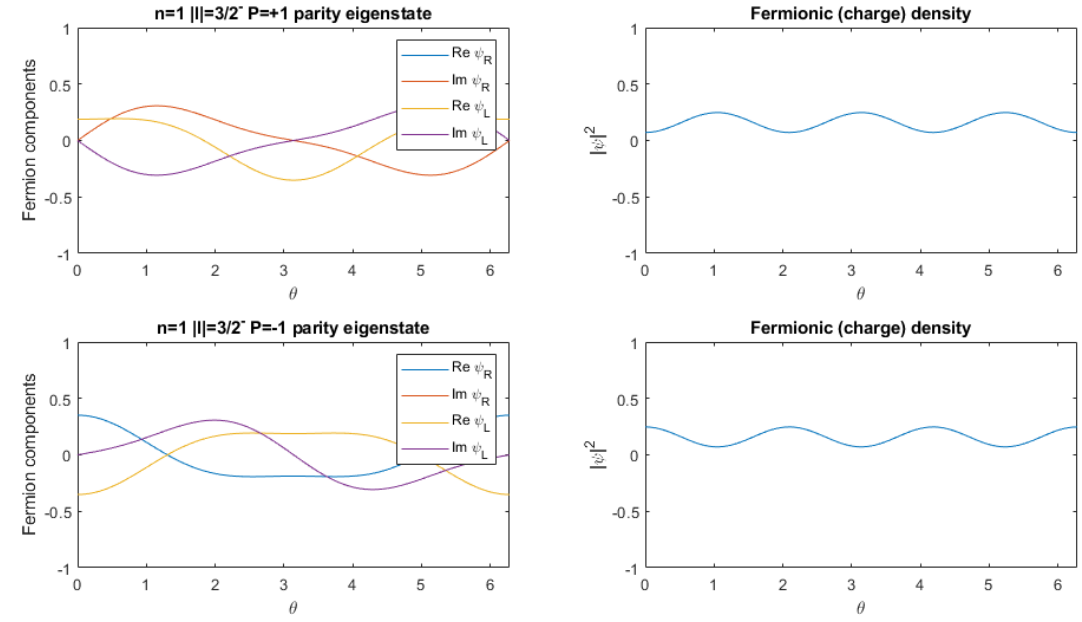

FIGURE 3.6: $|l|^{\pm} = \frac{3}{2}^{-}$ parity eigenstates

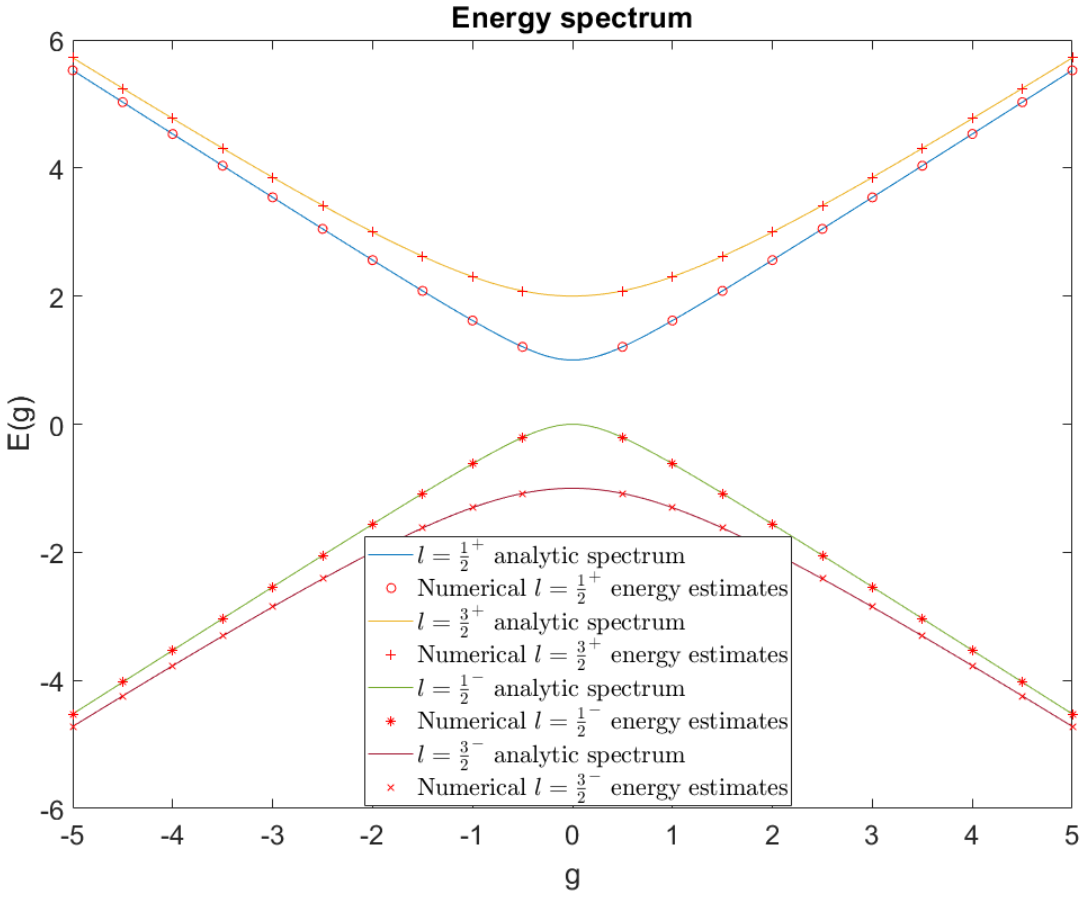

FIGURE 3.7: Some iteratively computed energy eigenvalues for low angular momentum n=1 solutions.

and the fermionic conjugate Dirac equation, as previously, in addition to a new equation of motion for the kink,

$$M^2 \partial_\mu \partial^\mu \phi + \mathrm{i} g \overline{\psi} \gamma^3 \mathrm{e}^{\mathrm{i}\gamma^3 \phi} \psi = 0. \tag{3.80}$$

By taking the Hermitian conjugate and using the anticommutation relations of the γ matrices, we see that this equation is real, as we require for the real kink. For clarity, let us now explicitly write out the d'Alembertian operator $\partial_\mu \partial^\mu$ in coordinates to demonstrate the role of the parameters M, ρ and g. The equation of motion for the kink may be written as

$$M^2 \frac{\partial^2 \phi}{\partial t^2} - \frac{M^2}{\rho^2} \frac{\partial^2 \phi}{\partial \theta^2} + \mathrm{i} g \overline{\psi} \gamma^3 \mathrm{e}^{\mathrm{i}\gamma^3 \phi} \psi = 0. \tag{3.81}$$

Note that we can bound the term involving the fermion (e.g. with the Cauchy-Schwarz inequality) by

$$|\overline{\psi} \gamma^3 \mathrm{e}^{\mathrm{i}\gamma^3 \phi} \psi| \leq |\psi|^2. \tag{3.82}$$

If we assume that $\rho > 1$, and that the maximal value of the fermion density $|\psi|^2$ is of the same order as the average density $\frac{T}{2\pi\rho}$, then we see that in the regime

$$M^2 \gg \rho g T, \tag{3.83}$$

the effect of the fermion on the kink vanishes, so the kink dynamics decouple from the fermion.[1] (Compare to the comments we made at the end of Section 3.2.)

As the Lagrangian density is explicitly independent of θ, the previous generalised angular momentum decouples into two distinct continuous symmetries: translation of the fields on the base space is now a symmetry in its

[1] If $\rho < 1$ then the time-dependence of the kink is more sensitive to the fermion than the space-dependence, but we will not consider this case.

own right, while there is also the internal symmetry of the fields

$$\psi(t,\theta) \mapsto e^{i\gamma^3 \frac{\alpha}{2}} \psi(t,\theta), \quad \phi(t,\theta) \mapsto \phi(t,\theta) - \alpha. \tag{3.84}$$

We refer to this as the axial transformation. The corresponding axial current is

$$J^\mu_{\text{axial}} = M^2 \, \partial^\mu \phi + \frac{\hbar}{2} \overline{\psi} \gamma^\mu \gamma^3 \psi, \tag{3.85}$$

with conservation equation $\partial_\mu J^\mu_{\text{axial}} = 0$, and time-independent total axial charge

$$Q^0_{\text{axial}} = \int_0^{2\pi} \left(M^2 \frac{\partial \phi}{\partial t} + \frac{\hbar}{2} \psi^\dagger \gamma^3 \psi \right) \rho \, \mathrm{d}\theta. \tag{3.86}$$

The Lagrangian also exhibits the following discrete parity symmetry:

$$\psi(t,\theta) \mapsto \gamma^0 \psi(t, 2\pi - \theta), \tag{3.87}$$

$$\phi(t,\theta) \mapsto 2n\pi - \phi(t, 2\pi - \theta). \tag{3.88}$$

The effect of the transformation on the kink is specifically chosen to preserve its overall homotopy class as n, rather than switching it to $-n$. This somewhat arbitrarily enforces that ϕ is a Lorentz pseudoscalar rather than scalar; we will comment further on this matter later. Note that the prescribed uniform kink $\phi(t,\theta) = n\theta$ is invariant under parity, and the parity transform on the system as a whole squares to the identity.

We take the ansatz that the kink is static, i.e. time-independent, and that the fermion is a stationary state, as before. Then the axial charge density W as defined at (3.61) is once again constant. Moreover, the axial current conservation in this static case gives a relationship between the fermionic charge density and the non-trivial behaviour of the kink:

$$\partial_\mu J^\mu_{\text{axial}} = -\frac{M^2}{\rho^2} \frac{\partial^2 \phi}{\partial \theta^2} - \frac{\hbar}{2\rho} \frac{\partial |\psi|^2}{\partial \theta} = 0. \tag{3.89}$$

Integrating twice, we fix the constants of integration by knowing the overall normalisation of the fermion and the homotopy class of the kink, to obtain:

$$|\psi|^2 = \frac{T}{2\pi\rho} + \frac{2M^2}{\hbar\rho}\left(n - \frac{\partial\phi}{\partial\theta}\right) \tag{3.90}$$

Writing the kink as

$$\phi(\theta) = n\theta + \eta(\theta), \tag{3.91}$$

the above becomes

$$|\psi|^2 = \frac{T}{2\pi\rho} - \frac{2M^2}{\hbar\rho}\frac{\partial\eta}{\partial\theta}. \tag{3.92}$$

Thus the fermion density only deviates from the mean by the derivative of the non-trivial behaviour of the kink, where by "trivial" behaviour we mean the uniform winding for its homotopy class. We will frequently refer to the function $\eta(\theta)$ defined here as the kink's *wobble*.

It is straightforward to check that any pair of fields (ϕ, ψ) of the form

$$(\phi(t,\theta) = n\theta, \psi(t,\theta) = \psi_{l,E^\pm}(t,\theta)) \tag{3.93}$$

solves all the equations of motion for the fully coupled model. This is a consequence of the *principle of symmetric criticality* [43, 50]. This principle states that if we have a field theory where we may impose a symmetry reduction, then under appropriate conditions, solutions of the symmetry reduction are in fact solutions of the full theory. One example of an appropriate condition is that the symmetry transformation is the action of a compact Lie group. This is precisely what we did in prescribing the kink to be uniform and then seeking angular momentum eigenfermion solutions in Section 3.3: we essentially restricted to a diagonal subgroup of the translation and axial symmetries of the fully coupled model, reducing over a factor of $U(1)$.

However, the fermionic parity solutions $\psi^P_{|l|,E^\pm}$ have non-constant local

density, so they do not remain solutions when paired with a uniformly winding kink $\psi(t,\theta) = n\theta$ because this violates the axial current conservation. (Of course, they specifically violate the reduced general angular momentum symmetry, so there is no reason to expect they would persist alongside the angular momentum solutions.)

3.4.2 Initial numerical treatment of the fully coupled model

To search for new static solutions to the system with non-zero wobble, we introduce the kink and its derivative as further unknown functions to our `bvp4c` code. Writing y_5 for ϕ and y_6 for $\frac{\partial\phi}{\partial\theta}$, and changing the label of the cumulative fermionic charge to y_7, we have a system of first order ODEs as follows:

$$y_1' = \frac{E}{a}y_2 - \frac{g}{a}y_4\cos(y_5) + \frac{g}{a}y_3\sin(y_5), \tag{3.94}$$

$$y_2' = -\frac{E}{a}y_1 + \frac{g}{a}y_3\cos(y_5) + \frac{g}{a}y_4\sin(y_5), \tag{3.95}$$

$$y_3' = -\frac{E}{a}y_4 + \frac{g}{a}y_2\cos(y_5) + \frac{g}{a}y_1\sin(y_5), \tag{3.96}$$

$$y_4' = \frac{E}{a}y_3 - \frac{g}{a}y_1\cos(y_5) + \frac{g}{a}y_2\sin(y_5), \tag{3.97}$$

$$y_5' = y_6, \tag{3.98}$$

$$y_6' = \frac{2g\rho}{M^2}\left[(y_1y_4 - y_2y_3)\cos(y_5) - (y_1y_3 + y_2y_4)\sin(y_5)\right], \tag{3.99}$$

$$y_7' = y_1^2 + y_2^2 + y_3^2 + y_4^2. \tag{3.100}$$

Including E, we have eight unknowns. We take the following boundary conditions:

$$y_1(0) = y_1(2\pi),\ y_2(0) = 0,\ y_3(0) = y_3(2\pi),\ y_4(0) = y_4(2\pi),$$
$$y_5(0) = 0,\ y_5(2\pi) = 2n\pi,\ y_7(0) = 0,\ y_7(2\pi) = T.$$

Observe that we can use the overall phase symmetry to make the right-handed fermion component (say) real at the origin, and to fix the initial value of the kink to 0 there also; we make the other fermion modes periodic, give the kink the correct homotopy class, and implement y_7 as the cumulative fermion charge density. Although we have not explicitly enforced that y_2 be periodic, we have found in practice that the periodicity boundary conditions on the other components suffice for `bvp4c` to converge to a solution also periodic in y_2, and we find the condition $\psi_R(0) \in \mathbb{R}$ to be more useful to compare and interpret results.

Similarly to the case of the uniform kink, we use the Fourier components of the previously known solutions as a template for our initial guess. Recalling that the current conservation law tells us that a non-zero wobble on the kink requires a non-uniform density profile for the fermion, we tweak these Fourier modes by multiplying them by a non-constant envelope function, for which we use a cubic polynomial in θ with roots at 0, π and 2π. The overall amplitude of this cubic is a parameter that we can vary for different initial guesses. We also add a small relative axial phase between the chiral components of the fermion, the magnitude of which is also a variable parameter.

It is straightforward to check that our previously known angular momentum eigensolutions paired with a uniform kink remain solutions to our more general static system. These solutions are easily recreated by the broader numerical process by taking the perturbation parameters to be extremely small or zero; see examples at Figure 3.8 and Figure 3.9.

We also found new solutions, with non-zero wobbles. To broad inspection, the wobbles appear to be simple trigonometric functions, and the numerical results demonstrate very little relative axial phase between the chiral components of the fermion in the most part. The number of nodes on the wobble persist, while their amplitude varies, with varying g. Examples follow in Figures 3.10-3.12. We compare these new fermionic solutions with our

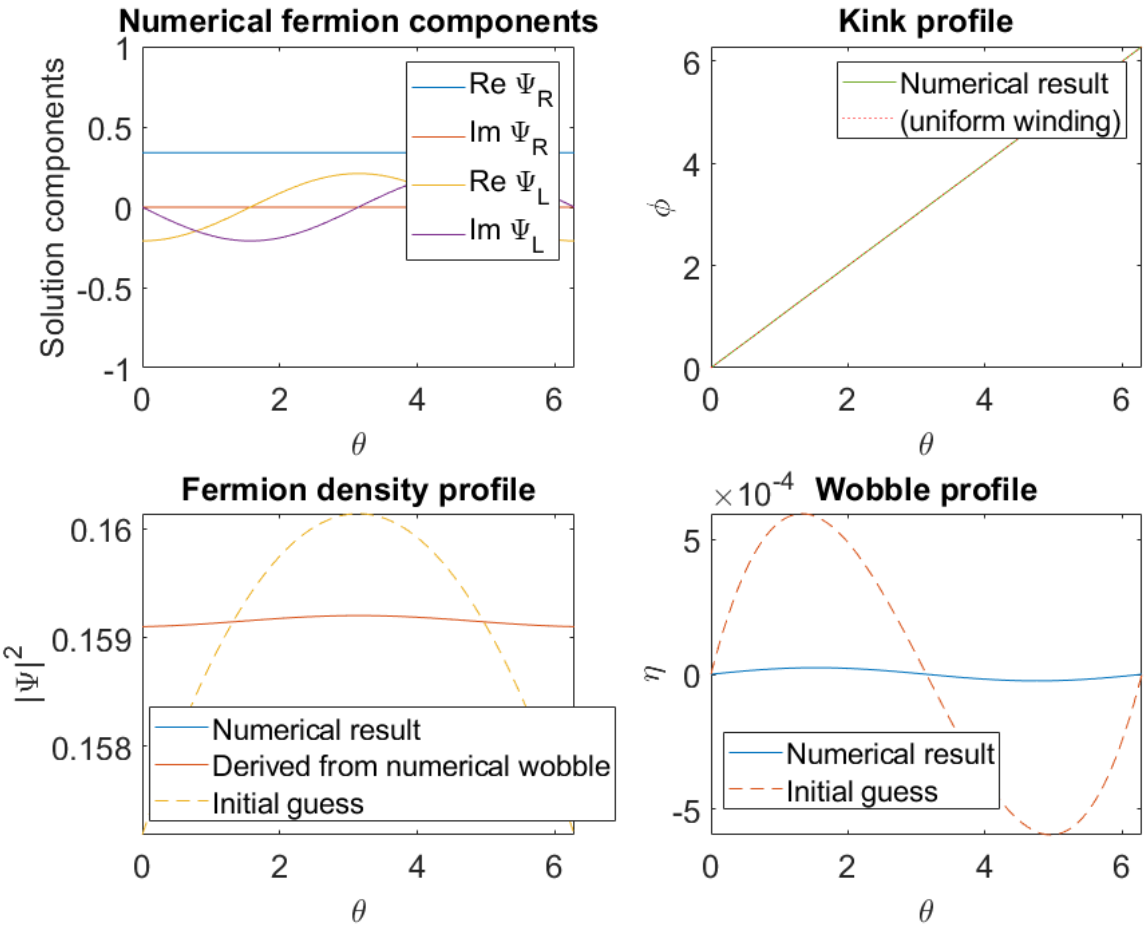

FIGURE 3.8: The $n = 1\, l = \frac{1}{2}$ (lower energy branch) eigensolution in the static system, generated numerically. The lower left figure compares the fermion density computed two different ways. In blue is plotted the total amplitude summed from the real and imaginary components appearing in the upper left, while in orange is plotted the result calculated by substituting the numerical wobble plotted in the lower right to the axial current conservation equation. The blue and orange curves overlap almost perfectly at the resolution plotted.

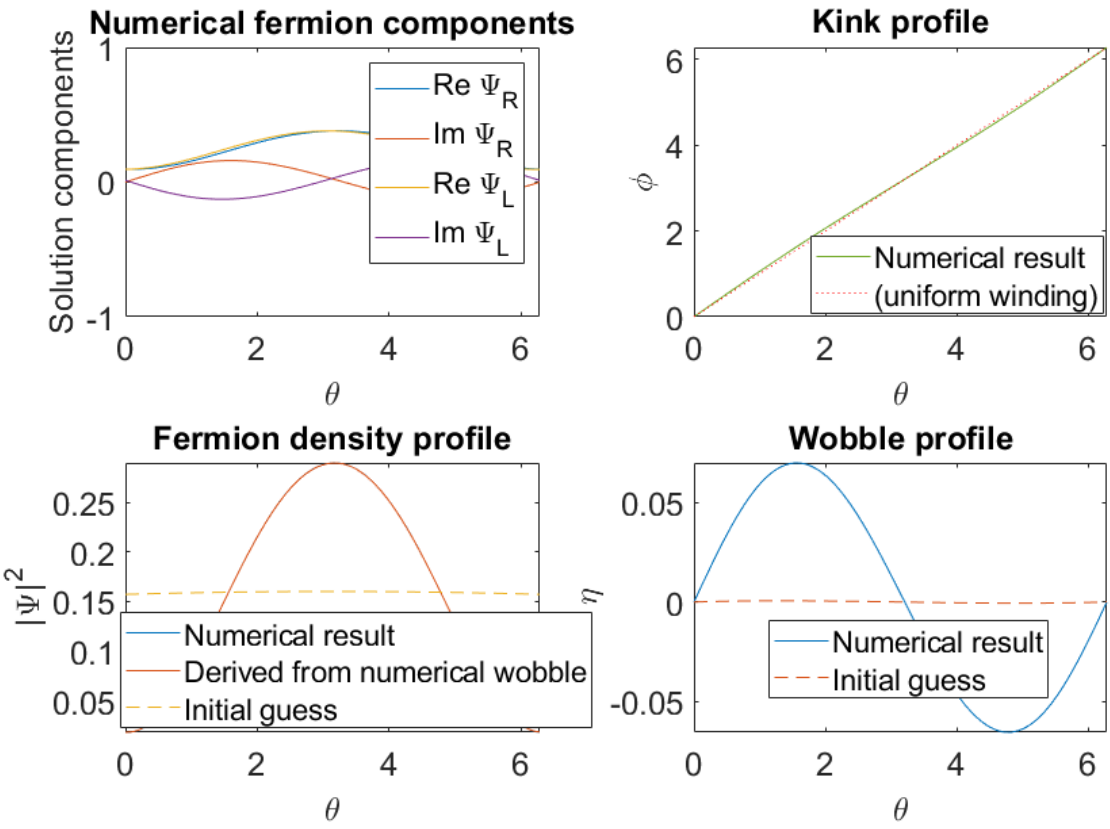

FIGURE 3.9: The $n = 1\, l = \frac{3}{2}$ (lower energy branch) eigensolution in the static system, generated numerically. The lower left figure compares the fermion density computed two different ways. In blue is plotted the total amplitude summed from the real and imaginary components appearing in the upper left, while in orange is plotted the result calculated by substituting the numerical wobble plotted in the lower right to the axial current conservation equation. The blue and orange curves overlap almost perfectly at the resolution plotted.

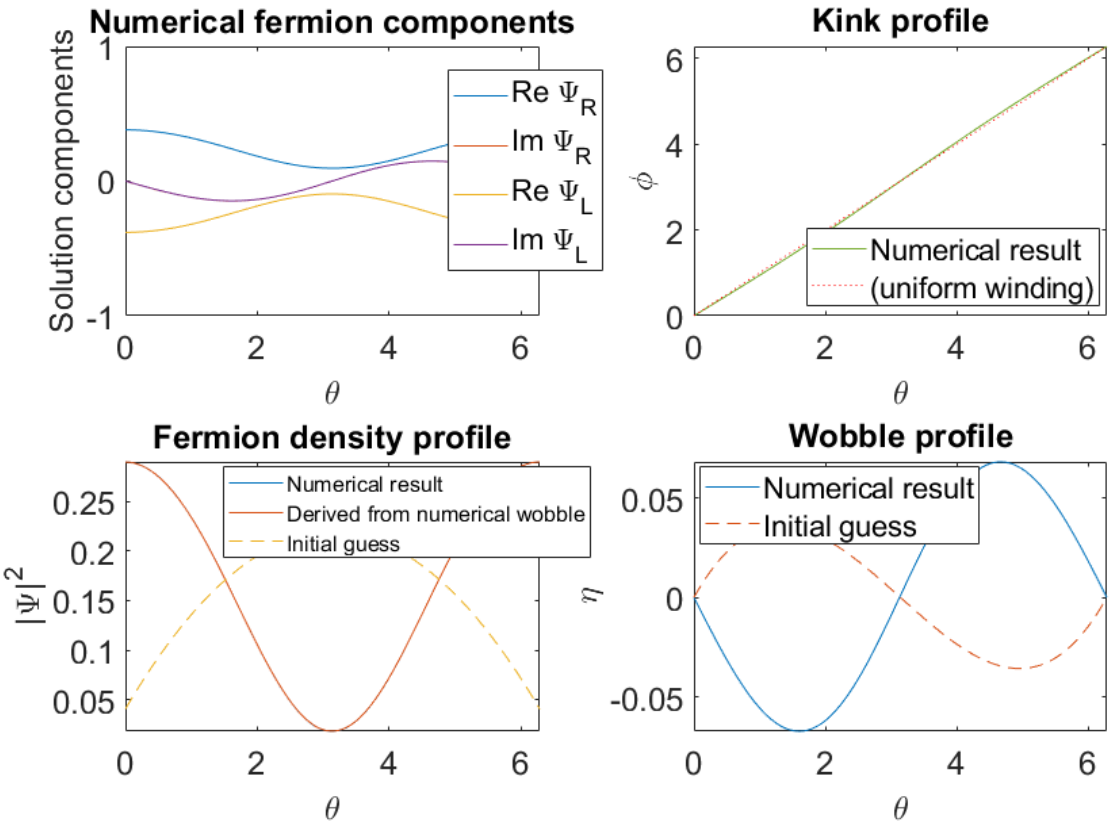

FIGURE 3.10: A non-trivial static solution with one-node wobble, at $g = 1$. The lower left figure compares the fermion density computed two different ways. In blue is plotted the total amplitude summed from the real and imaginary components appearing in the upper left, while in orange is plotted the result calculated by substituting the numerical wobble plotted in the lower right to the axial current conservation equation. The blue and orange curves overlap almost perfectly at the resolution plotted.

earlier plots of definite-parity solutions in the special case. From the similarity in the shapes of the profiles in the upper left plots of the real and imaginary components, it seems plausible by inspection that these new solutions have definite parity, i.e. that the solutions are preserved up to sign under the application of the discrete parity transformation given at (3.87-3.88). We have not yet tried to adapt our numerical approach to explicitly enforce parity, but we discuss this in our outlook.

The energy eigenvalue of a $2l$-node wobble appears to track closely to the

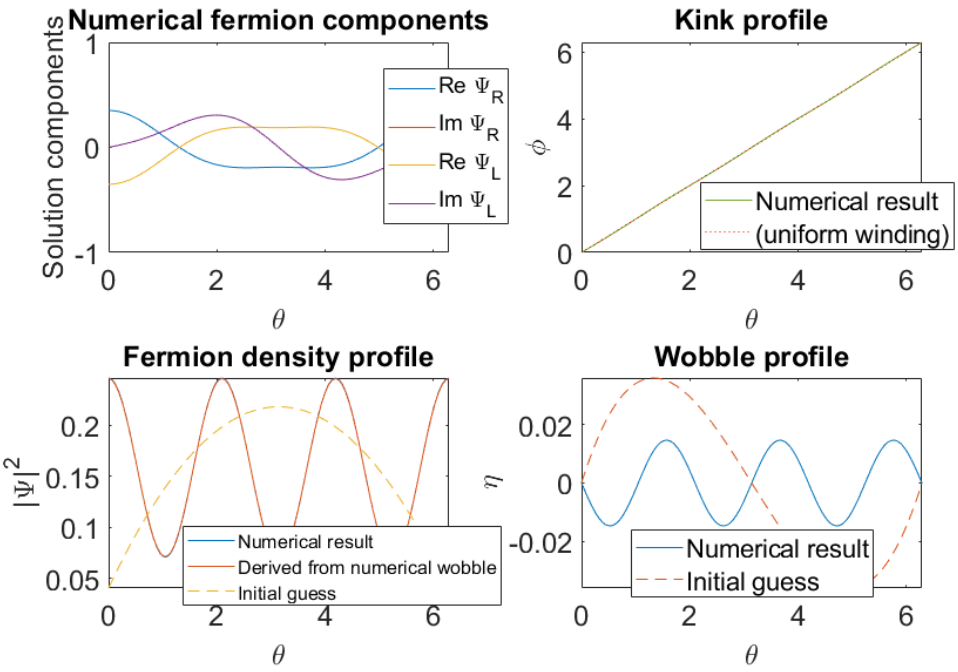

FIGURE 3.11: A non-trivial static solution with three-node wobble, at $g = 1$. The lower left figure compares the fermion density computed two different ways. In blue is plotted the total amplitude summed from the real and imaginary components appearing in the upper left, while in orange is plotted the result calculated by substituting the numerical wobble plotted in the lower right to the axial current conservation equation. The blue and orange curves overlap almost perfectly at the resolution plotted.

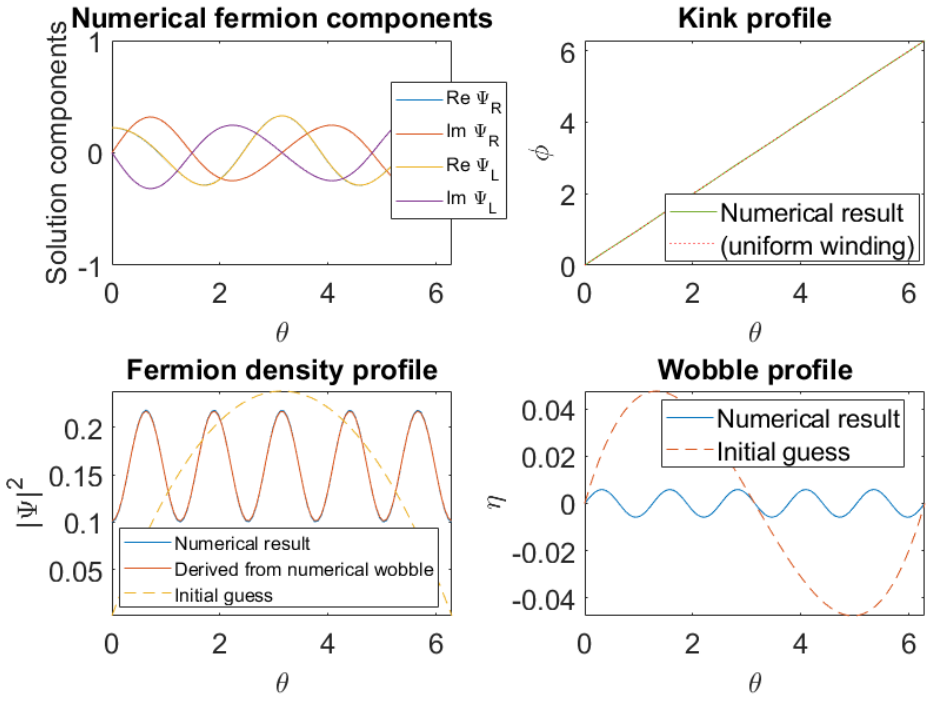

FIGURE 3.12: A non-trivial static solution with five-node wobble, at $g = 1$. The lower left figure compares the fermion density computed two different ways. In blue is plotted the total amplitude summed from the real and imaginary components appearing in the upper left, while in orange is plotted the result calculated by substituting the numerical wobble plotted in the lower right to the axial current conservation equation. The blue and orange curves overlap almost perfectly at the resolution plotted.

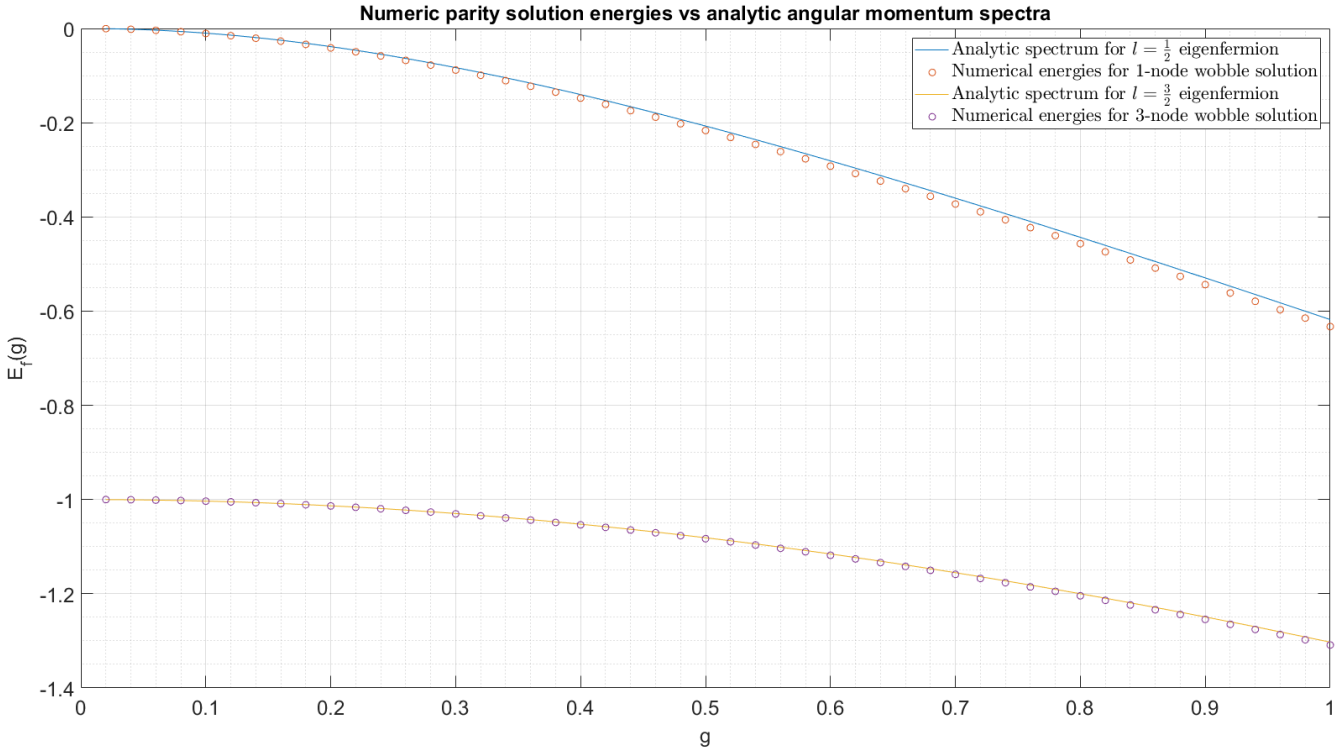

FIGURE 3.13: Energy eigenvalues of nontrivial solutions, $0.02 \leq g \leq 1$

known spectrum of the angular momentum $|l|$ eigenstates on the uniform kink, with greater divergence at greater $|g|$: see Figures 3.13 and 3.14.

Remark 3.1. We are grateful to Nick Manton for a stimulating conversation wherein he pointed out an oddity in these results. All of our parameters such as a, g, T, and so on, are of order 1 in these examples, and yet both the order of the kink wobble, and the effect on the energy, appear to be much smaller. The author believes this arises because of the inherent interval length of 2π that we have chosen by modelling this system on a circle of radius 1: it may be that this introduces a power of $\frac{1}{2\pi}$ into our calculated quantities. This is something we hope to explore in future work.

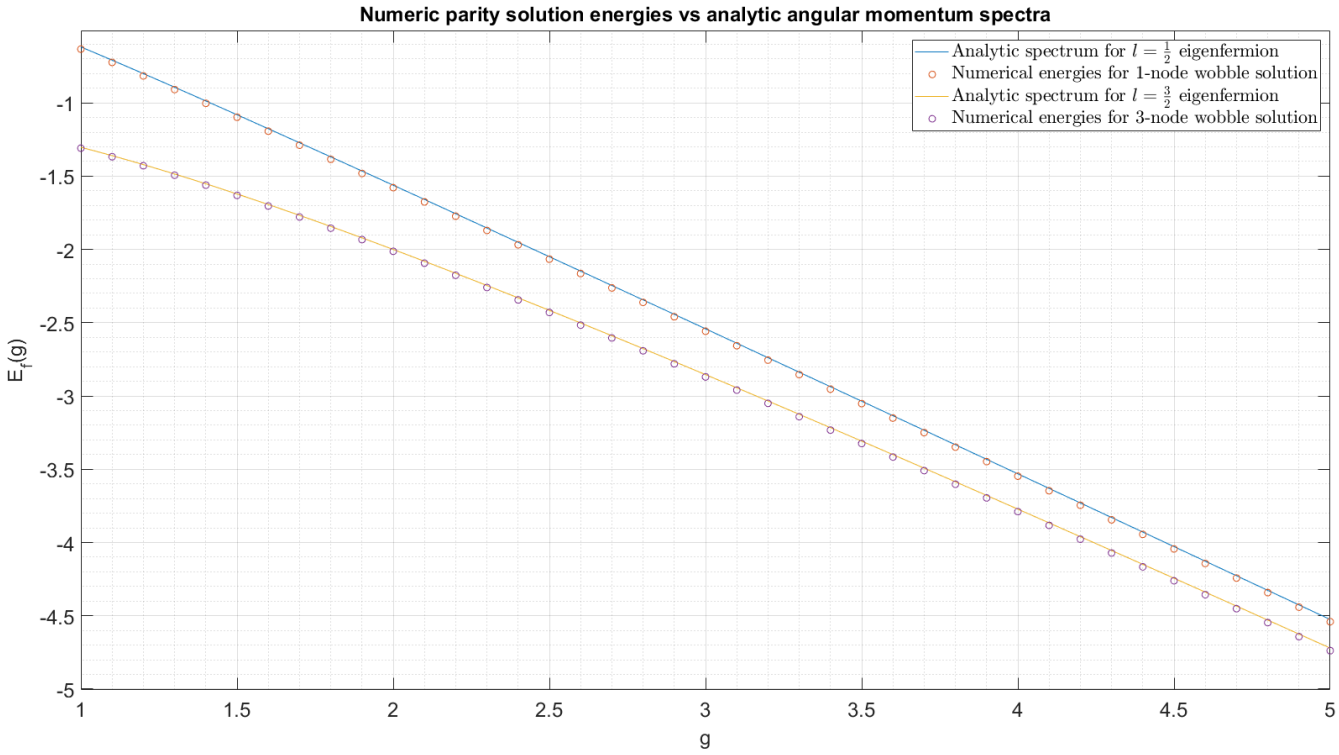

FIGURE 3.14: Energy eigenvalues of nontrivial solutions, $1 \leq g \leq 5$

3.5 Bispinor coordinates and static solutions

3.5.1 The $XYZW$ picture

We observe that the role of the kink in the coupling term $-g\overline{\psi}\mathrm{e}^{\mathrm{i}\gamma^3\phi}\psi$ appears to act like a local change of basis for the inner product of the fermion with itself. However, it is not a gauge connection: note that since (in the chiral representation) the matrix $\mathrm{e}^{\mathrm{i}\gamma^3\phi}$ is diagonal, it cannot be written as $\gamma^\mu A_\mu$ for some gauge connection A_μ. Nonetheless, we can learn something by absorbing this feature of the kink into the fermion, as follows.

Let us change variables to a new fermion field $\xi(x^\mu)$ given by

$$\xi(x^\mu) = \mathrm{e}^{\mathrm{i}\gamma^3 K(x^\mu)}\psi(x^\mu), \tag{3.101}$$

for some as yet unspecified function of spacetime $K(x^\mu)$. In the new coordinates, the fermionic part of the Lagrangian is

$$\mathcal{L}_f = \overline{\xi}\left(\mathrm{i}\hbar\partial\!\!\!/ - \hbar(\partial\!\!\!/ K)\gamma^3 - g\mathrm{e}^{\mathrm{i}\gamma^3(\phi+2K)}\right)\xi. \tag{3.102}$$

If we now take, for example, $K = -\frac{\phi}{2}$, the explicit appearance of the kink is removed from the Lagrangian, and we are left with

$$\mathcal{L} = \frac{M^2}{2}\partial_\mu\phi\partial^\mu\phi + \overline{\xi}\left(\mathrm{i}\hbar\partial\!\!\!/ + \frac{\hbar}{2}(\partial\!\!\!/\phi)\gamma^3 - g\right)\xi. \tag{3.103}$$

In these coordinates, the coupling constant g now appears as a mass term for the new fermion field ξ, and the kink itself does not explicitly appear, but we have introduced a coupling between the fermion and the derivative of the kink field.

Strictly speaking, the change of variables as written gives the new fermion ξ either periodic or antiperiodic boundary conditions, according to $\xi(t, \theta + 2\pi) = (-1)^n\xi(t,\theta)$. However, in the case of odd n, we could instead choose

to define e.g. $K = -\frac{\phi}{2} + n\pi$ to restore truly periodic boundary conditions to ξ while preserving the new form of the Lagrangian. It is straightforward to check that ξ still transforms as a Dirac spinor under parity in either case: $\hat{P}\xi(t,\theta) = \gamma^0\xi(t, 2\pi - \theta)$.

In a sense, the kink derivative now resembles a gauge connection even further: we could write the first two fermionic terms as $\overline{\xi}i\hbar\gamma^\mu(\partial_\mu + A_\mu)\xi$ where $A_\mu = -\frac{i}{2}\gamma^3\partial_\mu\phi = -\frac{i}{2}\hat{\varepsilon}^\nu{}_\mu\partial_\nu\phi$. However, recall that parity symmetry requires that ϕ is a pseudoscalar rather than scalar field, so this "gauge potential" A_μ would be a Lorentz pseudovector rather than vector. Moreover, even if the original coupling were not chiral (so γ^3 would not appear, and ϕ could be a true scalar field), the kinetic term for the kink would be a mass term for the gauge connection, $\frac{M^2}{2}A_\mu A^\mu$, rather than the typical Lagrangian contribution from the field strength $\sim F_{\mu\nu}F^{\mu\nu}$. As written, this would be a system with a zero-energy gauge field and where the gauge symmetry is explicitly broken by the kink activity, which would be interpreted as a mass for the gauge field.

The $U(1)$ phase action is unchanged from the previous coordinates, and the expression for the phase current retains the same form:

$$J^\mu = \hbar\overline{\psi}\gamma^\mu\psi = \hbar\overline{\xi}\gamma^\mu\xi. \tag{3.104}$$

We see that the new fermion ξ is in fact invariant under the axial transformation; in the new coordinates, then, that axial transformation is simply the internal translation of the kink. Concordantly, the axial current conservation equation is simply the Euler-Lagrange equation for ϕ derived from the new

Lagrangian:

$$0 = \partial_\mu \left(\frac{\partial L}{\partial(\partial_\mu \phi)} \right) = \partial_\mu J^\mu_{\text{axial}} \tag{3.105}$$

$$= \partial_\mu \left(M^2 \partial^\mu \phi + \frac{\hbar}{2} \overline{\xi} \gamma^\mu \gamma^3 \xi \right) \tag{3.106}$$

$$= \partial_\mu \left(M^2 \partial^\mu \phi + \frac{1}{2} \hat{\varepsilon}^\mu{}_\nu J^\nu \right). \tag{3.107}$$

Now consider the Lorentz covariant bispinors we can form using ξ. We have already seen that the phase current is such a Lorentz vector, $J^\mu = \hbar \overline{\xi} \gamma^\mu \xi$. Define variables X and W from its components according to $J^\mu = (\hbar X, -aW)$, so

$$X = \overline{\xi} \gamma^t \xi = \xi^\dagger \xi = \psi^\dagger \psi, \tag{3.108}$$

$$W = -\rho \overline{\xi} \gamma^\theta \xi = \xi^\dagger \gamma^3 \xi = \psi^\dagger \gamma^3 \psi. \tag{3.109}$$

Note that X and W are both real; moreover X is non-negative. Furthermore, X is the fermionic (phase charge) density, while W is the fermionic contribution to the axial charge density. X is invariant under parity, but W picks up a minus sign under a parity transformation: explicitly, $\hat{P} W(t, \theta) = -W(t, -\theta)$. There are two more real bispinors Y and Z we can form, defined as

$$Y = \overline{\xi} \xi = \xi^\dagger \gamma^0 \xi = \psi^\dagger \gamma^0 \mathrm{e}^{\mathrm{i} \gamma^3 \phi} \psi, \tag{3.110}$$

$$Z = \mathrm{i} \overline{\xi} \gamma^3 \xi = \mathrm{i} \xi^\dagger \gamma^1 \xi = \mathrm{i} \psi^\dagger \gamma^1 \mathrm{e}^{\mathrm{i} \gamma^3 \phi} \psi. \tag{3.111}$$

Again, Y is invariant under parity, while Z picks up a minus sign. (Here, Y is a true Lorentz scalar, while Z is pseudoscalar.)

Any other bispinor can be expressed in terms of these four real coordinates: note, for example, that if we construct the rank two Lorentz tensor

$V^{\mu\nu} = \overline{\xi}\gamma^\mu\gamma^\nu\xi$, we find

$$V^{\mu\nu} = \overline{\xi}\gamma^\mu\gamma^\nu\xi = \overline{\xi}\left(g^{\mu\nu} - \hat{\varepsilon}^{\mu\nu}\gamma^3\right)\xi = g^{\mu\nu}Y + \mathrm{i}\hat{\varepsilon}^{\mu\nu}Z. \tag{3.112}$$

It may be worth noting that since $g^{\mu\nu}$ and $\hat{\varepsilon}^{\mu\nu}$ are themselves invariant under Lorentz transforms, this tensor $V^{\mu\nu}$ is actually a complex Lorentz-invariant grade 2 multivector, sent to its complex conjugate under the parity transformation.

Many of the dynamical features of the kink-fermion system can be captured using these coordinates X, Y, Z and W, without reference to the underlying fermion ξ (or ψ). A key observation is that all possible evolutions of the system (not just classical solutions) take place on a three-dimensional cone in this $XYZW$ picture:

$$X^2 - W^2 - Y^2 - Z^2 = 0. \tag{3.113}$$

This is most easily demonstrated by passing to polar coordinates for the original complex components of ψ: writing

$$\psi(t,\theta) = \begin{pmatrix} R(t,\theta)\mathrm{e}^{\mathrm{i}\mu(t,\theta)} \\ L(t,\theta)\mathrm{e}^{\mathrm{i}\nu(t,\theta)} \end{pmatrix}, \tag{3.114}$$

with μ, ν periodic real functions and R, L non-negative real functions, it is easily seen that

$$X = R^2 + L^2, \tag{3.115}$$

$$W = R^2 - L^2, \tag{3.116}$$

$$Y = 2RL\cos(\phi + \mu - \nu), \tag{3.117}$$

$$Z = -2RL\sin(\phi + \mu - \nu), \tag{3.118}$$

from which (3.113) follows. This can be expressed in a manifestly Lorentz-invariant form: note that

$$J^\mu J_\mu = \hbar^2 (X^2 - W^2), \tag{3.119}$$

while, defining $V^{\mu\nu}$ as above at (3.112),

$$V^{\mu\nu} V_{\mu\nu} = 2(Y^2 + Z^2). \tag{3.120}$$

Thus the equation of the cone (3.113) can be expressed

$$\frac{J^\mu J_\mu}{\hbar^2} = \frac{1}{2} V^{\mu\nu} V_{\mu\nu}. \tag{3.121}$$

We stress that this does not require imposing the equations of motion: it is a consequence of Lorentz covariance alone.

Let us express the conservation laws for classical solutions in the $XYZW$ picture. We see that the global $\mathrm{U}(1)$ current conservation equation, $\partial_\mu J^\mu = 0$, takes the form

$$\hbar \left(\frac{\partial X}{\partial t} - \frac{1}{\rho} \frac{\partial W}{\partial \theta} \right) = 0. \tag{3.122}$$

The axial current conservation equation, $\partial_\mu J^\mu_{\text{axial}} = 0$, is expressed as

$$\hbar \left(\frac{\partial W}{\partial t} - \frac{1}{\rho} \frac{\partial X}{\partial \theta} \right) = -2M^2 \partial_\mu \partial^\mu \phi. \tag{3.123}$$

By comparison with the global $\mathrm{U}(1)$ current conservation, we see that we can write the left-hand side of (3.123) as $\hat{\varepsilon}^\mu{}_\nu \partial_\mu J^\nu$. This can be a convenient way to write both conservation laws in terms of the global $\mathrm{U}(1)$ current J^μ.

The Dirac equations for ξ and $\overline{\xi}$ are

$$\mathrm{i}\hbar \not{\partial} \xi + \frac{\hbar}{2}(\not{\partial}\phi)\gamma^3 \xi - g\xi = 0, \tag{3.124}$$

$$\mathrm{i}\hbar \overline{\xi} \not{\partial} + \frac{\hbar}{2}\overline{\xi}\gamma^3(\not{\partial}\phi) + g\overline{\xi} = 0. \tag{3.125}$$

These provide two further Lorentz-covariant equations of motion by contracting spinors and summing appropriately: one for each combination of derivatives of X and W seen above in the current conservation equations. The $\left(\frac{\partial X}{\partial t}, \frac{\partial W}{\partial \theta}\right)$ equation is equivalent to the phase current conservation equation $\partial_\mu J^\mu = 0$. For $\left(\frac{\partial W}{\partial t}, \frac{\partial X}{\partial \theta}\right)$ we obtain

$$\partial_\mu \hat{\varepsilon}^\mu{}_\nu J^\nu = \hbar\left(\frac{\partial W}{\partial t} - \frac{1}{\rho}\frac{\partial X}{\partial \theta}\right) = 2gZ, \tag{3.126}$$

which by comparison with axial current conservation tells us

$$-M^2 \partial^\mu \partial_\mu \phi = gZ. \tag{3.127}$$

Derivatives of Y and Z do not arise in such a neat (fermion-independent) manner, because for example the contraction needed to isolate $\frac{\partial Y}{\partial t}$ introduces the combination $\frac{\partial \overline{\xi}}{\partial \theta}\gamma^3 \xi - \overline{\xi}\gamma^3 \frac{\partial \xi}{\partial \theta}$, which is not directly expressible in terms of Z only. In total, the remaining four equations we can derive from the Dirac equations are:

$$\hbar \frac{\partial Y}{\partial t} = \hbar \frac{\partial \phi}{\partial t} Z - a\left[\frac{\partial \overline{\xi}}{\partial \theta}\gamma^3 \xi - \overline{\xi}\gamma^3 \frac{\partial \xi}{\partial \theta}\right], \tag{3.128}$$

$$a \frac{\partial Y}{\partial \theta} = a \frac{\partial \phi}{\partial \theta} Z - \hbar\left[\frac{\partial \overline{\xi}}{\partial t}\gamma^3 \xi - \overline{\xi}\gamma^3 \frac{\partial \xi}{\partial t}\right], \tag{3.129}$$

$$\hbar \frac{\partial Z}{\partial t} = -\hbar \frac{\partial \phi}{\partial t} Y - 2gW - \mathrm{i}a\left[\frac{\partial \overline{\xi}}{\partial \theta}\xi - \overline{\xi}\frac{\partial \xi}{\partial \theta}\right], \tag{3.130}$$

$$a \frac{\partial Z}{\partial \theta} = -a \frac{\partial \phi}{\partial \theta} Y - 2gX - \mathrm{i}\hbar\left[\frac{\partial \overline{\xi}}{\partial t}\xi - \overline{\xi}\frac{\partial \xi}{\partial t}\right]. \tag{3.131}$$

We determined these by expanding the left hand side according to e.g.

$$\hbar \frac{\partial Y}{\partial t} = -\mathrm{i}\overline{\xi}\left(\mathrm{i}\hbar \frac{\partial \xi}{\partial t}\right) - \mathrm{i}\left(\mathrm{i}\hbar \frac{\partial \overline{\xi}}{\partial t}\right)\xi, \tag{3.132}$$

and comparing this to the expressions obtained by e.g. contracting (3.124) with $-\mathrm{i}\overline{\xi}$ from the left and contracting (3.125) with $-\mathrm{i}\xi$ from the right.

3.5.2 Static kinks and stationary state fermions

We will not discuss here the general dynamics in terms of the $XYZW$ picture. Instead we will focus on the same ansätze as we did before in the special case:

$$\phi(t,\theta) = \phi(\theta) \text{ only}, \quad \psi(t,\theta) = \mathrm{e}^{-\frac{\mathrm{i}}{\hbar}E_f t}\psi(\theta). \tag{3.133}$$

The system will vastly simplify. To abbreviate this "*S*tatic kink and *S*tationary *S*tate fermion" ansatz, we will refer to it as the *3S* ansatz. Immediately, $\frac{\partial X}{\partial t}$ and $\frac{\partial W}{\partial t}$ vanish. Thus by (3.122), W is uniformly constant in both t and θ. Z is now directly proportional to $\frac{\partial X}{\partial \theta}$, as well as acting as a source for ϕ. Moreover, time-dependence for Y and Z can only possibly arise from the kink, so $\frac{\partial Y}{\partial t}$ and $\frac{\partial Z}{\partial t}$ also vanish. We are left with the much simpler system of ODEs:

$$-a\frac{\partial X}{\partial \theta} = \frac{2M^2}{\rho^2}\frac{\partial^2 \phi}{\partial \theta^2} = 2gZ, \tag{3.134}$$

$$a\frac{\partial Y}{\partial \theta} = \left(a\frac{\partial \phi}{\partial \theta} - 2E_f\right)Z, \tag{3.135}$$

$$a\frac{\partial Z}{\partial \theta} = \left(-a\frac{\partial \phi}{\partial \theta} + 2E_f\right)Y - 2gX. \tag{3.136}$$

Recall the definition of the total fermionic (phase charge) density (per unit radius of the spatial circle), T, as

$$T = \int_0^{2\pi} X(\theta)\,\rho\,\mathrm{d}\theta. \tag{3.137}$$

Then, we can integrate the first equation at (3.134) and use the known winding number n of the kink to write

$$\frac{\partial \phi}{\partial \theta} = n + \frac{\hbar \rho}{2M^2}\left(\frac{T}{2\pi\rho} - X(\theta)\right). \tag{3.138}$$

It is useful now to define two new constants:

$$\lambda = \frac{\hbar\rho}{2M^2}; \quad E' = E_f - \frac{a}{2}\left(n + \frac{T\lambda}{2\pi\rho}\right). \tag{3.139}$$

(Note that λ is a length scale, and may be written in terms of ρ and the dimensionless constant $\tilde{M}^2$ defined at (3.22) as $\lambda = \frac{\rho}{2\tilde{M}^2}$.) Substituting the expression for $\frac{\partial\phi}{\partial\theta}$ into the equations for $\frac{\partial Y}{\partial\theta}$ and $\frac{\partial Z}{\partial\theta}$, we observe that the problem is reduced to the system of four first-order ODEs:

$$\frac{\partial \phi}{\partial \theta} = n + \lambda\left(\frac{T}{2\pi\rho} - X\right), \tag{3.140}$$

$$a\frac{\partial X}{\partial \theta} = -2gZ, \tag{3.141}$$

$$a\frac{\partial Y}{\partial \theta} = -\left(2E' + a\lambda X\right)Z, \tag{3.142}$$

$$a\frac{\partial Z}{\partial \theta} = \left(2E' + a\lambda X\right)Y - 2gX. \tag{3.143}$$

In particular, the equations (3.141-3.143) for the bispinors X, Y and Z are not explicitly dependent on the kink ϕ. If we can solve for the bispinors first, we can then deduce the matching kink solution.

It is immediately clear that $X^2 - Y^2 - Z^2$ is a first integral of the system; of course, it equals W^2. Another first integral is apparent by substituting (3.141)

into (3.142):

$$2ag\frac{\partial Y}{\partial\theta} = \left(2E' + a\lambda X\right)\left(-2gZ\right) \tag{3.144}$$

$$= \left(2E' + a\lambda X\right)\left(a\frac{\partial X}{\partial\theta}\right) \tag{3.145}$$

$$= a\frac{\partial}{\partial\theta}\left[2E'X + \frac{a\lambda}{2}X^2\right] \tag{3.146}$$

Hence there is a constant C_0 given by

$$C_0 = 2agY - 2aE'X - \frac{a^2\lambda}{2}X^2. \tag{3.147}$$

This equation also determines Y in terms of X and C_0; so, finally, we can plug it and (3.141) into (3.143) to reduce the XYZ system to a single non-linear differential equation in X. It is convenient to express it in the following manner: multiplying (3.143) by $2ag$ gives

$$(2ag)a\frac{\partial Z}{\partial\theta} = (2E' + a\lambda X)(2agY) - 4ag^2X. \tag{3.148}$$

We can use (3.147) to eliminate Y from the right-hand side, and slightly rewrite the left:

$$a^2\left(2g\frac{\partial Z}{\partial\theta}\right) = (2E' + a\lambda X)\left(C_0 + 2aE'X + \frac{a^2\lambda}{2}X^2\right) - 4ag^2X. \tag{3.149}$$

Then we use (3.141) to eliminate Z from the left-hand side, and collect powers of X on the right to obtain:

$$a^2\left(-a\frac{\partial^2 X}{\partial\theta^2}\right) = \frac{a^3\lambda^2}{2}X^3 + 3a^2\lambda E'X^2 + \left(4a\left[E'^2 - g^2\right] + a\lambda C_0\right)X + 2E'C_0. \tag{3.150}$$

At the cost of introducing one more constant of integration, which we will call C_1, we can multiply by $2\frac{\partial X}{\partial \theta}$ and integrate once more, yielding

$$-a^3\left(\frac{\partial X}{\partial \theta}\right)^2 = \frac{a^3\lambda^2}{4}X^4 + 2a^2\lambda E' X^3 + \left(4a\left[E'^2 - g^2\right] + a\lambda C_0\right)X^2 + 4E'C_0X + C_1. \tag{3.151}$$

In general, a non-linear differential equation of this form can be solved by an elliptic function, possibly reducing to a trigonometric or hyperbolic function in certain degenerate cases [68]. However, the specific solution depends on the coefficients of the polynomial appearing on the RHS above, and at present the parameters E', C_0 and C_1 are all unknown. We can eliminate C_1 in terms of C_0 and W by comparing the equation (3.151) to the condition $X^2 - W^2 - Y^2 - Z^2 = 0$, from which we may eliminate Y and Z in a similar fashion. First, multiplying by $2a^2g$ and rearranging, we have

$$-a^2\left(2gZ\right)^2 = \left(2agY\right)^2 - 4a^2g^2X^2 + 4a^2g^2W^2. \tag{3.152}$$

Substituting (3.147) on the left-hand side and (3.143) on the right yields

$$-a^2\left(-a\frac{\partial X}{\partial \theta}\right)^2 = \left(C_0 + 2aE'X + \frac{a^2\lambda}{2}X^2\right)^2 - 4a^2g^2X^2 + 4a^2g^2W^2. \tag{3.153}$$

Expanding, and collecting powers of X on the left-hand side, we're left with

$$-a^4\left(\frac{\partial X}{\partial \theta}\right)^2 = \frac{a^4\lambda^2}{4}X^4 + 2a^3\lambda E' X^3 + \left(4a^2\left[E'^2 - g^2\right] + a^2\lambda C_0\right)X^2 + 4aE'C_0X + C_0^2 + 4a^2g^2W^2. \tag{3.154}$$

Hence $aC_1 = C_0^2 + 4a^2g^2W^2$. If we specifically consider definite-parity solutions where $W = 0$, then $aC_1 = C_0^2$, and in fact the quartic in X factorises into

two real quadratics, giving

$$-a^4\left(\frac{\partial X}{\partial\theta}\right)^2 = \left(\frac{a^2\lambda}{2}X^2 + 2a\left[E' - g\right]X + C_0\right)\left(\frac{a^2\lambda}{2}X^2 + 2a\left[E' + g\right]X + C_0\right). \tag{3.155}$$

It is convenient now to perform some rescaling. We rescale E', g and C_0 to be dimensionless by taking

$$\tilde{E}' = \frac{E'}{a}; \quad \tilde{g} = \frac{g}{a}; \quad \tilde{C}_0 = \frac{\lambda C_0}{a^2}. \tag{3.156}$$

This yields

$$\begin{aligned}-\left(\frac{\partial X}{\partial\theta}\right)^2 = \frac{\lambda^2}{4}X^4 + 2\lambda\tilde{E}'X^3 + \left(4\left[\tilde{E}'^2 - \tilde{g}^2\right] + \tilde{C}_0\right)X^2 \\ + \frac{4\tilde{E}'\tilde{C}_0}{\lambda}X + \frac{\tilde{C}_0^2}{\lambda^2} + 4\tilde{g}^2W^2.\end{aligned} \tag{3.157}$$

Finally, when λ is non-zero, we can also rescale X to remove the (remaining) leading coefficients of $\frac{\lambda}{2}$ on the quadratics by setting

$$\tilde{X}(\theta) = \frac{\lambda}{2}X(\theta), \tag{3.158}$$

leaving

$$\begin{aligned}-\left(\frac{\partial\tilde{X}}{\partial\theta}\right)^2 = \tilde{X}^4 + 4\tilde{E}'\tilde{X}^3 + \left(4\left[\tilde{E}'^2 - \tilde{g}^2\right] + \tilde{C}_0\right)\tilde{X}^2 \\ + 2\tilde{E}'\tilde{C}_0\tilde{X} + \frac{\tilde{C}_0^2}{4} + \lambda^2\tilde{g}^2W^2.\end{aligned} \tag{3.159}$$

3.6 Elliptic function solutions for $\tilde{X}$

We will use the properties of the Jacobi elliptic functions to examine solutions of (3.155) and its rescalings. We will not derive the theory of these function, but simply give some properties in Section 3.6.1, and use them as a toolkit.

References for the theory and its applications include Whittaker and Watson [68] and the Digital Library of Mathematical Functions [56, Chapter 22].

Our detailed focus is on the case $W = 0$, but we can describe features of the more general case by comparing, in the coming Section 3.7, the solutions of (3.155) to the solutions on the prescribed kink derived in Section 3.3.

3.6.1 Some properties of Jacobi elliptic functions

The Jacobi sn function may be implicitly defined in terms of an elliptic integral as follows:

$$\mathrm{sn}^{-1}(x,k) = \int_0^x \frac{\mathrm{d}z}{\sqrt{1-z^2}\sqrt{1-k^2z^2}}, \tag{3.160}$$

for an *elliptic modulus* $k \in \mathbb{C}$ satisfying $|k|^2 \in [0,1]$, and by analytic continuation otherwise. It is typical to choose the branch cut in the k-plane to be from $-\infty$ to 0 and from 1 to ∞.

Associated to the elliptic modulus k are two values called the *quarter periods*, $K(k)$ and $K'(k)$. These are defined as

$$K(k) = \mathrm{sn}^{-1}(1,k) = \int_0^1 \frac{\mathrm{d}z}{\sqrt{1-z^2}\sqrt{1-k^2z^2}}, \tag{3.161}$$

and $K'(k) = K(k')$ where $k^2 + k'^2 = 1$ and $k' \to 1$ as $k \to 0$. By definition, we see that $\mathrm{sn}(0,k) = 0$ and $\mathrm{sn}(K(k),k) = 1$. $\mathrm{i}K'(k)$ is a simple pole of $\mathrm{sn}(u,k)$ with residue $\frac{1}{k}$. For $|k| \leq 1$, both quarter periods are real. $\mathrm{sn}(u,k)$ is a doubly periodic meromorphic function of the u-plane, and satisfies

$$\mathrm{sn}\left(u + 2\alpha K(k) + 2\mathrm{i}\beta K'(k), k\right) = (-1)^{\alpha}\,\mathrm{sn}\left(u,k\right), \quad \alpha,\beta \in \mathbb{Z}. \tag{3.162}$$

Manipulation of the definition (3.161) establishes that for $|k|^2 > 1$,

$$K(k) = \frac{1}{k}\left(K\left(\frac{1}{k}\right) - \mathrm{i}K'\left(\frac{1}{k}\right)\right), \tag{3.163}$$

and that for $k \in \mathbb{R}$,

$$K(\mathrm{i}k) = \frac{1}{\sqrt{1+k^2}} K\left(\frac{k}{\sqrt{1-k^2}}\right). \tag{3.164}$$

These can be seen as particular cases of *Landen's transformation*, which may be written in the form

$$K\left(\frac{\sqrt{a^2-b^2}}{a}\right) = \frac{2a}{a+b} K\left(\frac{a-b}{a+b}\right). \tag{3.165}$$

It can also be established using these formulae that if k is on the unit circle, i.e. $k = \mathrm{e}^{\mathrm{i}\alpha}$, then [44]

$$K'\left(e^{i\alpha}\right) = e^{-i\frac{\alpha}{2}} K\left(\sin\left(\frac{\alpha}{2}\right)\right). \tag{3.166}$$

We often do not write the dependence on the elliptic modulus explicitly. There are similar Jacobi elliptic functions $\mathrm{cn}(u)$ and $\mathrm{dn}(u)$ whose zeroes, poles and double periodicity may also be understood by permuting the points $0, K, \mathrm{i}K'$ and $K + \mathrm{i}K'$ of the complex plane. They satisfy

$$\mathrm{cn}^2(u) = 1 - \mathrm{sn}^2(u), \quad \mathrm{dn}^2(u) = 1 - k^2\mathrm{sn}^2(u). \tag{3.167}$$

There are addition theorems expressing elliptic functions of a summand of each of these, e.g. $\mathrm{sn}(u+v)$, as rational functions of sn, cn and dn evaluated at the points u and v. In the limits $k = 0$ and $k = 1$ the Jacobi elliptic functions become trigonometric and hyperbolic functions respectively, according to

$$\mathrm{sn}(u,0) = \sin(u), \qquad \mathrm{cn}(u,0) = \cos(u), \quad \mathrm{dn}(u,0) = 1, \tag{3.168}$$

$$\mathrm{sn}(u,1) = \tanh(u), \quad \mathrm{cn}(u,1) = \mathrm{sech}(u), \quad \mathrm{dn}(u,1) = \mathrm{sech}(u). \tag{3.169}$$

We define the fundamental *elliptic integral of the second kind* $E(u) = E(u,k)$ to be

$$E(u) = \int_0^u \mathrm{dn}^2(z)\,\mathrm{d}z, \tag{3.170}$$

and subsequently we define the *Zeta function* $Z(u,k)$ (not to be confused with our bispinor coordinate Z) as

$$Z(u,k) = E(u,k) - u\frac{E\left(K(k)\right)}{K(k)}. \tag{3.171}$$

We further define the fundamental *elliptic integral of the third kind* $\Pi(u,a,k)$ for elliptic modulus k and *parameter* a to be

$$\Pi(u,a,k) = \int_0^u \frac{k^2\mathrm{sn}(a)\mathrm{cn}(a)\mathrm{dn}(a)\mathrm{sn}^2(z)}{1-k^2\mathrm{sn}^2(a)\mathrm{sn}^2(z)}\mathrm{d}z. \tag{3.172}$$

Then it is found that

$$\Pi(u,a,k) = \frac{1}{2}\int_{u-a}^{u+a} Z(z,k)\,\mathrm{d}z + uZ(a,k). \tag{3.173}$$

The utility of these definitions is that some quantities of interest will be expressed in terms of integrals of the form

$$\int \frac{A + B\mathrm{sn}^2(u)}{C + D\mathrm{sn}^2(u)}\mathrm{d}u. \tag{3.174}$$

These can be rewritten in terms of a fundamental elliptic integral of the third kind, and thus evaluated in terms of a Zeta function. The integral term in equation (3.173) is generically multivalued as $Z(u,k)$ has poles in the u-plane, but it is periodic with respect to the real period $2K(k)$. Thus, by clever choices of the domain of our integral, evaluating expressions such as (3.174) requires only computing the value $Z(a,k)$. This is a transcendental problem but can be approached numerically.

3.6.2 Parity eigensolutions

Performing the rescalings (3.156) and (3.158) on (3.155), we obtain

$$-\left(\frac{\partial \tilde{X}}{\partial \theta}\right)^2 = \left(\tilde{X}^2 + 2\left[\tilde{E}' - \tilde{g}\right]\tilde{X} + \frac{\tilde{C}_0}{2}\right)\left(\tilde{X}^2 + 2\left[\tilde{E}' + \tilde{g}\right]\tilde{X} + \frac{\tilde{C}_0}{2}\right). \quad (3.175)$$

Throughout this section, we will make use of the following nomenclature:

- Let $P(\tilde{X})$ refer to the real, monic polynomial of degree 4 appearing on the right-hand side of (3.175) above; then $P(\tilde{X})$ is equivalent to the right-hand side of (3.159) with the substitution $W = 0$.
- Let $P_-(\tilde{X})$ and $P_+(\tilde{X})$ label the given (real, monic) quadratic factors explicitly by the sign appearing between $\tilde{E}'$ and $\tilde{g}$ in the linear term of each.

Having scaled $P(\tilde{X})$ to be monic, there are now four roots $x_1, x_2, x_3, x_4 \in \mathbb{C}$ (not necessarily distinct or real) such that (3.175) is equivalent to

$$-\left(\frac{\partial \tilde{X}}{\partial \theta}\right)^2 = \left(\tilde{X} - x_1\right)\left(\tilde{X} - x_2\right)\left(\tilde{X} - x_3\right)\left(\tilde{X} - x_4\right). \quad (3.176)$$

A straightforward application of the chain rule to the integral definition (3.160) demonstrates that the solution to equation (3.176) may be written as

$$\tilde{X}(\theta) = \frac{x_1\left(x_2 - x_3\right) - x_2\left(x_1 - x_3\right)\mathrm{sn}^2\left(p(\theta - \theta_c), k\right)}{\left(x_2 - x_3\right) - \left(x_1 - x_3\right)\mathrm{sn}^2\left(p(\theta - \theta_c), k\right)}, \quad (3.177)$$

where θ_c is a constant of integration and

$$p = \frac{\mathrm{i}}{2}\sqrt{\left(x_1 - x_4\right)\left(x_2 - x_3\right)}, \quad (3.178)$$

$$k = \sqrt{\frac{\left(x_1 - x_3\right)\left(x_2 - x_4\right)}{\left(x_1 - x_4\right)\left(x_2 - x_3\right)}}. \quad (3.179)$$

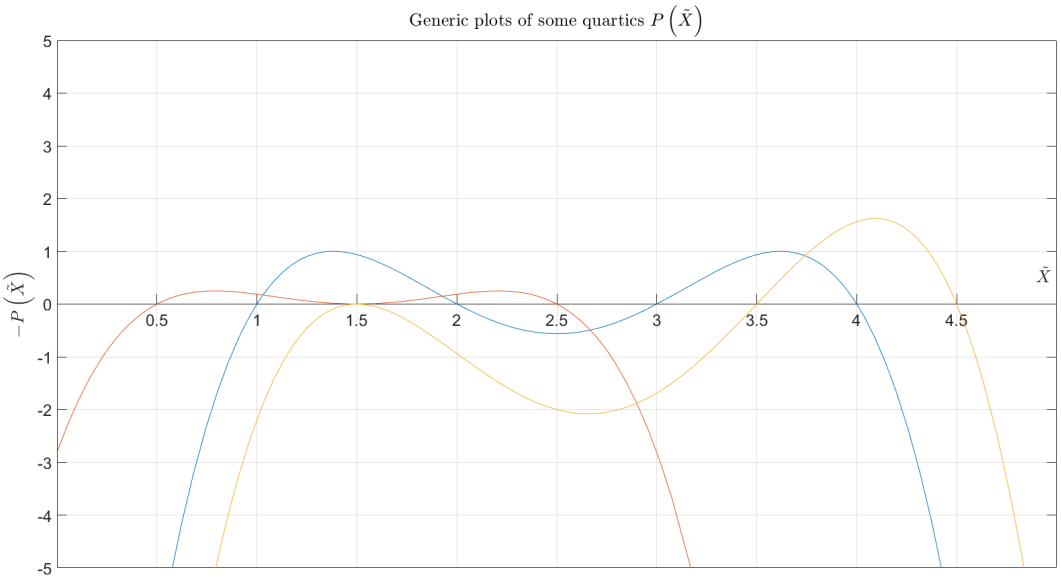

FIGURE 3.15: Some generic quartics $P\left(\tilde{X}\right)$ for the non-linear differential equation (3.176). Complex roots occur in conjugate pairs, so there must be an even number of real roots when counted with multiplicity. The graph of $-P\left(\tilde{X}\right)$ must open downwards.

Clearly the ordering of the roots in (3.176) is arbitrary, so there are many similar ways of expressing this generic solution with different orderings of the roots; the symmetries of the sn function guarantee that these describe the same meromorphic function $\tilde{X}(\theta)$. We will consequently use (3.177) as the canonical expressions for $\tilde{X}$, p and k in terms of the roots of $P(\tilde{X})$, and choose to label the roots x_i according to our convenience.

Observe that since $\mathrm{sn}(0) = 0$, $\tilde{X}(\theta_c) = x_1$. Moreover, since $\mathrm{i}K'$ is a pole of sn, then when $p(\theta' - \theta_c) = \mathrm{i}K'$, $\tilde{X}(\theta') = x_2$. Assuming that $\tilde{X}(\theta)$ remains real for $\theta \in \mathbb{R}$, then, x_1 and x_2 must correspond to extremal values of $\tilde{X}$. Considering interpreting (3.176) as a dynamical system in $\tilde{X}$ and $\frac{\partial \tilde{X}}{\partial \theta}$, and plotting $-P(\tilde{X})$ against $\tilde{X}$. Since $P(\tilde{X})$ is real, the graph of the quartic must have either zero, two or four real roots, counted with multiplicity, and $-P\left(\tilde{X}\right)$ must open downwards. We plot some generic possibilities at Figure 3.15.

Remark 3.2. We're grateful to Andy Hone for pointing out a geometric interpretation which makes the observations of the previous paragraphs more straightforward. The general solution given at (3.177) is quickly recognised as a Möbius transformation $\mathcal{M}$ applied to the sn^2 function appearing within it, and more specifically the Möbius transformation defined by the action on three points:

$$\mathcal{M}(0) = x_1, \mathcal{M}(\hat{\infty}) = x_2, \mathcal{M}(1) = x_3. \tag{3.180}$$

In principle, we could tell in advance that we're looking for some transformation of a Jacobi elliptic function whose image on the real line is bounded between extrema x_1 and x_2, so a Möbius transformation obeying the first two conditions of (3.180) is a sensible thing to try. It is somewhat simpler to start from this point in order to derive the remaining dependence of the Möbius map and the parameters p and k upon the roots of (3.176). We briefly comment a little further on this interpretation in our discussion in Section 3.9.

Physical solutions require that there are at least two non-negative real roots, so without loss of generality, we can restrict to considering $x_1, x_2 \in \mathbb{R}$ such that $0 \leq x_1 \leq x_2$. Moreover, since we suppose $\tilde{X}$ to be real, physicality further requires that $\left(\frac{\partial \tilde{X}}{\partial \theta}\right)^2 = -P(X) > 0$ for $x_1 < \tilde{X} < x_2$. We will for now discount the case that $x_1 = x_2$, since the fermionic solutions of fixed density are exactly the persistent angular momentum eigenstates of Section 3.3.2. We will moreover discount the case that $x_1 = 0$: we have not found any numeric solutions where the fermionic density has minimum zero, or where the computed value of $\tilde{C}_0$ is zero.

The factorisation of $P(\tilde{X}) = P_-(\tilde{X})P_+(\tilde{X})$ puts algebraic constraints on the generic roots x_i. To emphasise which roots belong to which quadratic factors, let us fashion an alternative labelling scheme for the roots as follows.

Let

$$P_-(\tilde{X}) = \left(\tilde{X}^2 + 2\left[\tilde{E}' - \tilde{g}\right]\tilde{X} + \frac{\tilde{C}_0}{2}\right) = \left(\tilde{X} - r_-\right)\left(\tilde{X} - s_-\right); \tag{3.181}$$

$$P_+(\tilde{X}) = \left(\tilde{X}^2 + 2\left[\tilde{E}' + \tilde{g}\right]\tilde{X} + \frac{\tilde{C}_0}{2}\right) = \left(\tilde{X} - r_+\right)\left(\tilde{X} - s_+\right). \tag{3.182}$$

Then we observe the requirements:

$$r_- s_- = \frac{\tilde{C}_0}{2} = r_+ s_+, \tag{3.183}$$

$$4\tilde{E}' = -r_- - s_- - r_+ - s_+, \tag{3.184}$$

$$4\tilde{g} = r_- + s_- - r_+ - s_+. \tag{3.185}$$

Now, $\lambda \geq 0$ (where we permit the limiting case $\lambda = 0$ corresponding to the kink as the background to the fermion, without backreaction). For illustrative purposes, let us suppose that the sign of $\tilde{E}'$ is always opposite that of $\tilde{C}_0$. The demand that the physical roots x_1, x_2 satisfy $0 < x_1 < x_2$ then significantly constrains the possible complex values of the remaining two roots x_3, x_4 into a handful of cases, depending on e.g. whether x_1 and x_2 belong to the same, or to distinct, quadratic factors of $P(\tilde{X})$, and the signs of the physical parameters. In particular, there will be two algebraic constraints on the roots x_3, x_4. This will allow us to eliminate them in terms of the physical roots x_1, x_2. For example, in the case that the physical roots belong to the quadratic factor $P_-(\tilde{X})$, then (3.183) and (3.185) give us the algebraic conditions

$$x_1 x_2 = x_3 x_4, \quad 4\tilde{g} = x_1 + x_2 - x_3 - x_4. \tag{3.186}$$

A further constraint on physically meaningful solutions is the translation symmetry $\theta \mapsto \theta + 2\pi$. Since we observe that x_1 and x_2 are specifically

obtained as extrema of $\tilde{X}$ when p is pure imaginary, and that $2\mathrm{i}K'$ is the corresponding period of sn, we desire that for some integer $j \in \mathbb{Z}$,

$$2\pi p = 2j\mathrm{i}K', \tag{3.187}$$

or equivalently

$$-\mathrm{i}\pi p = jK'. \tag{3.188}$$

In fact since sn is an odd function and it always appears squared in $\tilde{X}$, we can restrict to considering $j \in \mathbb{N}$. We see now that it is convenient to cancel the explicit factor of i in the definition of p at (3.178) above, and work instead in terms of

$$q = \frac{1}{2}\sqrt{(x_1 - x_4)\,(x_2 - x_3)}, \tag{3.189}$$

and thus with the constraint

$$\pi q = jK', j \in \mathbb{N}. \tag{3.190}$$

This is a transcendental constraint on the roots, expressed just in terms of the physical roots x_1 and x_2 after using (3.183-3.185) to eliminate x_3 and x_4.

Finally, we should consider the overall normalisation of the fermion, as we know this plays a role in the energy eigenvalue. Recall that we defined

$$\begin{aligned} T &= \int_0^{2\pi} X(\theta)\,\rho\,\mathrm{d}\theta \\ &= \frac{2\rho}{\lambda}\int_0^{2\pi} \tilde{X}(\theta)\,\mathrm{d}\theta, \end{aligned} \tag{3.191}$$

or equivalently we might define

$$\tilde{T} := \frac{T\lambda}{2\rho} = \int_0^{2\pi} \tilde{X}(\theta)\,\mathrm{d}\theta. \tag{3.192}$$

For numerical calculations, it is convenient to exploit the periodicity of the solution as expressed above at (3.190) to avoid integrating over the singularities of $\mathrm{sn}(u)$ at $u = \mathrm{i}K'$. Suppressing the constant of integration θ_c, we can express the above as

$$\tilde{T} = 2j \int_0^{\frac{\pi}{j}} \tilde{X}(\theta)\, \mathrm{d}\theta. \tag{3.193}$$

From (3.177), $\tilde{X}(\theta)$ takes the generic form:

$$\tilde{X}(\theta) = \frac{A + B\,\mathrm{sn}^2(p\theta)}{C + D\,\mathrm{sn}^2(p\theta)} = \frac{A}{C} + \left(\frac{BC - AD}{C^2}\right) \frac{\mathrm{sn}^2(p\theta)}{1 + \frac{D}{C}\,\mathrm{sn}^2(p\theta)}. \tag{3.194}$$

Therefore we expect we can express the integral on the right-hand side of (3.193) in terms of an incomplete elliptic integral of the third kind, as discussed in Section 3.6.1. By our preferred form of $\tilde{X}$, $\frac{A}{C} = x_1$ in the above expression. We also find

$$\frac{BC - AD}{C^2} = \frac{(x_1 - x_2)(x_1 - x_3)}{(x_2 - x_3)}, \tag{3.195}$$

and if we define the parameter χ of the incomplete elliptic integral of the third kind $\Pi(z, \chi, k)$ via

$$\frac{D}{C} = -k^2 \mathrm{sn}^2(\chi) = -\left(\frac{x_1 - x_3}{x_2 - x_1}\right) \tag{3.196}$$

then

$$\mathrm{sn}^2(\chi) = \frac{x_1 - x_4}{x_2 - x_4}; \tag{3.197}$$

consequently,

$$\begin{aligned} \mathrm{cn}^2(\chi) &= 1 - \mathrm{sn}^2(\chi) = 1 - \left(\frac{x_1 - x_4}{x_2 - x_4}\right) \\ &= \frac{x_2 - x_1}{x_2 - x_4}, \end{aligned} \tag{3.198}$$

and

$$\begin{aligned} \mathrm{dn}^2(\chi) = 1 - k^2\mathrm{sn}^2(\chi) &= 1 - \left(\frac{x_1 - x_3}{x_2 - x_1}\right) \\ &= \frac{x_2 - x_1}{x_2 - x_3}. \end{aligned} \tag{3.199}$$

Integrating (3.194),

$$\tilde{T} = 2j \int_0^{\frac{\pi}{j}} \tilde{X}(\theta)\, \mathrm{d}\theta = \frac{2j}{p} \int_0^{\frac{\pi p}{j}} \tilde{X}(\theta)\, \mathrm{d}(p\theta) \tag{3.200}$$

$$= \frac{2j}{p} \int_0^{\frac{\pi p}{j}} \left[x_1 + \frac{BC - AD}{C^2} \left(\frac{\mathrm{sn}^2(p\theta)}{1 - k^2\mathrm{sn}^2(\chi)\mathrm{sn}^2(p\theta)} \right) \right] \mathrm{d}(p\theta) \tag{3.201}$$

$$= 2\pi x_1 + \frac{BC - AD}{C^2 k^2 \mathrm{sn}(\chi)\mathrm{cn}(\chi)\mathrm{dn}(\chi)} \Pi\left(\frac{\pi p}{j}, \chi, k\right). \tag{3.202}$$

Combining the expressions from (3.195) to (3.198), we see that (up to a possible ambiguity in the sign of the square root, which we can fix)

$$\frac{BC - AD}{C^2 k^2 \mathrm{sn}(\chi)\mathrm{cn}(\chi)\mathrm{dn}(\chi)} = 2q. \tag{3.203}$$

Therefore we see that the normalisation of the fermion is expressed by the transcendental equation

$$\tilde{T} = 2\pi x_1 + 2q\, \Pi\left(\frac{\pi p}{j}, \chi, k\right), \tag{3.204}$$

and the parameters p, q, k and χ can all be written as functions of the physical roots x_1 and x_2 by employing the algebraic relations obtained at (3.183-3.185).

The upshot of this discussion is that in principle, the transcendental constraints given at Equations (3.190) and (3.193) can be reduced to finding intersections of transcendental curves in the (x_1, x_2)-plane. By setting the physical parameters $\lambda, \tilde{C}_0$ and $\tilde{g}$, intersections of the transcendental curves give the possible physical solutions of the kink-fermion system with these quantities, and moreover, by Equation (3.184), the shifted energy eigenvalue $\tilde{E}'$ can

be immediately determined by inspection once we identify the intersection point and determine the two remaining, non-physical, roots x_3 and x_4. We have not had time to follow this outlined approach further, but we hope to explore it in future work.

3.7 Angular momentum eigensolutions and the role of W

Let us consider how, from the $XYZW$ picture, solutions of the special case with background kink arise. Moving the kink to the background corresponds to taking the limit $M^2 \to \infty$ (for fixed ρ, g and T), which in the $XYZW$ picture corresponds to $\lambda \to 0$. In this limit we cannot perform the final rescaling (3.158), but (3.157) reduces to

$$-\left(\frac{\mathrm{d}X}{\mathrm{d}\theta}\right)^2 = 4\left(\tilde{E}'^2 - \tilde{g}^2\right)X^2 + 4\tilde{E}'\frac{\tilde{C}_0}{\lambda}X + \frac{\tilde{C}_0^2}{\lambda^2} + 4\tilde{g}^2W^2. \tag{3.205}$$

With a little algebra, we can complete the square and then solve the above with a standard arcsin integral. First we write the right-hand side simply as $AX^2 + BX + C$, with coefficients given by

$$A = 4\left(\tilde{E}'^2 - \tilde{g}^2\right), \quad B = 4\tilde{E}'\frac{\tilde{C}_0}{\lambda}, \quad C = \frac{\tilde{C}_0^2}{\lambda^2} + 4\tilde{g}^2W^2. \tag{3.206}$$

The discriminant of this quadratic is

$$\Delta = B^2 - 4AC = 16\tilde{g}^2\left[\frac{\tilde{C}_0^2}{\lambda^2} - 4W^2\left(\tilde{E}'^2 - \tilde{g}^2\right)\right]. \tag{3.207}$$

Completing the square, the differential equation (3.205) can be written as

$$\left(\frac{\mathrm{d}X}{\mathrm{d}\theta}\right)^2 = \frac{\Delta}{4A}\left[1 - \left(\frac{2A}{\sqrt{\Delta}}X + \frac{B}{\sqrt{\Delta}}\right)^2\right]. \tag{3.208}$$

Integrating, we obtain solutions of the form

$$X(\theta) = \frac{\sqrt{\Delta}}{2A} \sin\left(\pm\sqrt{A}\,(\theta - \theta_0)\right) - \frac{B}{2A}, \tag{3.209}$$

where θ_0 is the constant of integration, as long as $\sqrt{A} = k \in \mathbb{Z}$. Substituting in our specific values of A, B and C, we obtain two general solutions: one on each of two (positive and negative) energy branches, according to

$$X(\theta) = \frac{2}{k^2}\left[\tilde{g}\sqrt{\frac{\tilde{C}_0^2}{\lambda^2} - k^2W^2}\sin k\,(\theta - \theta_0) \mp \frac{\tilde{C}_0}{\lambda}\sqrt{\tilde{g}^2 + \frac{k^2}{4}}\right], \tag{3.210}$$

$$\tilde{E}' = \pm\sqrt{\tilde{g}^2 + \frac{k^2}{4}}. \tag{3.211}$$

We immediately see, for real solutions, the bound on W^2:

$$0 \leq W^2 \leq \frac{\tilde{C}_0^2}{k^2\lambda^2}. \tag{3.212}$$

We will show that we obtain the known parity eigenstates when $W^2 = 0$, and the known angular momentum eigenstates when $W^2 = \frac{\tilde{C}_0^2}{k^2\lambda^2}$; in each case, the interpretation of the mode k is that $k = 2l$ where l is the angular momentum eigenvalue.

Let us consider some effects of setting $\lambda = 0$ on the kink and physical invariants. From the known eigensolutions (either parity or angular momentum), we can exactly determine X, Y, Z and W, whence C_0, directly in terms of constants and invariants such as l, T, and so on. For the angular momentum solutions,

$$X = \frac{T}{2\pi\rho}, \quad Y = \pm\frac{g}{\sqrt{a^2l^2 + g^2}}\frac{T}{2\pi\rho}, \quad Z = 0, \quad W = \mp\frac{al}{\sqrt{a^2l^2 + g^2}}\frac{T}{2\pi\rho}, \tag{3.213}$$

with the choice of $\pm$ sign always corresponding to the energy branch. For the parity solutions, let $P = \pm 1$ be the parity. Then

$$X = \left[1 + P\frac{alg}{a^2l^2 + g^2}\cos 2l\,(\theta - \theta_0)\right]\frac{T}{2\pi\rho}, \tag{3.214}$$

$$Y = \left[\frac{g}{\sqrt{a^2l^2 + g^2}} + P\cos 2l\,(\theta - \theta_0)\right]\frac{T}{2\pi\rho}, \tag{3.215}$$

$$Z = \left[P\frac{a^2l^2}{a^2l^2 + g^2}\sin 2l\,(\theta - \theta_0)\right]\frac{T}{2\pi\rho}, \tag{3.216}$$

and by construction $W = 0$.

Consider again the quadratic on the RHS of 3.205. Its roots are

$$X = \frac{-\tilde{E}'\tilde{C}_0 \pm \tilde{g}\sqrt{\tilde{C}_0^2 - 4\left(\tilde{E}'^2 - \tilde{g}^2\right)\lambda^2 W^2}}{2\lambda\left(\tilde{E}'^2 - \tilde{g}^2\right)}. \tag{3.217}$$

For physical periodicity, we require that both roots are non-negative, since $\left(\tilde{E}'^2 - \tilde{g}^2\right) > 0$ for reality of (3.210). This gives the same physical bound on W^2, and in particular demonstrates the double root when the upper bound is saturated. But on such a physical solution where X is constant, by axial current conservation the kink is uniform – so we immediately reduce to the special case as a subset of the general case, implying that the solution is an angular momentum solution. Some straightforward algebra then demonstrates that the conditions in equations (3.213-3.216) are obtained in the respective bounds (3.212).

How do we interpret W in the special case of the prescribed kink? Fix an energy level $E^{\pm}$, determined by $|l| \neq 0$ and the choice of branch, and identify $k = 2l$. All such energy levels are two-dimensional; we have exhibited the angular momentum and parity bases. Individual elements of the parity basis $\{\psi^+, \psi^-\}$ have $W = 0$, while the individual elements of the angular momentum basis are proportional to linear combinations of the parity basis

solutions according to

$$\psi_{l^\pm} \sim (\psi^+ + \psi^-), \tag{3.218}$$

$$\psi_{-l^\pm} \sim (\psi^+ - \psi^-). \tag{3.219}$$

Now, a general solution (*of the special case*) in the chosen energy level may be expressed as a linear combination of the parity basis solutions,

$$\psi = u\psi^+ + v\psi^-, \quad u, v \in \mathbb{C}. \tag{3.220}$$

Calculating e.g. W, C_0, X, Y in terms of the known values for the parity basis, we find:

$$W = \mp \left(8al\sqrt{a^2l^2 + g^2} \right) (u^*v + v^*u), \tag{3.221}$$

$$C_0 = 16a^3l^2\sqrt{a^2l^2 + g^2} \left(|u|^2 + |v|^2 \right). \tag{3.222}$$

Then the bound $C_0^2 - (2alW)^2 \geq 0$ simply corresponds to the implication that, by positive-definiteness and linearity of the complex inner product,

$$|u + v|^2 \geq 0 \Rightarrow |u|^2 + |v|^2 \geq u^*v + v^*u. \tag{3.223}$$

In this sense, axial charge arises from the cross-terms in $|\psi|^2$ when expressed in the parity basis: the projection, or inner product, of the positive and negative parity components.

3.8 Consistency with the Dirac equations for $W = 0$

The $XYZW$ dynamical system was derived from the Dirac equations for the fermion field(s); it is necessary that any fermion solution must yield bispinors that satisfy the real dynamical system, but it is not necessary that every solution to the XYZ equations can arise from a valid solution for the underlying Dirac equations. For a solution $X(\theta)$ to actually provide a valid fermionic solution, we must be able to construct the fermionic components of ψ consistently. We will use the polar decomposition in terms of real functions $R(\theta), L(\theta), \mu(\theta)$ and $\nu(\theta)$ as discussed at (3.114). The general obstruction to obtaining solutions to the Dirac equations is that it is not necessarily clear that we can solve for the axial phase $\mu(\theta) - \nu(\theta)$.

For stationary state fermionic solutions, the Dirac equations expressed in these components are

$$E_f R\mathrm{e}^{\mathrm{i}\mu} = \mathrm{i}a\frac{\partial}{\partial\theta}\left[R\mathrm{e}^{\mathrm{i}\mu}\right] + gL\mathrm{e}^{-\mathrm{i}(\phi-\nu)}, \tag{3.224}$$

$$E_f L\mathrm{e}^{\mathrm{i}\nu} = -\mathrm{i}a\frac{\partial}{\partial\theta}\left[L\mathrm{e}^{\mathrm{i}\nu}\right] + gR\mathrm{e}^{\mathrm{i}(\phi+\mu)}. \tag{3.225}$$

Let us restrict to the case $W = 0$. We have observed that in this case $R(\theta) = L(\theta)$, so

$$E_f R\mathrm{e}^{\mathrm{i}\mu} = \mathrm{i}a\left(\frac{\partial R}{\partial\theta} + \mathrm{i}\frac{\partial\mu}{\partial\theta}R\right)\mathrm{e}^{\mathrm{i}\mu} + gR\mathrm{e}^{-\mathrm{i}(\phi-\nu)}, \tag{3.226}$$

$$E_f R\mathrm{e}^{\mathrm{i}\nu} = -\mathrm{i}a\left(\frac{\partial R}{\partial\theta} + \mathrm{i}\frac{\partial\nu}{\partial\theta}R\right)\mathrm{e}^{\mathrm{i}\nu} + gR\mathrm{e}^{\mathrm{i}(\phi+\mu)}. \tag{3.227}$$

Next we restrict the appearance of complex phases to the coupling terms,

and write the equations explicitly in terms of their real and imaginary components:

$$E_f R = -a\frac{\partial \mu}{\partial \theta} R + \mathrm{i}a\frac{\partial R}{\partial \theta} + gR\left(\cos(\phi+\mu-\nu) - \mathrm{i}\sin(\phi+\mu-\nu)\right), \quad (3.228)$$

$$E_f R = a\frac{\partial \nu}{\partial \theta} R - \mathrm{i}a\frac{\partial R}{\partial \theta} + gR\left(\cos(\phi+\mu-\nu) + \mathrm{i}\sin(\phi+\mu-\nu)\right). \quad (3.229)$$

Comparing the real parts demonstrates that

$$\frac{\partial \mu}{\partial \theta} = -\frac{\partial \nu}{\partial \theta}, \quad (3.230)$$

$$\text{i.e. } \nu(\theta) = \nu_0 - \mu(\theta) \text{ for some constant } \nu_0. \quad (3.231)$$

In fact this constant ν_0 is easily determined by the requirement that $W = 0$ solutions are parity eigenstates; we can show that it is 0 for the positive parity eigenstate and π for the negative parity eigenstate. (An equivalent means of deriving this would have been to substitute the polar component decomposition and the ansatz $W = 0$ into equations (3.128-3.131).)

We have reduced to a pair of real equations relating R, μ and ϕ; recall that since $X(\theta)$ is considered to be already determined, so are R and ϕ. For this solution $X(\theta)$ to admit a fermion solution, we seek a consistent solution for $\mu(\theta)$ from the remaining pair of equations:

$$E_f = -a\frac{\partial \mu}{\partial \theta} + g\cos(\phi + 2\mu - \nu_0), \quad (3.232)$$

$$0 = a\frac{\partial R}{\partial \theta} - gR\sin(\phi + 2\mu - \nu_0). \quad (3.233)$$

In principle, (3.233) can be solved for μ in terms of the arcsin of a logarithmic derivative of R, but it is then not so straightforward to determine whether that complicated expression for μ will be consistent with (3.232) by resulting in a constant right-hand side. Instead let us differentiate (3.232), and then use

(3.233) to eliminate the explicit appearance of trigonometric functions. Thus,

$$0 = -a\frac{\partial^2\mu}{\partial\theta^2} - g\left(\sin(\phi + 2\mu - v_0)\right)\left(\frac{\partial\phi}{\partial\theta} + 2\frac{\partial\mu}{\partial\theta}\right), \tag{3.234}$$

$$= -a\frac{\partial^2\mu}{\partial\theta^2} - a\left(\frac{1}{R}\frac{\partial R}{\partial\theta}\right)\left(\frac{\partial\phi}{\partial\theta} + 2\frac{\partial\mu}{\partial\theta}\right). \tag{3.235}$$

Now,

$$X = 2R^2 \Rightarrow \frac{1}{R}\frac{\partial R}{\partial\theta} = \frac{1}{2X}\frac{\partial X}{\partial\theta}, \tag{3.236}$$

and from the axial current conservation for the static kink (3.138), we had

$$\frac{\partial\phi}{\partial\theta} = n + \frac{T\lambda}{2\pi\rho} - \lambda X \tag{3.237}$$

$$= 2\left(\tilde{E}_f - \tilde{E}'\right) - \lambda X. \tag{3.238}$$

That is,

$$\frac{\partial^2\mu}{\partial\theta^2} + \frac{1}{2X}\frac{\partial X}{\partial\theta}\left(2\left(\tilde{E}_f - \tilde{E}'\right) - \lambda X + 2\frac{\partial\mu}{\partial\theta}\right) = 0, \tag{3.239}$$

or

$$\frac{\partial^2\mu}{\partial\theta^2} + \frac{1}{X}\frac{\partial X}{\partial\theta}\frac{\partial\mu}{\partial\theta} = \left(\tilde{E}' - \tilde{E}_f + \frac{\lambda}{2}\right)\frac{\partial X}{\partial\theta}. \tag{3.240}$$

Taking an integrating factor of simply $X(\theta)$ we see

$$\frac{\partial}{\partial\theta}\left(X\frac{\partial\mu}{\partial\theta}\right) = \left(\tilde{E}' - \tilde{E}_f + \frac{\lambda}{2}\right)X\frac{\partial X}{\partial\theta}, \tag{3.241}$$

$$\Rightarrow X\frac{\partial\mu}{\partial\theta} = \frac{\lambda}{4}X^2 + \left(\tilde{E}' - \tilde{E}_f\right)X + C_2, \tag{3.242}$$

$$\Rightarrow \frac{\partial\mu}{\partial\theta} = \frac{\lambda}{4}X + \left(\tilde{E}' - \tilde{E}_f\right) + \frac{C_2}{X}. \tag{3.243}$$

As we know $X(\theta)$ is a particularly simple rational function of Jacobi sn functions, we can therefore integrate this equation to obtain an expression for $\mu(\theta)$ as an incomplete elliptic integral of the third kind – *if* we can find an appropriate value for the constant of integration C_2 that we introduced during

these manipulations. Thankfully, the Dirac equations also let us determine the consistent value of C_2. To see this, we will eliminate the messy trigonometric functions by relating them algebraically, rather than differentiating one into the other. We will substitute (3.233) into (3.232) by writing

$$\cos(\phi + 2\mu - \nu_0) = \pm\sqrt{1 - \sin^2(\phi + 2\mu - \nu_0)} \tag{3.244}$$

$$= \pm\sqrt{1 - \left(\frac{1}{\tilde{g}R}\frac{\partial R}{\partial \theta}\right)^2} \tag{3.245}$$

$$= \pm\sqrt{1 - \left(\frac{1}{2\tilde{g}X}\frac{\partial X}{\partial \theta}\right)^2}. \tag{3.246}$$

Substituting this and (3.243) into (3.232),

$$\tilde{E}_f = -\left(\frac{\lambda}{4}X + (\tilde{E}' - \tilde{E}_f) + \frac{C_2}{X}\right) \pm \tilde{g}\sqrt{1 - \left(\frac{1}{2\tilde{g}X}\frac{\partial X}{\partial \theta}\right)^2}. \tag{3.247}$$

If we multiply by $2X$ and rearrange, we see

$$\frac{\lambda}{2}X^2 + 2\tilde{E}'X + 2C_2 = \pm\sqrt{4\tilde{g}^2X^2 - \left(\frac{\partial X}{\partial \theta}\right)^2}. \tag{3.248}$$

This is beginning to look very familiar! We square both sides to find

$$-\left(\frac{\partial X}{\partial \theta}\right)^2 = \left(\frac{\lambda}{2}X^2 + 2\tilde{E}'X + 2C_2\right)^2 - (2\tilde{g}X)^2. \tag{3.249}$$

This difference of two squares gives us *exactly* the elegant factorisation appearing in the defining differential equation of the XYZ system when $W = 0$, as long as we take $2C_2 = \frac{\tilde{C}_0}{\lambda}$. This also clarifies that $\tilde{C}_0$ is related to the evolution of the phase of the chiral fermion components, which was not obvious when we first introduced it as a constant of integration.

Returning to (3.243), we've now obtained

$$\frac{\partial \mu}{\partial \theta} = \frac{\lambda}{4}X(\theta) + (\tilde{E}' - \tilde{E}_f) + \frac{\tilde{C}_0}{2\lambda}\frac{1}{X(\theta)}. \tag{3.250}$$

In section 3.6.2 we demonstrated how to write a schematic solution for $\tilde{X}(\theta)$ as an integrand for an incomplete elliptic integral of the third kind. We can do similarly for the function $\frac{1}{\tilde{X}(\theta)}$ by relabelling the coefficients A, B, C and D, being careful to note that the parameter χ will also be changed by this rearrangement. Observe from (3.194),

$$\frac{1}{\tilde{X}(\theta)} = \frac{C + D\,\mathrm{sn}^2(p\theta)}{A + B\,\mathrm{sn}^2(p\theta)} = \frac{C}{A} + \left(\frac{AD - BC}{A^2}\right) \frac{\mathrm{sn}^2(p\theta)}{1 + \frac{B}{A}\,\mathrm{sn}^2(p\theta)}, \tag{3.251}$$

and we should now define

$$\frac{B}{A} = -k^2 \mathrm{sn}^2(\chi'). \tag{3.252}$$

Making similar use of identities for the Jacobi elliptic functions and the expressions for the roots of the quartic $P(\tilde{X})$, we find:

$$\mathrm{sn}^2(\chi') = \frac{x_2\,(x_1 - x_4)}{x_1\,(x_2 - x_4)}, \tag{3.253}$$

$$\mathrm{cn}^2(\chi') = \frac{x_4\,(x_2 - x_1)}{x_1\,(x_2 - x_4)}, \tag{3.254}$$

$$\mathrm{dn}^2(\chi') = \frac{x_3\,(x_2 - x_1)}{x_1\,(x_2 - x_3)}, \tag{3.255}$$

$$\frac{AD - BC}{A^2} = -\frac{(x_1 - x_2)\,(x_1 - x_3)}{x_1^2\,(x_2 - x_3)}, \tag{3.256}$$

and so, up to the sign of a square root,

$$\frac{AD - BC}{A^2 k^2 \mathrm{sn}(\chi')\mathrm{cn}(\chi')\mathrm{dn}(\chi')} = \pm\frac{2q}{\sqrt{x_1 x_2 x_3 x_4}}. \tag{3.257}$$

Observe that when $W = 0$, $x_1 x_2 x_3 x_4 = \tilde{C}_0^2$, so finally,

$$\frac{1}{\tilde{X}(\theta)} = \frac{1}{x_1} \pm \frac{2q}{\tilde{C}_0}\left[\frac{k^2 \mathrm{sn}(\chi')\mathrm{cn}(\chi')\mathrm{dn}(\chi')\mathrm{sn}^2(p\theta)}{1 - k^2 \mathrm{sn}^2(\chi')\mathrm{sn}^2(p\theta)}\right], \tag{3.258}$$

where the term in square brackets is the integrand of the incomplete elliptic

integral of the third kind $\Pi(p\theta, \chi', k)$. Thus, in principle, when $W = 0$, it is completely possible to solve for the function $\mu(\theta)$ and evaluate it numerically. Equipped with that, we can therefore construct all components of the Dirac spinor ψ from the XYZ solution, with a guarantee that this ψ satisfied the Dirac equation.

3.9 Discussion

For such a seemingly simple model, our kink-fermion system on $\mathbb{R} \times \mathrm{S}^1$ has revealed a surprisingly elaborate structure. The ability to recast the dynamics of a fermion field into the language and technology of elliptic functions was unexpected at the outset of this project.

There are some outstanding questions which we had initially hoped to pursue during our research, but were unable to address in time, at least in part owing to the effects of the COVID-19 pandemic. We made some simplifying assumptions in our illustrative remarks of the framework when we were discussing the roots of the quartic $P\left(\tilde{X}\right)$ in Section 3.6.2. In particular, we assumed that the lowest nonnegative root was in fact positive, and moreover that the sign of $\tilde{E}'$ was always opposite the sign of $\tilde{C}_0$. These assumptions arose because they were satisfied by a very limited set of numerical solutions derived by the methods of Section 3.4.2. To substantiate these claims we would like to systematically generate a large number of numerical solutions in order to see whether they hold true. Alternatively, without making *a priori* assumptions about the relationships between the physical quantities $\tilde{E}', \lambda$ and $\tilde{C}_0$, we could examine all the possible effects of permuting the quartic roots in the expressions of equations (3.181-3.182), and derive the corresponding transcendental constraints analogous to equations (3.190) and (3.193) in each case. A preliminary investigation suggests that there are

physical solutions just when the resulting elliptic modulus k arising according to equation (3.179) lies on the complex unit circle; then by the identity (3.166), the quarter period relevant to (3.190) can be evaluated. The fact that this condition is sufficient to give a physical solution follows from the geometric perspective outlined in Remark 3.2. Möbius transformations of $\mathbb{CP}^1$ map circles and lines to circles and lines, and the values 0,1 and $\hat{\infty}$ lie on a line, so their images x_1, x_2 and x_3 must lie on a circle or a line. If x_3 and x_4 are not real, then they are complex conjugates, so (for x_3 to lie on a circle with x_1 and x_2) they must have real part strictly between x_1 and x_2 and lie on the circle for which $x_1 x_2$ is a diameter. But then it is easily seen that as the square root of the cross ratio $[x_1, x_2, x_3, x_4]$, k must lie on the complex unit circle.

In fact, we see that in terms of the Möbius map $\mathcal{M}$ implicitly defined at (3.177),

$$x_4 = \mathcal{M}\left(\frac{1}{k^2}\right). \tag{3.259}$$

We pointed out at (3.180) that that $x_3 = \mathcal{M}(1)$, but we should perhaps clarify that, in terms of the quarter period $K(k)$, this can be written

$$x_3 = \mathcal{M}(\mathrm{sn}\, K). \tag{3.260}$$

So all of the roots of the quartic $P(\tilde{X})$ can be related to properties of the "generic" Jacobi elliptic function $\mathrm{sn}(z, k)$ appearing in the preimage of the Möbius map. We feel that we have certainly not exploited all of this geometric structure yet. We therefore confidently hope that we will be able push this perspective further in order to simplify the case-by-case treatment of our outline for "hunting" physical solutions in the (x_1, x_2) plane by numerically solving for the intersection of two transcendental curves.

Although we have some understanding in the $XYZW$ picture of the role of the quantities E' and C_0, they are lacking a physical interpretation in the original system. We postulate that E' is a sort of "free energy" of the fermion,

accounting for the proportion of its energy that is not used to "bind" to the kink; and also that C_0 can be interpreted as a sort of regularised fermionic pressure, which remains well-behaved in the limit $\lambda \to 0$. However, we have not yet rigourised these ideas.

Of the physical quantities of the system, the axial charge W appears to be of primary importance. All of the numerical solutions derived by the methods of Section (3.4.2) converged to states with $W = 0$, but not by our design. It seems the `bvp4c` algorithm simply preferred to converge to these states. We could add boundary conditions to our numerics enforcing W to be non-zero, in a similar manner to how we fixed the cumulative value of T, and therefore generate numerical solutions with non-zero axial charge. We would like to understand what happens to a known $W = 0$ solution if we perturb the value of W. Consider that, owing to the role of W in Equation (3.159), this corresponds somewhat to "pushing down" on the graph of $-P(\tilde{X})$. Then the allowed domain of the density $\tilde{X}(\theta)$ becomes smaller and smaller, until a critical point where the physical roots of $P\left(\tilde{X}\right)$ coincide, and the upper bound on W at equation (3.212) is saturated. We illustrate this in Figure 3.16.

As mentioned at Remark 3.1, we believe there is some very small parameter inherent to our choice of ρ explaining why full coupling gives only a tiny deviation to the fermion energy spectra. Our guess is that is more appropriate to normalise the fermion so that it has density 1 per unit length, rather than 1 per length ρ. This would be more appropriate for modelling a periodic fermion beam, rather than a fermion with periodic boundary conditions localised on a circle. As a very preliminary example, we adapted our iterative numerical process to begin with a $l = \frac{1}{2}$ state with $T = 1$ at $g = 1$, and find solutions evolving T up to a value of 2π. The result is plotted in Figure 3.17. We observe that at $T = 2\pi$, the wobble on the kink has become of order 1. The change in the energy eigenvalue is still quite small; as a function of T it is very well fitted to a quadratic curve. The density function $X(\theta)$ appears

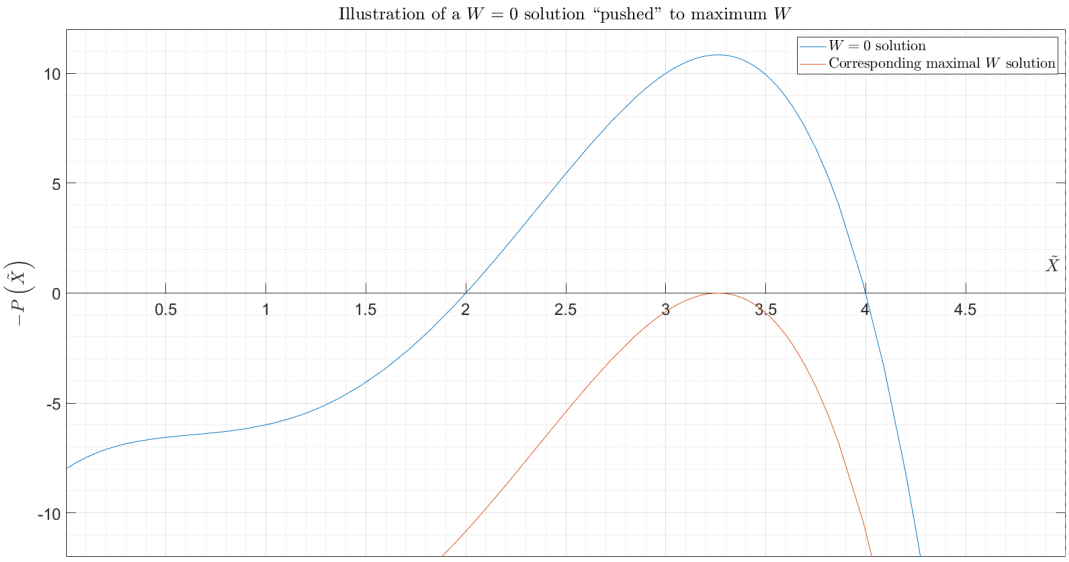

FIGURE 3.16: Illustration of modifying a quartic $P\left(\tilde{X}\right)$ by "pushing" W to a maximal value where only an angular momentum solution exists. (Illustrative only – the blue curve is not a guaranteed physical solution.)

broader.

We discuss some other potential areas of future work in Section 5.2.1.

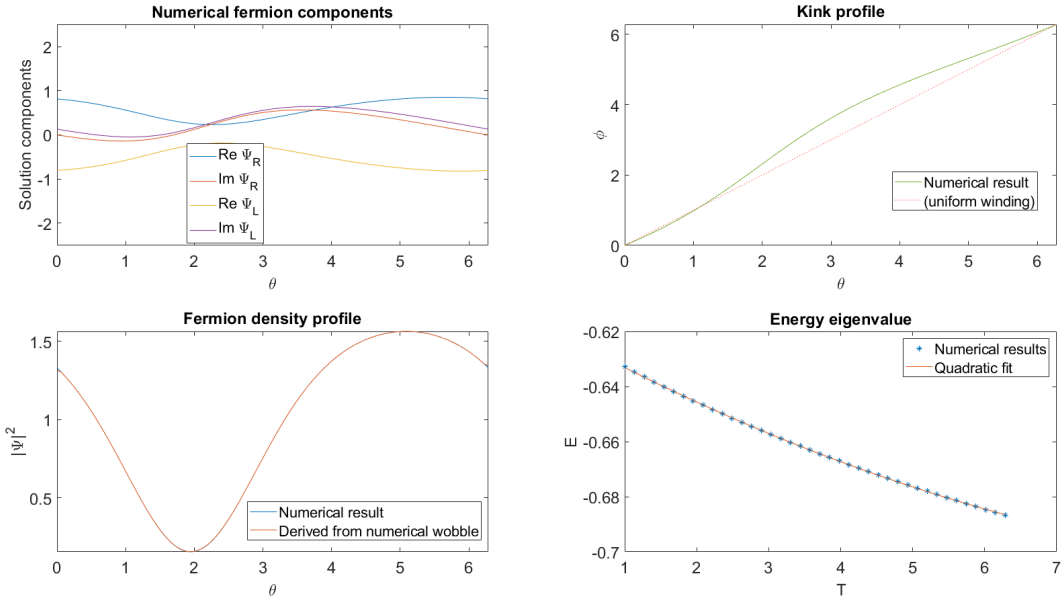

FIGURE 3.17: A numerical $l = \frac{1}{2}$ with $T = 2\pi$ obtained by starting with a $T = 1$ solution and slowly iterating T.

Chapter 4

Spin-isospin fermion-baby Skyrmion coupling on $\mathrm{S}^2 \times \mathbb{R}$

In this chapter, we examine a model of fermion-baby Skyrmion coupling on $\mathbb{R} \times \mathrm{S}^2$. By analogy with the simplicity of the $B = 1$ BPS Skyrmion on S^3 [23, 36, 37, 40], we begin with a fixed scalar field taking values in S^2 in the background of the fermion, prescribed to wind uniformly azimuthally n times over a period of the base space. We will use a Lagrangian analogous to that at (2.10) for the dynamical fermion field, but we will first need to take conventions for the spin and isospin representations, and determine the spin connection on S^2.

Once we have done that preliminary work, we can begin the investigation proper of the fermion dynamics. The ansatz of simple azimuthal winding in the baby Skyrmion permits a straightforward definition of generalised angular momentum about the polar axis. Separating variables, we reduce the eigenvalue problem to solving the latitude profile function of the fermion, which is a function of the polar angle θ. We observe that the differential equation for the latitude profile is Fuchsian when considered to extend to the entire complex plane, and therefore amenable to solution by Frobenius series. We check the Fuchs relations and observe that, up to the critical exponent factor, normalisable solutions are polynomials. This algebra on a fourth-order system is quite taxing to perform by hand; rather than exhibiting the details,

we include a Maple worksheet in Appendix B.1 which performs the necessary manipulations.

We will then specialise to the case $n = 1$, where it is particularly appropriate to use such a simple isovector map as a model of the baby Skyrmion [59]. Here we find that angular momentum corresponding to the azimuthal winding extends to a full $SU(2)$ symmetry of the fermion. We can use the additional symmetry alongside the Fuchsian analysis to solve the problem explicitly by looking for the lowest-weight states of the irreducible representations of $SU(2)$. We are able to determine the exact energy spectrum in this case, as well as outline the constructive algorithm for explicitly determining components of the fermion eigensolutions.

Our treatment of the fermion on $\mathbb{R} \times S^2$ in terms of Fuchsian analysis and the $SU(2)$ representations draws heavily on the approach of Abrikosov [1], who solved the spectrum of the Dirac operator for Euclidean spinors on S^2. We wish to comment that in the absence of isospin, a "pure" Dirac fermion for our purposes is a Lorentzian spinor on $\mathbb{R} \times S^2$ rather than a Euclidean spinor on S^2. We are solving the eigenvalue problem for the fermionic Hamiltonian on our spacetime, which differs from the Euclidean Dirac operator by a factor of γ^0 owing to the difference in the metric signature. Therefore, to ensure we don't accidentally compare apples and oranges, we have also included a Maple worksheet in Appendix B.2 which performs the analogous treatment to Abrikosov's for our Lorentzian Dirac operator. We find that the key results are unchanged. Eigenstates are classified by their half-integer total angular momentum l, their half-integer angular momentum about the polar axis m, and their parity. The energy E_f of a state of total angular momentum l and parity $P = \pm 1$ is

$$E_f = P\left(l + \frac{1}{2}\right). \tag{4.1}$$

This is an illustration of the Lichnerowicz or Lichnerowicz-Weitzenböck theorem, which states that on a pseudo-Riemannian manifold with positive scalar curvature, the square of the Dirac operator is strictly positive [38, 45].

4.1 Constructing the model

4.1.1 Conventions and representations for spinors and isospinors

Here we will briefly review the standard behaviour of spinors on flat space under rotation, in order to clarify the specific conventions for, and differences between, Lorentz spinors and Euclidean isospinors.

Consider the local Clifford algebra for $\mathbb{R} \times S^2$ with Minkowski metric $\eta_{\mu\nu} = \mathrm{diag}(1, -1, -1)$. The Lie algebra $\mathfrak{so}(1,2)$ has three generators: J corresponding to a positive spatial rotation, and K^1, K^2 corresponding to positive boosts in the x^1, x^2 directions respectively. In the vector representation they are

$$J = \begin{pmatrix} 0 & 0 & 0 \\ 0 & 0 & -1 \\ 0 & 1 & 0 \end{pmatrix}, \quad K^1 = \begin{pmatrix} 0 & 1 & 0 \\ 1 & 0 & 0 \\ 0 & 0 & 0 \end{pmatrix}, \quad K^2 = \begin{pmatrix} 0 & 0 & 1 \\ 0 & 0 & 0 \\ 1 & 0 & 0 \end{pmatrix}. \tag{4.2}$$

Let us rewrite them as M^μ, where $(M^0, M^1, M^2) = (J, K^2, -K^1)$. Then M^μ rotates or boosts the $(x^{\mu+1}, x^{\mu+2})$ plane (addition modulo 3) and respects this orientation. Define the totally alternating tensor $\varepsilon^{\lambda\mu\nu}$ by $\varepsilon^{012} = 1$ with indices raised and lowered by η. It's then easily seen that

$$(M^\mu)^\lambda{}_\rho = \varepsilon^{\mu\lambda}{}_\rho \tag{4.3}$$

and

$$[M^\mu, M^\nu] = -\varepsilon^{\mu\nu}{}_\kappa M^\kappa. \tag{4.4}$$

A general Lorentz transformation is given in terms of parameters a_0, a_1, a_2 by

$$\Lambda^\mu{}_\nu = \left(e^{a_\lambda M^\lambda}\right)^\mu{}_\nu. \tag{4.5}$$

The usual (chiral) representation of the Pauli matrices is

$$\sigma_1 = \begin{pmatrix} 0 & 1 \\ 1 & 0 \end{pmatrix}, \quad \sigma_2 = \begin{pmatrix} 0 & -\mathrm{i} \\ \mathrm{i} & 0 \end{pmatrix}, \quad \sigma_3 = \begin{pmatrix} 1 & 0 \\ 0 & -1 \end{pmatrix}. \tag{4.6}$$

They have composition $\sigma_i\sigma_j = \delta_{ij} + \mathrm{i}\varepsilon_{ijk}\sigma_k$. The Clifford algebra is generated by the gamma matrices γ^μ obeying $\{\gamma^\mu, \gamma^\nu\} = 2\eta^{\mu\nu}\mathbb{I}$. For our purposes, it is convenient in this chapter to take the so-called standard representation of the gamma matrices,

$$\gamma^0 = \sigma_3 = \begin{pmatrix} 1 & 0 \\ 0 & -1 \end{pmatrix}, \quad \gamma^1 = -\mathrm{i}\sigma_1 = \begin{pmatrix} 0 & -\mathrm{i} \\ -\mathrm{i} & 0 \end{pmatrix}, \quad \gamma^2 = -\mathrm{i}\sigma_2 = \begin{pmatrix} 0 & -1 \\ 1 & 0 \end{pmatrix}. \tag{4.7}$$

They act on the space of Dirac spinors $\mathbb{C}^2$ by standard multiplication. We contrast this representation with the choice of a chiral basis for the (1+1)-dimensional system of the previous chapter: then, both of the gamma matrices corresponding to space and time directions had only off-diagonal components non-zero, while the chiral gamma matrix was diagonal. Here, in (2+1) dimension, the product $\gamma^0\gamma^1\gamma^2$ is proportional to the identity, so there is no further decomposition of the Dirac spinor into Weyl spinors; i.e. there is no special "chiral gamma matrix." On the other hand, the standard representation easily distinguishes between the diagonal γ^0 corresponding to the time direction, and the off-diagonal γ^1, γ^2 corresponding to space directions. We

will also see that this representation is convenient for the changes of coordinates we will make use of later.

Recall that the Lorentz action on Dirac spinors is usually given by constructing a set of spin generators,

$$S^{\mu\nu} = \frac{i}{4}\left[\gamma^\mu, \gamma^\nu\right], \tag{4.8}$$

and showing that these form a representation of the Lorentz algebra. Working in $(2+1)$ dimensions, there is no need to have two indices on the spin generators. For brevity, let us define

$$S^\mu = -\frac{i}{2}\varepsilon^\mu{}_{\nu\lambda} S^{\nu\lambda}, \tag{4.9}$$

and we find that $S^\mu = -\frac{i}{2}\gamma^\mu$. It's then easily checked that

$$[S^\mu, S^\nu] = -\varepsilon^{\mu\nu}{}_\kappa S^\kappa, \tag{4.10}$$

so these S^μ do form a representation of the M^μ. Thus, for any Lorentz action Λ which in the vector representation has $\Lambda = e^{a_\lambda M^\lambda}$, we can define its action on spinors $S[\Lambda]$ via

$$(S[\Lambda])^\alpha{}_\beta = \left(e^{a_\lambda S^\lambda}\right)^\alpha{}_\beta. \tag{4.11}$$

Let $\Psi \in \mathbb{C}^2$ be a Dirac spinor. The spinor conjugate $\overline{\Psi}$ is defined as $\overline{\Psi} = \Psi^\dagger\gamma^0$. It remains to show that the spinor bilinear $\overline{\Psi}\gamma^\mu\Psi$ belongs to the vector representation, i.e.

$$\overline{(S[\Lambda]\Psi)}\gamma^\mu\,(S[\Lambda]\Psi) = \Lambda^\mu{}_\nu(\overline{\Psi}\gamma^\nu\Psi) = \overline{\Psi}\Lambda^\mu{}_\nu\gamma^\nu\Psi. \tag{4.12}$$

Recall that $\overline{(S[\Lambda]\Psi)} = \Psi^\dagger S[\Lambda]^\dagger\gamma^0 = \overline{\Psi}S[\Lambda]^{-1}$, so it is sufficient to check that $S[\Lambda]^{-1}\gamma^\mu S[\Lambda] = \Lambda^\mu{}_\nu\gamma^\nu$. Expanding the transformations as exponentials,

that is (suppressing spinor indices)

$$e^{-a_\lambda S^\lambda} \gamma^\mu e^{a_\kappa S^\kappa} = \left(e^{a_\rho M^\rho}\right)^\mu{}_\nu \gamma^\nu \tag{4.13}$$

$$\Leftrightarrow (1 - a_\lambda S^\lambda)\gamma^\mu(1 + a_\kappa S^\kappa) = (1 + a_\rho M^\rho)^\mu{}_\nu \gamma^\nu + O(a^2). \tag{4.14}$$

Hence it is sufficient to show that $[\gamma^\mu, S^\lambda] = \left(M^\lambda\right)^\mu{}_\nu \gamma^\nu$. By comparison with (4.10) above, we see that

$$[\gamma^\mu, S^\lambda] = -\varepsilon^{\mu\lambda}{}_\nu \gamma^\nu = \varepsilon^{\lambda\mu}{}_\nu \gamma^\nu = \left(M^\lambda\right)^\mu{}_\nu \gamma^\nu, \tag{4.15}$$

as required. Thus indeed the spinor bilinear $\overline{\Psi}\gamma^\mu\Psi$ is a Lorentz vector.

We proceed similarly for the isospinor, which is constructed as the "Dirac" spinor for $\mathfrak{so}(0,3) = \mathfrak{so}(3)$. The Euclidean metric is just the Kronecker delta δ_{ij}. As the metric is of definite signature, there is no need to distinguish between covariant and contravariant indices, so we will write all indices downstairs. $\mathfrak{so}(3)$ is generated by the three elements J_i, each of which generates a positive rotation in the (x_{i+1}, x_{i+2}) plane (addition modulo 3). In the vector representation they have matrix elements

$$(J_i)_{jk} = -\varepsilon_{ijk}. \tag{4.16}$$

(In particular, J_1 is the same as the J given above for $\mathfrak{so}(1,2)$.) They obey the familiar commutation relation

$$[J_i, J_j] = \varepsilon_{ijk} J_k. \tag{4.17}$$

A rotation of $\mathbb{R}^3$ parametrised by the components of a vector $\boldsymbol{\theta} = (\theta_1, \theta_2, \theta_3)$ is given by

$$R_{ij} = \left(e^{\boldsymbol{\theta}\cdot\boldsymbol{J}}\right)_{ij} = \left(e^{\theta_k J_k}\right)_{ij}. \tag{4.18}$$

Here the Pauli matrices satisfy to generate the Clifford algebra, as they certainly obey $\{\sigma_i, \sigma_j\} = 2\delta_{ij}\mathbb{I}$. They act by standard multiplication on an *isospinor* $\Xi \in \mathbb{C}^2$. Again, to find "spin generators" proportional to commutators $[\sigma_i, \sigma_j]$ it is sufficient to simply rescale the σ_i. Let

$$\Sigma_i = -\frac{\mathrm{i}}{2}\sigma_i. \tag{4.19}$$

It is immediate that these form a representation of the J_i as

$$[\Sigma_i, \Sigma_j] = \varepsilon_{ijk}\Sigma_k. \tag{4.20}$$

Thus a rotation $R = \mathrm{e}^{\boldsymbol{\theta}\cdot\boldsymbol{J}}$ induces an action on an isospinor according to

$$(S[R])_{ab} = \left(\mathrm{e}^{\boldsymbol{\theta}\cdot\boldsymbol{\Sigma}}\right)_{ab}. \tag{4.21}$$

However, in contrast to the spinors in indefinite signature, we see that for the isospinors the corresponding identity to (4.15) is

$$[\sigma_i, \Sigma_j] = -\frac{\mathrm{i}}{2}[\sigma_i, \sigma_j] = \varepsilon_{ijk}\sigma_k = -(J_i)_{jk}\sigma_k. \tag{4.22}$$

The relative minus sign here implies that the isospinor bilinear, $\Xi^\dagger\sigma_i\Xi$, in fact belongs to the conjugate of the vector representation: it rotates *backwards* under the action of rotations, i.e.

$$(S[R]\Xi)^\dagger\sigma_i(S[R]\Xi) = \Xi^\dagger(R^{-1})_{ij}\sigma_j\Xi. \tag{4.23}$$

Thus, to create a rotation-invariant scalar of the form $\Xi^\dagger\boldsymbol{\phi}\cdot\boldsymbol{\sigma}\Xi$, the object $\boldsymbol{\phi}$ should also be in the dual (iso)vector representation, and transform backwards under (iso)rotations.

We wish to clarify that this is not an accidental inconsistency between a

left action and a right action. It is rather a consequence of our convention to write all our indices downstairs, and thus not distinguish between the indices of vector components and basis vectors in Euclidean isospace. We can demonstrate explicitly that the action given above at (4.23) is consistent with the requirement that S is a homomorphism from $\mathrm{SO}(3)$ to $\mathrm{Spin}(3)$. Let $R = R_1 R_2$. Then consider:

$$\begin{aligned}
(S[R_1R_2])^\dagger \, \sigma_i \, (S[R_1R_2]) &= (S[R_1]S[R_2])^\dagger \, \sigma_i \, (S[R_1]S[R_2]) && (4.24)\\
&= S[R_2]^\dagger S[R_1]^\dagger \, \sigma_i \, S[R_1]S[R_2] && (4.25)\\
&= S[R_2]^\dagger \left[(R_1^{-1})_{ij} \, \sigma_j \right] S[R_2] && (4.26)\\
&= (R_2^{-1})_{ik} (R_1^{-1})_{kj} \, \sigma_j && (4.27)\\
&= (R_2^{-1} R_1^{-1})_{ij} \, \sigma_j && (4.28)\\
&= ([R_1R_2]^{-1})_{ij} \, \sigma_j. && (4.29)
\end{aligned}$$

Note also that the constant of proportionality of the spin generators to the basis elements of the Clifford algebras, which was $-\frac{\mathrm{i}}{2}$ in both (4.9) and (4.19) above, was fixed by the desire to equate the commutator in each case. In particular, our choice of orientation fixed the sign, and hence our conclusion that the isospinor bilinear transformed backwards relative to the spinor bilinear. Simply setting $\Sigma_i = +\frac{\mathrm{i}}{2}\sigma_i$ instead at (4.19), for example, would not have made the isospinor bilinear transform forwards, because the commutator would break the orientation of the algebra.

4.1.2 Geometry of the spinor bundle

Formally, a spinor field over a manifold M is a section of a spinor bundle Λ over M. An obstacle to the construction of the required spin structure is the second Stiefel-Whitney class, $w_2(M) \in H^2(M, \mathbb{Z}_2)$ [46]. When $w_2(M)$

vanishes, the manifold is said to be "spin". All orientable 3-manifolds are spin [35].

At each point p of the spin manifold M, we endow the local spinor space $\Lambda_p(M)$ with our chosen representation of the Dirac γ matrices. To construct a Dirac operator for local coordinates x^μ on a chart U of M, we glue these γ matrices to a local orthonormal frame $e_a{}^\mu$, so that coordinate γ matrices are defined

$$\gamma^\mu = e_a{}^\mu \gamma^a. \tag{4.30}$$

We therefore expect that under any change of coordinates, we will also implicitly change the basis of the spinor space.

Let us consider this in general before making specific choices of coordinates. Suppose we have two sets of coordinates, x^μ and $\tilde{x}^\mu$; and corresponding to each, a respectively preferred local orthonormal frame, $e^a{}_\mu$ and $\tilde{f}^a{}_\mu$. We must assume that the components of a Dirac spinor ψ with γ matrices associated to the frame e and coordinates x^μ will transform according to an element S of the spin group when viewed in the coordinates $\tilde{x}^\mu$ and against the frame $\tilde{f}$; that is,

$$\psi \mapsto \tilde{\psi} = S\psi. \tag{4.31}$$

We have seen that we may construct a Lorentz vector V from the spinor bilinear $\overline{\psi}\gamma\psi$. In the respective coordinates, then,

$$V = V^\mu \frac{\partial}{\partial x^\mu} = \tilde{V}^\nu \frac{\partial}{\partial \tilde{x}^\nu}, \tag{4.32}$$

where the contravariant components are

$$V^\mu = \overline{\psi}\gamma^\mu\psi = \overline{\psi} e_a{}^\mu \gamma^a \psi, \tag{4.33}$$

$$\tilde{V}^\nu = \overline{\tilde{\psi}}\tilde{\gamma}^\nu\tilde{\psi} = \overline{\tilde{\psi}} \tilde{f}_a{}^\nu \gamma^a \tilde{\psi}. \tag{4.34}$$

These contravariant components transform according to $\tilde{V}^\nu = \frac{\partial \tilde{x}^\nu}{\partial x^\mu} V^\mu$. Therefore, the spinor transition function S must satisfy

$$\overline{(S\psi)}\tilde{f}_a{}^\nu \gamma^a S\psi = \frac{\partial \tilde{x}^\nu}{\partial x^\mu}\overline{\psi} e_b{}^\mu \gamma^b \psi, \tag{4.35}$$

$$\text{i.e. } S^\dagger \gamma^0 \tilde{f}_a{}^\nu \gamma^a S = \frac{\partial \tilde{x}^\nu}{\partial x^\mu}\gamma^0 e_b{}^\mu \gamma^b \tag{4.36}$$

Now, by definition, $\frac{\partial \tilde{x}^\nu}{\partial x^\mu} e_b{}^\mu$ is $\tilde{e}_b{}^\nu$, the expression of the frame e in the coordinates $\tilde{x}^\nu$. It is still a local orthonormal frame, so it is simply an orthogonal rotation of the elements of the "preferred" frame $\tilde{f}_a{}^\nu$ we associated with the $\tilde{x}^\nu$ coordinates. Let us denote that local rotation as follows:

$$\tilde{e}_b{}^\nu = \tilde{T}_b{}^a \tilde{f}_a{}^\nu. \tag{4.37}$$

Thus, the condition on the spinor transition function S may be expressed just in terms of local orthonormal coordinates as

$$S^\dagger \gamma^0 \gamma^a S = \gamma^0 \tilde{T}_b{}^a \gamma^b. \tag{4.38}$$

Note that once we have specified coordinates and frames, we determine the local rotation matrix $\tilde{T}_b{}^a$. We use this to solve for the spin transition function S. In general there will be two possibilities, since if S is a solution then so is $-S$. This corresponds to the double cover of the spin group over the isometry group of the manifold. We will comment further on this in the next section, in the specific case of coordinate transformation involving polar coordinates. It will illustrate the spin-$\frac{1}{2}$ nature of the fermion, naturally having half-integer angular momentum eigenvalues.

We are nearly ready to construct the Dirac operator on the manifold M. As is typical on curved manifolds, we must make it covariant with respect to the local change of basis by augmenting it with a connection term. We define

the covariant Dirac operator D_μ with respect to coordinate x^μ as

$$D_\mu = \partial_\mu + \Omega_\mu, \tag{4.39}$$

where the *spin connection* Ω is a 1-form taking value in the Lie algebra of the spin group. Under a coordinate transformation $x^\mu \mapsto \tilde{x}^\nu$ with induced spin transformation S, we desire that the covariant derivative of a spinor transforms both as a spinor and a vector;

$$D_\mu \psi \mapsto \tilde{D}_\nu \tilde{\psi} = \frac{\partial x^\mu}{\partial \tilde{x}^\nu} S D_\mu \psi. \tag{4.40}$$

Thus D transforms as

$$D_\mu \mapsto \frac{\partial x^\mu}{\partial \tilde{x}^\nu} S \left(\partial_\mu + \Omega_\mu\right) S^{-1}, \tag{4.41}$$

$$= \frac{\partial x^\mu}{\partial \tilde{x}^\nu} \left(\partial_\mu + S\left[\partial_\mu S^{-1}\right] + S\Omega_\mu S^{-1}\right), \tag{4.42}$$

and so the spin connection satisfies

$$\tilde{\Omega}_\nu = \frac{\partial x^\mu}{\partial \tilde{x}^\nu} \left(S\left[\partial_\mu S^{-1}\right] + S\Omega_\mu S^{-1}\right). \tag{4.43}$$

This is satisfied by contracting the *connection 1-form* $\omega^a{}_b$ with the spin generators:

$$\Omega_\mu = -\frac{\mathrm{i}}{2} \omega_\mu{}^{ab} S_{ab}. \tag{4.44}$$

The connection 1-form $\omega^a{}_b$, taking values in the Lie algebra of the isometry group, is the expression of the Levi-Civita connection in the local frame. To derive its local components, it is easiest to use the metric compatibility (antisymmetry) condition,

$$\omega_{ab} = -\omega_{ba}, \tag{4.45}$$

with the first of Cartan's structure equations expressing that the connection is torsion-free,

$$\mathrm{d}\hat{\theta}^a + \omega^a{}_b \wedge \hat{\theta}^b = 0 \quad (= T^a)\,. \tag{4.46}$$

Here, the $\hat{\theta}^a$ are the dual frame basis,

$$\hat{\theta}^a = e^a{}_\mu \mathrm{d}X^\mu. \tag{4.47}$$

Recall that the torsion 2-form $T^a \in T(M) \otimes \Omega^2 M)$ is obtained as follows. Given a connection ∇, the torsion tensor in the physicist's convention[1] is the type-(1,2) tensor T defined by

$$T(X, Y, \omega) = \omega(\nabla_X Y - \nabla_Y X - [X, Y]). \tag{4.48}$$

Its components are $T^a{}_{bc} = T(\hat{e}_b, \hat{e}_c, \hat{\theta}^a)$, and then the torsion 2-form is obtained by contracting

$$T^a = \frac{1}{2} T^a{}_{bc} \hat{\theta}^b \wedge \hat{\theta}^c. \tag{4.49}$$

In terms of the local frame, the connection components are defined via

$$\nabla_{\hat{e}_a}(\hat{e}_b) = \Gamma^c{}_{ab} \hat{e}_c, \tag{4.50}$$

and the connection 1-form is obtained by the contraction

$$\omega^a{}_b = \Gamma^a{}_{cb} \hat{\theta}^c. \tag{4.51}$$

A developed treatment of the connection 1-form and Cartan structure equations can be found in textbooks such as Nakahara [48].

Again, once we have chosen specific coordinates and frames, we may

[1] The mathematician's convention carries an overall relative minus sign.

solve Cartan's structure equation for the components of the connection 1-form. This allows us to determine the spin connection and complete the construction of the Dirac operator.

4.1.3 Coordinates and transformations on the sphere

To treat Dirac fermions on the sphere, we will employ both spherical polar coordinates and stereographic projection. Polar coordinates will allow us to exploit the symmetries of the sphere, and describe fermion solutions in terms of Fourier modes in the azimuthal angle ϕ and functions of the polar angle θ akin to spherical harmonics. The description of the spectrum of the Dirac operator for spinors without isospin on S^2 in terms of so-called "spinor spherical harmonics" has been achieved by Abrikosov [1]. To check the behaviour of the fermion at the north and south poles of the sphere where the polar coordinates are singular, we will transform to the coordinates of stereographic projections from the opposite pole, respectively.

For clarity, we will describe these coordinates and their charts in terms of the usual embedding of our spacetime manifold $\mathbb{R} \times S^2$ in $\mathbb{R} \times \mathbb{R}^3$, with coordinates $x^\mu = (t, x, y, z)$ such that $x^2 + y^2 + z^2 = 1$. The time coordinate t will be equivalent in all charts, so we will simply describe our charts in terms of the spatial manifold S^2. Thus when we speak of "removing a point" of S^2, we really mean removing the line of points from spacetime corresponding to that spatial location for all time. As we will break the full Lorentz invariance by considering stationary state spinors in a preferred time coordinate, we will not worry about the effects of Lorentz boosts: the spatial submanifold will always be a perfect sphere.

We consider three charts and respective local coordinates:

1. The south chart (U_S, φ_S), where the point with $z = 1$, which we call the north pole, is removed from the sphere. The local coordinates are given

by stereographic projection from the north pole,

$$\varphi_S^\mu = X^\mu = (t, X, Y) = \left(t, \frac{x}{1-z}, \frac{y}{1-z}\right). \tag{4.52}$$

It is convenient to define the radial distance in these stereographic coordinates, R, according to

$$R^2 = X^2 + Y^2. \tag{4.53}$$

2. Similarly, the north chart (U_N, φ_N), where the south pole with $z = -1$ is removed from the sphere, and coordinates are given by stereographic projection from the south pole,

$$\varphi_N^\mu = \tilde{X}^\mu = (t, \tilde{X}, \tilde{Y}), = \left(t, \frac{x}{1+z}, \frac{-y}{1+z}\right). \tag{4.54}$$

Again, we define radial distance $\tilde{R}$ according to

$$\tilde{R}^2 = \tilde{X}^2 + \tilde{Y}^2. \tag{4.55}$$

It is easy to establish the *inversion* symmetry between the stereographic projections from opposite poles:

$$\tilde{R} = \frac{1}{R}. \tag{4.56}$$

3. The polar coordinate chart (U_p, φ_p) with both poles removed from the sphere, and with local coordinates including the usual spherical polar coordinates,

$$\varphi_p^\mu = x_p^\mu = (t, \theta, \phi) = \left(t, \arctan\frac{\sqrt{x^2+y^2}}{z}, \arctan\frac{y}{x}\right). \tag{4.57}$$

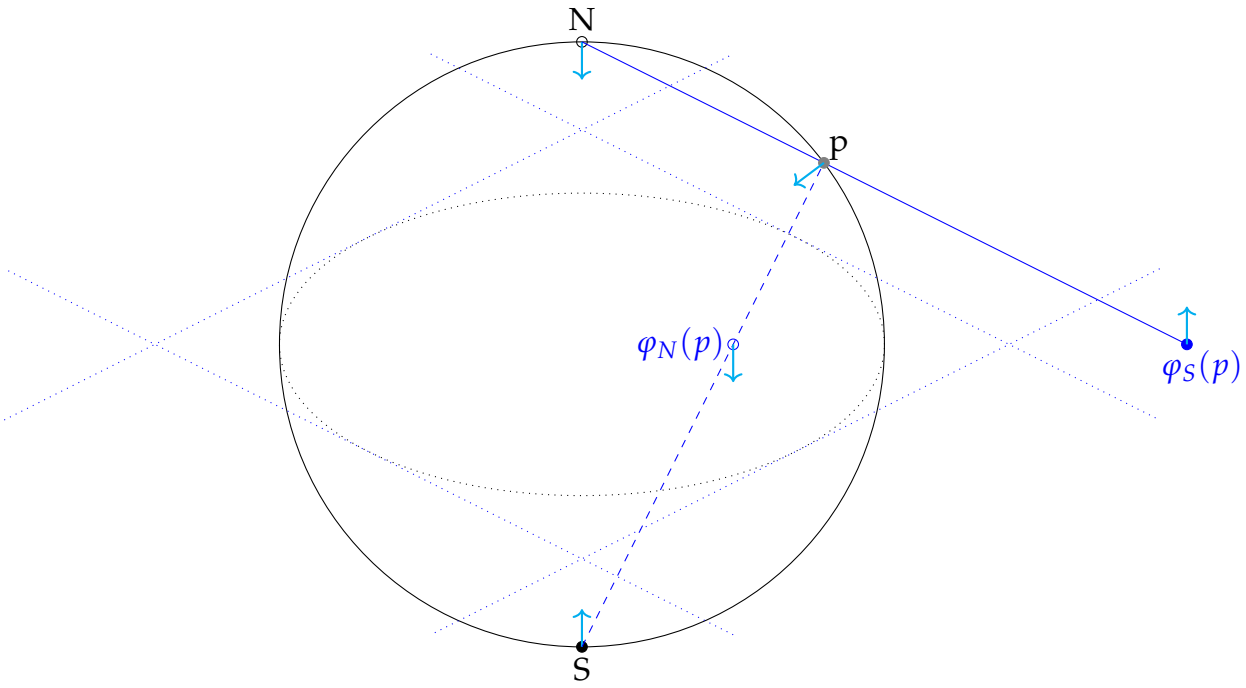

FIGURE 4.1: Stereographic projections of a point p on S^2 to the real plane $\mathbb{R}^2$, in the north and south charts. Observe the arrows indicating the relative orientations induced by the respective coordinates.

Observe that there is a relevant reversal of orientation between the north and south charts, as illustrated at Figure 4.1, corresponding to the coordinate transformation identities

$$\tan\phi = \frac{y}{x} = \frac{Y}{X} = -\frac{\tilde{Y}}{\tilde{X}}. \tag{4.58}$$

Note that we have denoted the local coordinates in the northern stereographic projections a tilde, and subscripted a p to the generalised polar coordinates. We will replicate this convention throughout this section, in order to clarify exactly which local coordinates we are using to express components. So, for example, the metric we obtain by pulling back the flat Minkowski metric, $\eta_{\mu\nu} = \mathrm{diag}(1,-1,-1,-1)$, will be denoted g in coordinates X^μ, $\tilde{g}$ in coordinates $\tilde{X}^\mu$, and g_p in coordinates x_p^μ; and similarly for coordinate-dependent presentations of other objects such as the local orthonormal frames.

Thus from each chart we take, respectively:

1. On U_S,

$$g_{\mu\nu}\mathrm{d}X^\mu \mathrm{d}X^\nu = \mathrm{d}t^2 - \frac{4}{(1+X^2+Y^2)^2}\left(\mathrm{d}X^2 + \mathrm{d}Y^2\right). \tag{4.59}$$

A canonical orthonormal frame e is given by

$$e^a{}_\mu = \mathrm{diag}\left(1, -\frac{2}{1+X^2+Y^2}, -\frac{2}{1+X^2+Y^2}\right) \tag{4.60}$$

$$\Rightarrow e_a{}^\mu = \mathrm{diag}\left(1, -\frac{1+X^2+Y^2}{2}, -\frac{1+X^2+Y^2}{2}\right). \tag{4.61}$$

2. On U_N,

$$\tilde{g}_{\mu\nu}\mathrm{d}\tilde{X}^\mu \mathrm{d}\tilde{X}^\nu = \mathrm{d}t^2 - \frac{4}{(1+\tilde{X}^2+\tilde{Y}^2)^2}\left(\mathrm{d}\tilde{X}^2 + \mathrm{d}\tilde{Y}^2\right). \tag{4.62}$$

A canonical orthonormal frame f is given by

$$\tilde{f}^a{}_\mu = \mathrm{diag}\left(1, -\frac{2}{1+\tilde{X}^2+\tilde{Y}^2}, -\frac{2}{1+\tilde{X}^2+\tilde{Y}^2}\right) \tag{4.63}$$

$$\Rightarrow \tilde{f}_a{}^\mu = \mathrm{diag}\left(1, -\frac{1+\tilde{X}^2+\tilde{Y}^2}{2}, -\frac{1+\tilde{X}^2+\tilde{Y}^2}{2}\right). \tag{4.64}$$

3. On U_p,

$$g_{p\,\mu\nu}\mathrm{d}x_p^\mu \mathrm{d}x_p^\nu = \mathrm{d}t^2 - \mathrm{d}\theta^2 - \sin^2\theta\,\mathrm{d}\phi^2. \tag{4.65}$$

A canonical orthonormal frame h is given by

$$h_p{}^a{}_\mu = \mathrm{diag}\left(1, -1, -\sin\theta\right) \tag{4.66}$$

$$\Rightarrow h_p{}_a{}^\mu = \mathrm{diag}\left(1, -1, -\frac{1}{\sin\theta}\right). \tag{4.67}$$

Explicit calculations to determine the connection 1-form(s) and the spinor transition functions are contained in Appendix A. In summary, we find that

in the coordinates X^μ of U_S, the Dirac operator is

$$\not{D} = \gamma^0 \frac{\partial}{\partial t} - \gamma^i \left(\frac{(1+R^2)}{2} \frac{\partial}{\partial X^i} - \frac{X^i}{2} \right), \tag{4.68}$$

while in polar coordinates, it is

$$\not{D} = \gamma^0 \frac{\partial}{\partial t} - \gamma^1 \left(\frac{\partial}{\partial \theta} + \frac{1}{2} \cot\theta \right) - \gamma^2 \frac{1}{\sin\theta} \frac{\partial}{\partial \phi}. \tag{4.69}$$

We further find that the spinor transition function for changing from polars to stereographic coordinates is $S_{(p\to S)} = \gamma^1 \mathrm{e}^{\frac{\mathrm{i}}{2}\phi\gamma^0}$, i.e.

$$\psi_{(S)} = \gamma^1 \mathrm{e}^{\frac{\mathrm{i}}{2}\phi\gamma^0} \psi_{(p)}. \tag{4.70}$$

We next wish to introduce the (baby) Skyrme field via the real triplet isovector $\boldsymbol{\phi}$, so the fermion field should also be in a spinor representation for isospin. We construct our representation as the tensor product of representations (Spin) $\otimes$ (Isospin): we promote the spin matrices (i.e. Dirac matrices) to

$$\hat{\gamma}^\mu = \gamma^\mu \otimes \mathbb{I}, \tag{4.71}$$

and take standard (flat) isospin matrices

$$\boldsymbol{\tau} = \mathbb{I} \otimes \boldsymbol{\sigma}, \tag{4.72}$$

where $\boldsymbol{\sigma}$ is the usual vector of Pauli matrices. The spin-isospin coupling is modelled by a term of the form

$$g\overline{\Psi}\boldsymbol{\tau} \cdot \boldsymbol{\phi}\Psi, \tag{4.73}$$

where g is a coupling constant. This term is Lorentz invariant. By construction, it is also invariant under isorotation assuming that $\boldsymbol{\phi}$ is a true dynamical

field (in the correct representation). If instead $\boldsymbol{\phi}$ is a fixed background field, the symmetry of this term will involve a transformation of the fermion involving both a spacetime rotation and an internal isorotation, analogous to the symmetry of the prescribed kink of Section 3.3.

4.1.4 The Lagrangian for the spin-isospin coupled fermion and baby Skyrmion

The simplest fermionic Lagrangian including spin-isospin coupling will be

$$\mathcal{L}_f = \overline{\Psi}(i\hbar\hat{\not{D}} - g\boldsymbol{\tau}\cdot\boldsymbol{\phi})\Psi, \tag{4.74}$$

where now $\hat{\not{D}} = \hat{\gamma}^\mu D_\mu = \hat{\gamma}^\mu(\partial_\mu + \Omega_\mu)$, $\Psi(x^\mu)$ is the spin-isospin fermion field, and $\overline{\Psi} = \Psi^\dagger\hat{\gamma}^0$ is the spinor conjugate.

Note that the fermion now has four independent complex components as it is in the tensor product of fundamental representations of both spin and isospin. We label these components as

$$\Psi_{\alpha,a},\ \alpha, a \in \{1,2\}, \tag{4.75}$$

where the first index denotes the spin component and the second denotes the isospin component. We will typically represent this as a vector in $\mathbb{C}^4$, ordering the components as follows:

$$\Psi = \begin{pmatrix} \Psi_{1,1} \\ \Psi_{1,2} \\ \Psi_{2,1} \\ \Psi_{2,2} \end{pmatrix}. \tag{4.76}$$

With this convention, the spin and isospin matrices defined above at (4.71) and (4.72) as tensor products have straightforward representations as block

matrices in $\mathcal{M}_{4\times4}(\mathbb{C})$. For completeness, we note that there is another representation of the fermion Ψ as a 2×2 complex matrix as follows:

$$\Psi = \begin{pmatrix} \Psi_{1,1} & \Psi_{1,2} \\ \Psi_{2,1} & \Psi_{2,2} \end{pmatrix} \in \mathcal{M}_{2\times2}(\mathbb{C}). \tag{4.77}$$

Each row of this 2×2 matrix comprises a spin component, and each column comprises an isospin component. In this convention, the spin matrices $\hat{\gamma}^\mu$ act on the Ψ field via multiplication by the 2×2 γ^μ matrices from the left, and the isospin matrices τ_i act via multiplication by $-\sigma_2\sigma_i\sigma_2$ from the right. This schematic representation is generally available for models of spin-isospin fermions, such as those that couple to Skyrmions on S^3. [23, 37]

We prescribe the soliton field to be static, and to have all of its topology captured simply by uniform azimuthal winding: we model the "baby Skyrmion" of topological charge n as the field $\boldsymbol{\phi} : \mathbb{R} \times \mathrm{S}^2 \to \mathrm{S}^2$, with Euclidean isospace components defined in terms of polar coordinates on spacetime according to

$$\boldsymbol{\phi}(t, \theta, \phi) = \begin{pmatrix} \sin\theta\cos n\phi \\ \sin\theta\sin n\phi \\ \cos\theta \end{pmatrix}. \tag{4.78}$$

This is effectively a very simple hedgehog ansatz for the baby Skyrmion. In Scoccola and Bes [59], the authors found that for $n = 1$ (in our present convention), such a simple profile for the θ-dependence arises when the potential term in the Skyrme model is very weak, or the radius of the spatial 2-sphere is small. To identify our ansatz with their model, we note that we must reverse the boundary conditions on the θ-profile. For our present purposes, this is equivalent to simply "turning isospace upside-down", which might be achieved either by reflecting through the $\phi_1\phi_2$ plane, or rotating by π about any axis perpendicular to the ϕ_3 axis. Without a true, independent

Skyrmion comprising a set of degrees of freedom in the configuration space, we are not concerned with how this relates to a condition of energy finiteness.

4.2 Stationary state ansatz and separation of variables

4.2.1 The Hamiltonian and the generalised angular momentum k

Varying the fermionic Lagrangian (4.74) with respect to $\overline{\Psi}$, we obtain the canonical Dirac equation:

$$\left(\mathrm{i}\hbar\hat{\not{D}} - g\boldsymbol{\tau}\cdot\boldsymbol{\phi}\right)\Psi = 0, \tag{4.79}$$

or in spherical polars,

$$\begin{aligned}\mathrm{i}\hbar\hat{\gamma}^0\frac{\partial\Psi}{\partial t} - \mathrm{i}\hbar\hat{\gamma}^1\left(\frac{\partial\Psi}{\partial\theta} + \frac{1}{2}\cot\theta\,\Psi\right) - \mathrm{i}\hbar\hat{\gamma}^2\frac{1}{\sin\theta}\frac{\partial\Psi}{\partial\phi}\\ -g\left(\sin\theta\cos n\phi\,\tau_1 + \sin\theta\sin n\phi\,\tau_2 + \cos\theta\,\tau_3\right)\Psi = 0.\end{aligned} \tag{4.80}$$

We make the ansatz that the fermion is a stationary state,

$$\Psi(t,\theta,\phi) = \mathrm{e}^{-\mathrm{i}\frac{E_f}{\hbar}t}\,\Psi(\theta,\phi), \tag{4.81}$$

and obtain the Schrödinger-like equation,

$$\begin{aligned}E_f\Psi(\theta,\phi) = \hat{H}_f\Psi := \hat{\gamma}^0\Bigg[\mathrm{i}\hbar\hat{\gamma}^1\left(\frac{\partial}{\partial\theta} + \frac{1}{2}\cot\theta\right) + \mathrm{i}\hbar\hat{\gamma}^2\frac{1}{\sin\theta}\frac{\partial}{\partial\phi}\\ + g\left(\sin\theta\cos n\phi\,\tau_1 + \sin\theta\sin n\phi\,\tau_2 + \cos\theta\,\tau_3\right)\Bigg]\Psi.\end{aligned} \tag{4.82}$$

As usual, the operator implicitly defined here as $\hat{H}_f$ is the *fermionic Hamiltonian*, and $\Psi^\dagger \hat{H}_f \Psi$ is the energy component $\vartheta^t{}_t$ of the energy-momentum tensor $\vartheta^\mu{}_\nu$ associated with the fermionic Lagrangian (4.74). $\hat{H}_f$ is self-adjoint, and the fermionic energy eigenvalue E_f is real.

In these polar coordinates, the Hamiltonian is expressed in matrix form acting on the $\mathbb{C}^4$ representation of the fermion as

$$\hat{H} = \begin{pmatrix} g\cos\theta & g\mathrm{e}^{-\mathrm{i}n\phi}\sin\theta & \hat{H}_a & 0 \\ g\mathrm{e}^{\mathrm{i}n\phi}\sin\theta & -g\cos\theta & 0 & \hat{H}_a \\ \hat{H}_b & 0 & -g\cos\theta & -g\mathrm{e}^{-\mathrm{i}n\phi}\sin\theta \\ 0 & \hat{H}_b & -g\mathrm{e}^{\mathrm{i}n\phi}\sin\theta & g\cos\theta \end{pmatrix}, \tag{4.83}$$

where, simply for brevity and ease of typesetting, we have named the expressions

$$\hat{H}_a = \frac{\partial}{\partial\theta} - \frac{\mathrm{i}}{\sin\theta}\frac{\partial}{\partial\phi} + \frac{1}{2}\cot\theta, \tag{4.84}$$

$$\hat{H}_b = -\frac{\partial}{\partial\theta} - \frac{\mathrm{i}}{\sin\theta}\frac{\partial}{\partial\phi} - \frac{1}{2}\cot\theta = -\hat{H}_a^*. \tag{4.85}$$

The fermionic Lagrangian (4.74) in polar coordinates admits the continuous symmetry whereby

$$\Psi(t,\theta,\phi) \mapsto \mathrm{e}^{-\mathrm{i}\alpha\frac{n}{2}\tau_3}\Psi(t,\theta,\phi-\alpha). \tag{4.86}$$

The Dirac term is certainly invariant under the spatial rotation, and the isorotations cancel. For the coupling term, we take the same perspective on the prescribed baby Skyrmion as we did for the prescribed kink in section 3.3: as it is fixed in the background, we are not free to rotate it azimuthally in the manner we rotate the fermion. The isorotation of the fermion, however,

exactly acts to transform the isovector $\boldsymbol{\phi}$ according to

$$\boldsymbol{\tau} \cdot \boldsymbol{\phi}(t, \theta, \phi) \mapsto \mathrm{e}^{\mathrm{i}\alpha \frac{n}{2}\tau_3} \boldsymbol{\tau} \cdot \boldsymbol{\phi}(t, \theta, \phi) \mathrm{e}^{-\mathrm{i}\alpha \frac{n}{2}\tau_3} = \boldsymbol{\tau} \cdot \boldsymbol{\phi}(t, \theta, \phi - \alpha), \tag{4.87}$$

and so overall the effect of this transformation is just to change ϕ to $\phi - \alpha$ throughout the Lagrangian. We denote the generator of this symmetry as $\hat{K}_3$:

$$\hat{K}_3 = \hbar \left(-\mathrm{i} \frac{\partial}{\partial \phi} + \frac{n}{2} \tau_3 \right). \tag{4.88}$$

$\hat{K}_3$ is self-adjoint and it is not difficult to check that it commutes with $\hat{H}_f$ (and in fact it commutes with the full Dirac operator $\hat{\not{D}}$). We will therefore seek a joint eigenbasis of $\hat{H}_f$ and $\hat{K}_3$ in which to solve the Dirac equation. We will suppose that $\hat{K}_3$ has eigenvalues $\hbar k$, so we will work over a basis of fermion states Ψ_k in which

$$\hat{K}_3 \Psi_k(\theta, \phi) = \hbar k \Psi_k(\theta, \phi). \tag{4.89}$$

(Typically, we will ignore the factors of $\hbar$ on both $\hat{K}_3$ and its eigenvalue from here forwards.) We refer to this value k as the *generalised angular momentum*, or the *grand spin*, about the azimuthal axis. Solving (4.89) shows that Ψ_k must be of the form

$$\Psi_k(\theta, \phi) = \begin{pmatrix} \Psi_{1,1}(\theta, \phi) \\ \Psi_{1,2}(\theta, \phi) \\ \Psi_{2,1}(\theta, \phi) \\ \Psi_{2,2}(\theta, \phi) \end{pmatrix} = \mathrm{e}^{\mathrm{i}\left(k - \frac{n}{2}\tau_3\right)\phi} \Theta_k(\theta) = \begin{pmatrix} \mathrm{e}^{\mathrm{i}\left(k - \frac{n}{2}\right)\phi} \Theta_{1,1}(\theta) \\ \mathrm{e}^{\mathrm{i}\left(k + \frac{n}{2}\right)\phi} \Theta_{1,2}(\theta) \\ \mathrm{e}^{\mathrm{i}\left(k - \frac{n}{2}\right)\phi} \Theta_{2,1}(\theta) \\ \mathrm{e}^{\mathrm{i}\left(k + \frac{n}{2}\right)\phi} \Theta_{2,2}(\theta) \end{pmatrix}, \tag{4.90}$$

for the as-yet undetermined profile functions of just the θ-coordinate, $\Theta_{\alpha,a}(\theta)$. Note that in general the solutions $\Theta_{\alpha,a}(u)$ will also depend on k, but we suppress that label for notational convenience when working directly with these component profile functions.

As the fermion is in the spin-$\frac{1}{2}$ representation of Lorentz spin, the Fourier modes must be strictly half-integers, i.e.

$$k \pm \frac{n}{2} \in \mathbb{Z} + \frac{1}{2}. \tag{4.91}$$

Thus the generalised angular momentum k will be strictly either an integer or half-integer, depending on the parity of the baby Skyrmion azimuthal winding number n:

$$k \in \begin{cases} \mathbb{Z} & \text{for } n \text{ odd}, \\ \mathbb{Z} + \frac{1}{2} & \text{for } n \text{ even}. \end{cases} \tag{4.92}$$

Before investigating the profile functions $\Theta_{\alpha,a}$, we will comment further on this rotational symmetry for Dirac spinors in the context of our coordinate choices.

4.2.2 Aside: angular momentum of spinors and polar coordinates

Let us consider the standard Dirac spinor without isospin. We've seen at (4.69) that the Dirac operator in polar coordinates is

$$\not{D} = \gamma^0 \frac{\partial}{\partial t} - \gamma^1 \left(\frac{\partial}{\partial \theta} + \frac{1}{2} \cot\theta \right) - \gamma^2 \frac{1}{\sin\theta} \frac{\partial}{\partial \phi}.$$

It's obvious that the azimuthal rotation generator $-\mathrm{i}\frac{\partial}{\partial \phi}$ commutes with $\not{D}$. Eigenstates of azimuthal angular momentum are thereby just the Fourier modes:

$$-\mathrm{i}\frac{\partial \psi}{\partial \phi} = k\psi \Rightarrow \psi(\theta, \phi) = \mathrm{e}^{\mathrm{i}k\phi}\Theta(\theta), \tag{4.93}$$

where this $\Theta(\theta)$ is a Dirac spinor. But why, the reader may wonder, do we take the Fourier wavenumber k to be strictly a half-integer? And why do we not explicitly see a spin generator S^μ acting on the fermion? The answer to

these questions is the choice of polar coordinates, and the effect they have on the local neighbourhood of the spinor bundle $\Lambda(U_p)$ living above the polar coordinate chart U_p.

Let's compare to the symmetry of the Dirac fermion in the southern stereographic coordinates on U_S. We saw at (4.68) that the Dirac operator in these coordinates is

$$\not{D} = \gamma^0 \frac{\partial}{\partial t} - \gamma^i \left(\frac{(1+R^2)}{2} \frac{\partial}{\partial X^i} - \frac{X^i}{2} \right).$$

Now, the generator of azimuthal spacetime rotation takes the usual form for rotation in the plane:

$$\hat{L}_3 = \mathrm{i} \left(Y \frac{\partial}{\partial X} - X \frac{\partial}{\partial Y} \right). \tag{4.94}$$

This alone does not commute with $\hat{\not{D}}$, but we would not expect it: over (2+1)-dimensional Minkowski space, we would need to add the spin generator $S^{12} = \frac{\mathrm{i}}{4}\left[\gamma^1, \gamma^2\right] = \frac{1}{2}\gamma^0$ corresponding to rotation in the xy-plane. The curvature of the stereographic coordinate system does not affect azimuthal rotation, and indeed we see that the spinor angular momentum generator

$$\hat{J}_3 = \mathrm{i} \left(Y \frac{\partial}{\partial X} - X \frac{\partial}{\partial Y} \right) + \frac{1}{2}\gamma^0 \tag{4.95}$$

does commute with the Dirac operator:

$$\left[\hat{J}_3, \not{D}\right] = 0. \tag{4.96}$$

Changing from the Dirac operator $\not{D}$ to the associated Hamiltonian $\hat{H}$ only removes the time derivative, and adds another factor of γ^0, with which $\hat{J}_3$ certainly commutes, so we can seek a joint basis of energy and azimuthal angular momentum eigenstates. Then an eigenstate ψ_k of $\hat{J}_3$ satisfying

$$\hat{J}_3 \psi_k = k \psi_k \tag{4.97}$$

is of the form

$$\psi_k(X,Y) = \mathrm{e}^{\mathrm{i}\left(k-\frac{1}{2}\gamma^0\right)\phi}\Theta(\theta) = \begin{pmatrix} \mathrm{e}^{\mathrm{i}\left(k-\frac{1}{2}\right)\phi} f_1(R) \\ \mathrm{e}^{\mathrm{i}\left(k+\frac{1}{2}\right)\phi} f_2(R) \end{pmatrix}, \tag{4.98}$$

where, formally, when we write ϕ it is shorthand for a branch of $\arctan(\frac{Y}{X})$, such that the spinor $\psi_k(X,Y)$ is continuous at the origin $(0,0)$. This expression for the spinor ψ_k is therefore uniquely well-defined for each point of the XY-plane, so *these* Fourier wavenumbers $k \pm \frac{1}{2}$ must be integers. The local fibre neighbourhood $\Lambda(U_S)$ of the spinor bundle over the neighbourhood U_S is just a topologically trivial Cartesian product, $U_S \times \mathbb{C}^2$. Under an *active* transformation where we rotate the spinor by 2π, we effectively parallel transport from the location we started, and the fibre coordinate changes; nonetheless, we stress that the integrality of $k \pm \frac{1}{2}$ is just a question of a *given* spinor being well-defined. This is illustrated in Figure 4.2.

To express this eigenstate in spherical coordinates, we must apply the spinor transition function $S_{(S\to p)}$ derived in Appendix A.2. Thus,

$$\begin{aligned} (\psi_k)_{(p)} &= S_{(S\to p)}\,(\psi_k)_{(S)} \\ &= -\gamma^1 \mathrm{e}^{\frac{\mathrm{i}}{2}\phi\gamma^0}\,(\psi_k)_{(S)} \\ &= \begin{pmatrix} 0 & \mathrm{i}\mathrm{e}^{-\frac{\mathrm{i}}{2}\phi} \\ \mathrm{i}\mathrm{e}^{\frac{\mathrm{i}}{2}\phi} & 0 \end{pmatrix} \begin{pmatrix} \mathrm{e}^{\mathrm{i}\left(k-\frac{1}{2}\right)\phi} f_1\left(R(\theta)\right) \\ \mathrm{e}^{\mathrm{i}\left(k+\frac{1}{2}\right)\phi} f_2\left(R(\theta)\right) \end{pmatrix} \\ &= \mathrm{i} \begin{pmatrix} \mathrm{e}^{\mathrm{i}k\phi} f_2(\theta) \\ \mathrm{e}^{\mathrm{i}k\phi} f_1(\theta) \end{pmatrix}. \end{aligned} \tag{4.99}$$

The change of coordinates has removed the explicit visible effect of the spin generator on the angular momentum eigenstates. Since $k \pm \frac{1}{2} \in \mathbb{Z}$, we maintain that k must be strictly half-integer. There is no contradiction in having a particular choice of spinor be well defined because the neighbourhood U_p

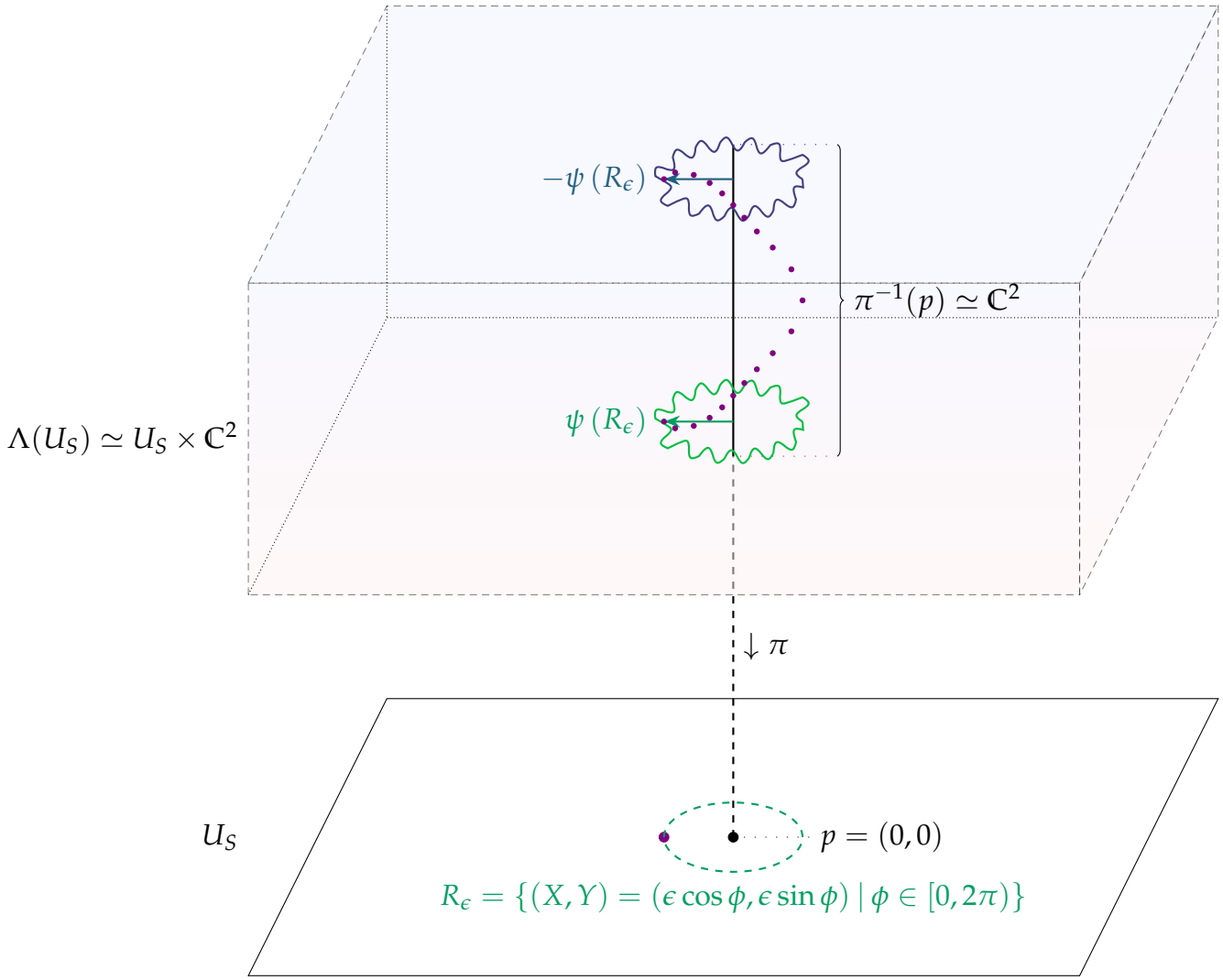

FIGURE 4.2: Illustration of the spinor bundle structure over the contractible neighbourhood U_S. We evaluate a section ψ (green) on a small circle R_ϵ near the south pole: it is periodic under rotation by 2π. However, if we start at a particular reference point on U_S and then actively rotate azimuthally (purple points), after a 2π rotation we find the section has picked up a factor of -1.

is not contractible. It has coordinate singularities at $\theta = 0$ and π, which are connected by a branch cut at some value $\phi = \phi_c$ determined by our choice of the branch of $\arctan(\frac{Y}{X})$. The local fibre neighbourhood $\Lambda(U_p)$ is not the topologically trivial space $U_p \times \mathbb{C}^2$, but instead has a twist like a Möbius strip. The length in the ϕ direction of a closed section is therefore 4π: all of its sections (which are spinor fields) are antiperiodic under $\phi \mapsto \phi + 2\pi$ but periodic under $\phi \mapsto \phi + 4\pi$. Therefore it is perfectly well-defined for the Fourier wavenumber to be the strict half-integer k. This is illustrated in Figure 4.3.

4.2.3 Equations of motion for the profile functions $\Theta_{\alpha,a}$

We return to the spin-isospin fermion where the generalised angular momentum has picked up the $\frac{n}{2}\tau_3$ contribution. We have fully separated the dependence of the fermion on the spacetime coordinates when we introduced the $\Theta_{\alpha,a}$ functions at (4.90). The Dirac eigenvalue problem is reduced to solving this system of four coupled first-order differential equations with eigenvalues E_f and k; explicitly, taking $\hbar = 1$ henceforth,

$$E_f\Theta_{1,1} = g\cos\theta\,\Theta_{1,1} + g\sin\theta\,\Theta_{1,2} + \left[\frac{\mathrm{d}}{\mathrm{d}\theta} + \frac{1}{2}\cot\theta + \frac{\left(k-\frac{n}{2}\right)}{\sin\theta}\right]\Theta_{2,1}, \quad (4.100)$$

$$E_f\Theta_{1,2} = -g\cos\theta\,\Theta_{1,1} + g\sin\theta\,\Theta_{1,1} + \left[\frac{\mathrm{d}}{\mathrm{d}\theta} + \frac{1}{2}\cot\theta + \frac{\left(k+\frac{n}{2}\right)}{\sin\theta}\right]\Theta_{2,2}, \quad (4.101)$$

$$E_f\Theta_{2,1} = -g\cos\theta\,\Theta_{2,1} - g\sin\theta\,\Theta_{2,2} - \left[\frac{\mathrm{d}}{\mathrm{d}\theta} + \frac{1}{2}\cot\theta + \frac{\left(-k+\frac{n}{2}\right)}{\sin\theta}\right]\Theta_{1,1}, \quad (4.102)$$

$$E_f\Theta_{2,2} = g\cos\theta\,\Theta_{2,2} - g\sin\theta\,\Theta_{2,1} - \left[\frac{\mathrm{d}}{\mathrm{d}\theta} + \frac{1}{2}\cot\theta + \frac{\left(-k-\frac{n}{2}\right)}{\sin\theta}\right]\Theta_{1,2}. \quad (4.103)$$

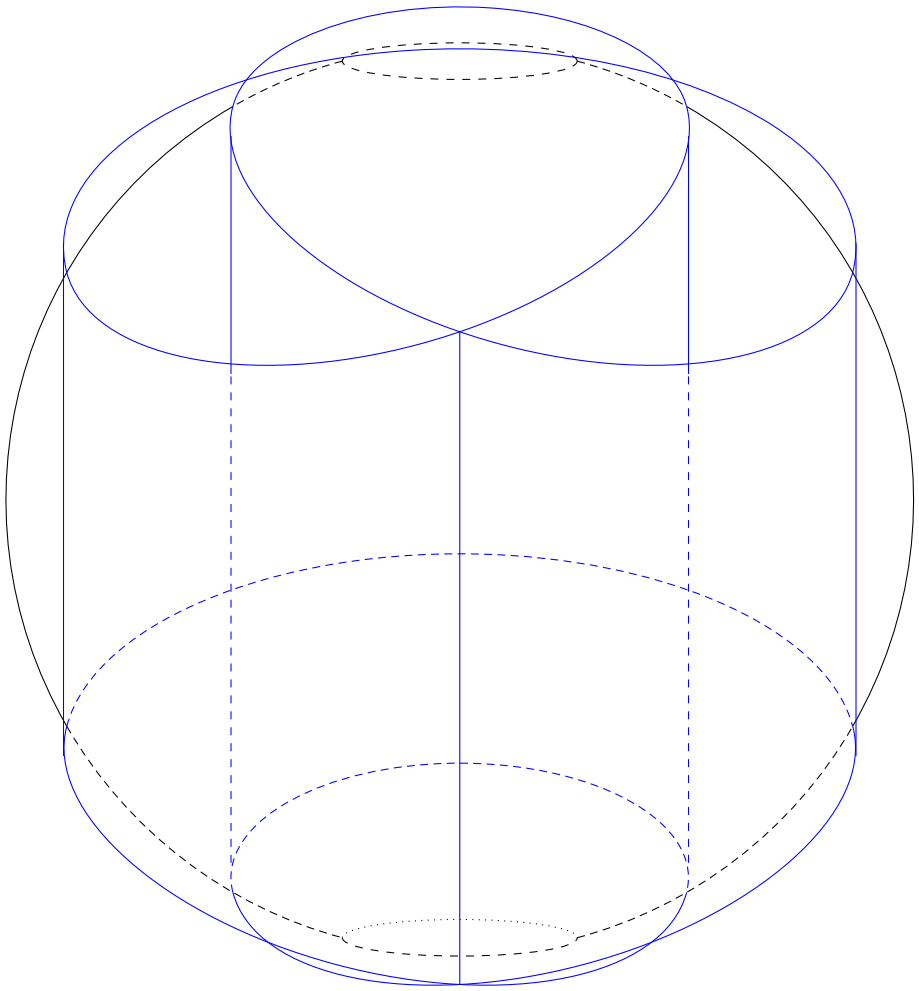

FIGURE 4.3: An illustration of the spinor bundle structure over the non-contractible neighbourhood U_p. U_p (black) is topologically a cylinder: the sphere with neighbourhoods around each pole removed. In contrast, the fibre neighbourhood by $\pi^{-1}(U_p)$ (blue) is non-trivial, and wraps around the cylinder twice. In polar coordinates, a spinor is a section of the blue bundle, and also winds around U_p twice.

Making the change of variables

$$u = \cos\theta, \tag{4.104}$$

we can unambiguously take $\sin\theta = \sqrt{1-u^2}$; moreover, $\frac{\mathrm{d}}{\mathrm{d}\theta} = -\sqrt{1-u^2}\frac{\mathrm{d}}{\mathrm{d}u}$. The system (4.100-4.103) becomes:

$$(E_f - gu)\Theta_{1,1} - g\sqrt{1-u^2}\Theta_{1,2} - \left[-\sqrt{1-u^2}\frac{\mathrm{d}}{\mathrm{d}u} + \frac{u}{2\sqrt{1-u^2}} + \frac{(k-\frac{n}{2})}{\sqrt{1-u^2}}\right]\Theta_{2,1} = 0, \tag{4.105}$$

$$(E_f + gu)\Theta_{1,2} - g\sqrt{1-u^2}\Theta_{1,1} - \left[-\sqrt{1-u^2}\frac{\mathrm{d}}{\mathrm{d}u} + \frac{u}{2\sqrt{1-u^2}} + \frac{(k+\frac{n}{2})}{\sqrt{1-u^2}}\right]\Theta_{2,2} = 0, \tag{4.106}$$

$$(-E_f - gu)\Theta_{2,1} - g\sqrt{1-u^2}\Theta_{2,2} - \left[-\sqrt{1-u^2}\frac{\mathrm{d}}{\mathrm{d}u} + \frac{u}{2\sqrt{1-u^2}} + \frac{(-k+\frac{n}{2})}{\sqrt{1-u^2}}\right]\Theta_{1,1} = 0, \tag{4.107}$$

$$(-E_f + gu)\Theta_{2,2} - g\sqrt{1-u^2}\Theta_{2,1} - \left[-\sqrt{1-u^2}\frac{\mathrm{d}}{\mathrm{d}u} + \frac{u}{2\sqrt{1-u^2}} + \frac{(-k-\frac{n}{2})}{\sqrt{1-u^2}}\right]\Theta_{1,2} = 0. \tag{4.108}$$

We can reduce the system (4.105-4.108) first to a coupled pair of second-order differential equations by eliminating two of the four $\Theta_{\alpha,a}$ component functions; then, we can ultimately reduce to a single fourth-order differential equation in just one component function. This algebraic process is made much less taxing with the assistance of a computer. We used Maple 2022 to perform the reduction, and for the subsequent Fuchsian analysis. We have included that code in Appendix B.1.

Observe that in each equation, the profile function which multiplies E_f is coupled to the two other profile functions with which it shares a spin or isospin state, but not to the component of the opposite state in both spin and isospin: e.g. in (4.105), $\Theta_{1,1}$ couples to $\Theta_{1,2}$ via g and $\Theta_{2,1}$ via spatial derivative, but not to $\Theta_{2,2}$. This has the effect of making the algebra the simplest if the two components we eliminate are opposite in both senses. We

will therefore begin the reduction by eliminating $\Theta_{1,2}$ and $\Theta_{2,1}$, to result in the pair of second-order equations coupling $\Theta_{1,1}$ and $\Theta_{2,2}$ as follows:

$$\begin{aligned}
&\left(u^2-1\right)^2\left(E_f+gu\right)\frac{\mathrm{d}^2\Theta_{1,1}}{\mathrm{d}u^2}+\left(u^2-1\right)^2\left(gu^2+2E_fu+g\right)\frac{\mathrm{d}\Theta_{1,1}}{\mathrm{d}u}\\
&+\left\{-\frac{1}{4}gu^3+\left[\frac{E_f}{4}+(2k-n)\,g\right]u^2-\left[k-\frac{n}{2}\right]\left[\left(k-\frac{n}{2}\right)g-E_f\right]u\right.\\
&\qquad\left.-\left[k-\frac{n}{2}\right]g-E_f\left[\frac{1}{2}+k^2+\frac{n^2}{4}-kn\right]+\left[u^2-1\right]\left[g^2-E_f^2\right]\left[E_f+gu\right]\right\}\Theta_{1,1}\\
&\qquad=g\left[\left(E_f-gn\right)u-E_fn+g\right]\left(u^2-1\right)\Theta_{2,2}, \qquad (4.109)\\
&\left(u^2-1\right)^2\left(E_f+gu\right)\frac{\mathrm{d}^2\Theta_{2,2}}{\mathrm{d}u^2}+\left(u^2-1\right)^2\left(gu^2+2E_fu+g\right)\frac{\mathrm{d}\Theta_{2,2}}{\mathrm{d}u}\\
&+\left\{-\frac{1}{4}gu^3+\left[\frac{E_f}{4}-(2k+n)\,g\right]u^2-\left[k+\frac{n}{2}\right]\left[\left(k+\frac{n}{2}\right)g+E_f\right]u\right.\\
&\qquad\left.+\left[k+\frac{n}{2}\right]g-E_f\left[\frac{1}{2}+k^2+\frac{n^2}{4}+kn\right]+\left[u^2-1\right]\left[g^2-E_f^2\right]\left[E_f+gu\right]\right\}\Theta_{2,2}\\
&\qquad=g\left[\left(E_f-gn\right)u-E_fn+g\right]\left(u^2-1\right)\Theta_{1,1}. \qquad (4.110)
\end{aligned}$$

(Observe that these equations are transformed into each other by the combination of swapping $\Theta_{1,1}$ with $\Theta_{2,2}$ and swapping k to $-k$. This suggests that when $k=0$, we might make ansätze that $\Theta_{1,1}=\pm\Theta_{2,2}$; we will return to this observation later.)

There are frequent factors of u^2-1 in the above differential equations: this is unsurprising, as the points $u=\pm1$ correspond to the poles of the sphere, where we will find coordinate singularities. However, we see that the spin-isospin coupling has also introduced two other factors which may give rise to singular behaviour when $g\neq0$:

1. $\left(E_f+gu\right)$, which vanishes at

$$u=-\frac{E_f}{g}; \qquad (4.111)$$

2. $\left[\left(E_f-gn\right)u-E_fn+g\right]$, which vanishes at

$$u=\frac{g-nE_f}{gn-E_f}. \qquad (4.112)$$

We should pay careful attention to the behaviour of any potential solutions at these points. Observe in particular that for $n = \pm 1$, the point given by (4.112) coalesces with the pole $u = \pm 1$ respectively, so will certainly contribute to singular behaviour there. We therefore refer to that value of u henceforth as the *coalescent pole*.

Finally, we can substitute (4.109) into (4.110) to obtain the single, fourth-order differential equation for $\Theta_{1,1}(u)$. We may sometimes refer to this as the *master* equation in this context. It takes the schematic form

$$R_1(u)\frac{\mathrm{d}^4\Theta_{1,1}}{\mathrm{d}u^4} + R_2(u)\frac{\mathrm{d}^3\Theta_{1,1}}{\mathrm{d}u^3} + R_3(u)\frac{\mathrm{d}^2\Theta_{1,1}}{\mathrm{d}u^2} + R_4(u)\frac{\mathrm{d}\Theta_{1,1}}{\mathrm{d}u} + R_5(u)\Theta_{1,1}(u) = 0, \tag{4.113}$$

for coefficient functions $R_i(u)$. The expressions for these functions get quite long, particularly $R_4(u)$ and $R_5(u)$, and we have not found any elegant way of making them presentable. Therefore, we will not set out the explicit expressions here. Maple code which will generate these functions explicitly is contained in Appendix B.1.1. For now, we will rewrite them in the format

$$R_i(u) = \left(u^2-1\right)^{a_i}\left(E_f+gu\right)^{b_i}\left[g\left(\left(E_f-gn\right)u - E_f n + g\right)\right]^{c_i}\hat{R}_i(u), \tag{4.114}$$

so that the structure of the singularities may be easily observed. We may take $\hat{R}_1(u) = 1$ WLOG. We obtain:

$$R_1(u) = \left(u^2-1\right)^4\left(E_f+gu\right)^2\left[g\left(\left(E_f-gn\right)u - E_f n + g\right)\right]^2, \tag{4.115}$$

$$R_2(u) = \left(u^2-1\right)^3\left(E_f+gu\right)^2\left[g\left(\left(E_f-gn\right)u - E_f n + g\right)\right]\hat{R}_2(u), \tag{4.116}$$

$$R_3(u) = \left(u^2-1\right)^2\left(E_f+gu\right)^2\hat{R}_3(u), \tag{4.117}$$

$$R_4(u) = \left(u^2-1\right)\left(E_f+gu\right)^2\hat{R}_4(u), \tag{4.118}$$

$$R_5(u) = \left(E_f+gu\right)^2\hat{R}_5(u). \tag{4.119}$$

It is immediately clear that the north and south poles of the sphere corresponding to $u = \pm 1$ are regular singular points of the differential equation (4.113). Since the power of $\left(E_f + gu\right)$ is the same in each term, these may be cancelled without issue, and we determine that the point $u = -\frac{E_f}{g}$ is not actually a singularity. On the other hand, the coalescent pole (4.112) is a singularity, but it is also a regular singular point.

By making the substitution $u = \frac{1}{v}$ throughout, we can also determine that the point $v = 0$ is a regular singular point of (4.113). Physically, u only takes values between -1 and 1, but if we allow it to take values on the Riemann sphere $\hat{\mathbb{C}} = \mathbb{C} \cup \{\infty\}$, then we have seen that the differential equation (4.113) for $\Theta_{1,1}(u)$ has no essential singularities in the complex variable u. We can therefore seek to find Frobenius series solutions in the neighbourhoods of each regular singular point.

4.2.4 Fuchsian analysis for general n

If a differential equation for a function $y(u)$ of a complex variable u has a regular singular point at $u = u_0$, then a Frobenius series about u_0 is a power series of the form

$$w(u) = (u - u_0)^r \left[1 + \sum_{m=1}^{\infty} a_m (u - u_0)^m\right]. \tag{4.120}$$

The value r is a real number called the *exponent* of the pole u_0. By substituting the Frobenius series into the differential equation for $y(u)$, a condition on r called the *indicial equation* is obtained, which says that r is a root of a degree m polynomial, where m is the order of the differential equation. There is always a series solution corresponding to the strictly greatest value of r that solves the indicial equation, with a non-negative radius of convergence. Other roots of the indicial equation will also provide distinct and independent Frobenius power series solutions if the exponents do not differ by an

Pole	Exponent	Roots of indicial equation
$u = 1$	μ	$\pm\frac{1}{2}\left(k+\frac{n}{2}+\frac{1}{2}\right)+1, \pm\frac{1}{2}\left(k-\frac{n}{2}-\frac{1}{2}\right)$
$u = -1$	ν	$\pm\frac{1}{2}\left(k+\frac{n}{2}-\frac{1}{2}\right)+1, \pm\frac{1}{2}\left(k-\frac{n}{2}+\frac{1}{2}\right)$
$u = \frac{E_f n - g}{E_f - gn}$	κ	$0, 1, 3, 4$
$u = \hat{\infty}$	λ	$\pm\frac{\sqrt{1+4\left(E_f-gn\right)+4\left(E_f^2-g^2\right)}}{2}, \pm\frac{\sqrt{1-4\left(E_f-gn\right)+4\left(E_f^2-g^2\right)}}{2}$

TABLE 4.1: The poles and respective exponents of (4.113).

integer (including zero). However, if two roots of the indicial equation do differ by an integer, the corresponding solutions may pick up logarithmic behaviour about the pole. (This is similar to the behaviour of special functions "of the second type" that exist for certain Sturm-Liouville problems, such as Bessel functions, and especially special functions which are generalisations of families of orthogonal polynomials, such as the Legendre functions.) This logarithmic behaviour notwithstanding, there will exist locally at every point of $\hat{\mathbb{C}}$ excepting the poles a family of m distinct solutions for $y(u)$ in this manner whenever the *Fuchs relation* is satisfied:

$$\sum_{u_i \text{ a pole in } \hat{\mathbb{C}}} \left(\sum_{r \text{ an exponent at } u_i} r \right) = \frac{m(m-1)(p-1)}{2}, \tag{4.121}$$

where m is the order of the differential equation and p is the number of *finite* poles in $\mathbb{C}$. In this calculation, the exponents at $u = \hat{\infty}$ are taken to be the roots of the indicial polynomial for $v = \frac{1}{u}$ about $v = 0$. A rigorous development of the above analysis is developed in Whittaker and Watson [68] and in Ince [29].

The Maple code in Appendix B.1.2 determines and solves the indicial equations at $u = 1, -1, \hat{\infty}$ and at the coalescent pole. We summarise the results in Table 4.1. For convenience and clarity, we have labelled the possible exponents distinctly at each pole.

We make a number of observations. First, the Fuchs relation is satisfied:

the sum of all possible exponents is 12, which matches the RHS of (4.121) since $m = 4$ and $p = 3$. Second, the exponents at $u = 1$ and $u = -1$ are interchanged if we exchange k and n with $-k$ and $-n$, respectively. This can be interpreted as the fact that reflecting both space and isospace about their azimuthal axes is equivalent to reversing both the winding number n of the soliton and the azimuthal Fourier mode k of the fermion. There appear to be further discrete symmetries of the energy spectrum under transformations which also involve reversing the signs of E_f and g, but we have not determined the transformation of the system which exhibits this symmetry.

Fourth, we see that the energy eigenvalue E_f actually contributes to the exponents λ at infinity. Solving for allowed values of E_f in terms of λ, we find:

$$E_f = \pm_A \frac{1}{2} \pm_B \sqrt{\lambda^2 + g\,(g \mp_A n)}. \tag{4.122}$$

By the subscript on the signs $\pm_A$ we indicate that these signs are not independent but must take identical values. The sign $\pm_B$ is independent of the paired signs $\pm_A$.

Equation (4.122) establishes the following:

Remark 4.1 (The energy spectrum of the spin-isospin coupled Dirac fermion on S^2, in terms of profile function asymptotics)**.** Any solution of the Dirac equation (4.79) which

1. is regular on the spatial manifold S^2,
2. is a joint eigenstate of both energy and azimuthal grand spin, and
3. for which $\Theta_{1,1}(u) \sim u^s$ asymptotically, i.e.

$$\Theta_{1,1}(u) \in O(u^s) \iff s \leq -\lambda, \tag{4.123}$$

has fermionic energy eigenvalue E_f equal to one of the four values

$$\pm_A \frac{1}{2} \pm_B \sqrt{\lambda^2 + g\,(g \mp_A n)}.$$

Strictly, this remark also holds if we relax to allow the solution to be singular at $u = 1, -1$ and at most one other finite point. However, we are only interested in solutions which are regular for all $u \in [-1, 1]$.

4.2.5 Polynomial solutions and energy levels

Our general philosophy from here forwards is to use the Fuchsian analysis to seek "polynomial" solutions for the profile functions $\Theta_{\alpha,a}(u)$. By this, we mean solutions $w(u)$ where the generically infinite sum in the local Frobenius series (4.120) terminates at finite degree about one (or more) of the regular singular points:

$$w(u) = (u - u_0)^r\, P(u - u_0), \quad P(u - u_0) = 1 + \sum_{m=1}^{N} a_m\, (u - u_0)^m\,; \quad (4.124)$$

i.e. strictly it is $P(u - u_0) = (u - u_0)^{-r}\, w(u)$ which is polynomial, but we will be a little imprecise in our terminology and refer to the full solution $w(u)$ as "polynomial". Often, it is only possible to seek a solution which is polynomial about at most one of the poles: when r is not an integer, then the analytic continuation of $(u - u_0)^r$ into the neighbourhood of a different pole $u_1 \neq u_0$ will not have a terminating power series.

In light of Remark 4.1, the energy E_f of a polynomial solution can be determined in terms of the polynomial degree $N = \deg P$. At large values of $|u|$, the asymptotic behaviour of the polynomial solution (4.124) is

$$w(u) \sim (u - u_0)^{r+N} \sim u^{r+N}. \quad (4.125)$$

Regardless of the placement of the finite poles, this solution extends to a neighbourhood of ∞. But in such a neighbourhood, we have derived the local solution

$$\begin{aligned} w(u) &= u^{-\lambda}\left(1 + \sum_{m=1}^{\infty} b_m u^{-m}\right) \\ &\sim u^{-\lambda}. \end{aligned} \tag{4.126}$$

Equating these expressions, we obtain

$$-\lambda = r + N. \tag{4.127}$$

Here, r is an exponent at one of the poles, and we observed in Table 4.1 that the exponents at the north and south pole are defined in terms of the azimuthal grand spin k (as well as the winding number n). This introduces k into the expression(s) for the energy E_f (4.122). k alone does not determine the value of λ, but, for fixed n, we see that the combination of k and N does explicitly determine the value of (each possible branch of) E_f. We therefore see that it is extremely plausible that most energy levels will be degenerate: there will be a (finite) degeneracy given by the number of partitions of λ into k and N. For general n, it is not a priori clear how to control for the permitted values of λ, N and k. However, in the special case $n = 1$ we will show that our joint eigenstates of E_f and k fall into irreducible $\mathrm{SU}(2)$ representations, and we can therefore completely solve for and classify the energy spectrum.

4.3 The case $n = 1$

The case $n = 1$ is the simplest model of the fermion coupled to a baby Skyrmion with non-zero topological charge. As we have mentioned, Scoccola and Bes [59] shows that our simple prescribed hedgehog form of the

Pole	Exponent	Roots of indicial equation
$u = 1$	μ	$\pm\frac{1}{2}(k+1)+2, \pm\frac{1}{2}(k-1)$
$u = -1$	ν	$\pm\frac{k}{2}+1, \pm\frac{k}{2}$
$u = \infty$	λ	$\pm\frac{\sqrt{1+4\left(E_f-g\right)+4\left(E_f^2-g^2\right)}}{2}, \pm\frac{\sqrt{1-4\left(E_f-g\right)+4\left(E_f^2-g^2\right)}}{2}$

TABLE 4.2: The poles and respective exponents of (4.113) for $n = 1$.

baby Skyrmion is similar to an actual solution in the baby Skyrmion model with a weak potential. This case is also analogous to the model of the Skyrmion on S^3 studied by Krusch and Goatham [23, 37].

4.3.1 The effect of the coalescent pole

As we mentioned earlier, for $n = 1$ the coalescent pole given by (4.112) coincides with the north pole of the sphere $u = 1$. We should therefore redo the Fuchsian analysis for general k in the case $n = 1$. The code is in Appendix B.1.3 and the results are contained in Table 4.2. We observe that the effect of the coalescent pole at $u = 1$ is to change the exponents which in the general case (Table 4.1) were of the form

$$\pm\frac{1}{2}\left(k+\frac{n}{2}+\frac{1}{2}\right)+1 \tag{4.128}$$

to now be of the form

$$\pm\frac{1}{2}\left(k+\frac{n}{2}+\frac{1}{2}\right)+2. \tag{4.129}$$

The Fuchs relation is satisfied for the new exponents with just the two finite poles at $u = 1$ and $u = -1$.

The $n = 1$ eigensolution for general k takes the polar coordinate form, according to (4.90), of

$$\Psi_p(u,\phi) = \begin{pmatrix} \mathrm{e}^{\mathrm{i}\left(k-\frac{1}{2}\right)\phi}\Theta_{1,1}(u) \\ \mathrm{e}^{\mathrm{i}\left(k+\frac{1}{2}\right)\phi}\Theta_{1,2}(u) \\ \mathrm{e}^{\mathrm{i}\left(k-\frac{1}{2}\right)\phi}\Theta_{2,1}(u) \\ \mathrm{e}^{\mathrm{i}\left(k+\frac{1}{2}\right)\phi}\Theta_{2,2}(u) \end{pmatrix}. \tag{4.130}$$

Using our now familiar spinor transition functions, we see that in the stereographic coordinates we obtain

$$\Psi(u,\phi) = \begin{pmatrix} \mathrm{e}^{\mathrm{i}(k-1)\phi}\Theta_{2,1}(u) \\ \mathrm{e}^{\mathrm{i}k\phi}\Theta_{2,2}(u) \\ \mathrm{e}^{\mathrm{i}k\phi}\Theta_{1,1}(u) \\ \mathrm{e}^{\mathrm{i}(k+1)\phi}\Theta_{1,2}(u) \end{pmatrix}, \quad \tilde{\Psi}(u,\phi) = \begin{pmatrix} \mathrm{e}^{\mathrm{i}k\phi}\Theta_{2,1}(u) \\ \mathrm{e}^{\mathrm{i}(k+1)\phi}\Theta_{2,2}(u) \\ \mathrm{e}^{\mathrm{i}(k-1)\phi}\Theta_{1,1}(u) \\ \mathrm{e}^{\mathrm{i}k\phi}\Theta_{1,2}(u) \end{pmatrix}. \tag{4.131}$$

We see therefore that $\mu = 0$ is appropriate only for $k = 1$, and $\nu = 0$ is appropriate only for $k = 0$.

4.3.2 The generalised angular momentum algebra for $n = 1$

Our hedgehog ansatz preserves the azimuthal axial symmetry of the sphere, but for general n it breaks the two other independent symmetries of S^2. In the case $n = 1$, however, the isovector $\boldsymbol{\phi}$ is simply the identity map from spatial S^2 to isospace S^2, and so the full symmetry group is preserved. For the Dirac fermion on S^2 in the absence of isospin, Abrikosov [1] shows that the fundamental $\mathrm{SU}(2)$ representation on S^2 is intimately linked to the spectrum of the Dirac operator. Complementary to

$$\hat{L}_3 = -\mathrm{i}\frac{\partial}{\partial\phi}, \tag{4.132}$$

the other angular momentum generators may be expressed

$$\hat{L}_1 = \mathrm{i}\sin\phi\frac{\partial}{\partial\theta} + \mathrm{i}\cos\phi\cot\theta\frac{\partial}{\partial\phi} + \frac{1}{2}\frac{\cos\phi}{\sin\theta}\gamma^0, \tag{4.133}$$

$$\hat{L}_2 = -\mathrm{i}\cos\phi\frac{\partial}{\partial\theta} + \mathrm{i}\sin\phi\cot\theta\frac{\partial}{\partial\phi} + \frac{1}{2}\frac{\sin\phi}{\sin\theta}\gamma^0. \tag{4.134}$$

These satisfy the $\mathrm{SU}(2)$ Lie algebra,

$$\left[\hat{L}_i, \hat{L}_j\right] = \mathrm{i}\epsilon_{ijk}\hat{L}_k, \tag{4.135}$$

and all commute with Abrikosov's Dirac operator:

$$\left[\hat{L}_i, \not{D}\right] = 0. \tag{4.136}$$

This permits a classification of the Dirac spectrum in terms of joint eigenstates of $\hat{L}_3$ and $\hat{\boldsymbol{L}}^2 = \hat{L}_1\hat{L}_1 + \hat{L}_2\hat{L}_2 + \hat{L}_3\hat{L}_3$.

An identical approach can be taken for Lorentz spinors on $\mathbb{R} \times \mathrm{S}^2$ in the absence of isospin, with the same $\mathrm{SU}(2)$ representation (4.132-4.134). We will not re-invent the wheel by giving the details of the calculations, but we include a demonstration in the Maple worksheet in Appendix B.2.

We have seen that with the inclusion of isospin, the appropriate generalisation of the total angular momentum operator $\hat{L}_3$ is our $\hat{K}_3$ given at equation (4.88), in this case

$$\hat{K}_3 = -\mathrm{i}\frac{\partial}{\partial\phi} + \frac{1}{2}\tau_3. \tag{4.137}$$

In the case $n = 1$ where we expect to preserve the full symmetry group of S^2, an obvious attempt at compatible operators is to simply add the appropriate

τ matrices to $\hat{L}_1$ and $\hat{L}_2$:

$$\hat{K}_1 = \mathrm{i}\sin\phi\frac{\partial}{\partial\theta} + \mathrm{i}\cos\phi\cot\theta\frac{\partial}{\partial\phi} + \frac{1}{2}\frac{\cos\phi}{\sin\theta}\hat{\gamma}^0 + \frac{1}{2}\tau_1, \tag{4.138}$$

$$\hat{K}_2 = -\mathrm{i}\cos\phi\frac{\partial}{\partial\theta} + \mathrm{i}\sin\phi\cot\theta\frac{\partial}{\partial\phi} + \frac{1}{2}\frac{\sin\phi}{\sin\theta}\hat{\gamma}^0 + \frac{1}{2}\tau_2. \tag{4.139}$$

Since $[\gamma^a, \tau_i] = 0$ for all a and i, it is immediate that these operators satisfy the $\mathrm{SU}(2)$ Lie algebra

$$\left[\hat{K}_i, \hat{K}_j\right] = \mathrm{i}\epsilon_{ijk}\hat{K}_k. \tag{4.140}$$

A little algebra shows that, in the case $n = 1$,

$$\left[\hat{K}_1, \hat{H}_f\right] = 0 = \left[\hat{K}_2, \hat{H}_f\right]. \tag{4.141}$$

Define the *total generalised angular momentum*, or *total grand spin*, operator by

$$\hat{\boldsymbol{K}}^2 = \hat{K}_1\hat{K}_1 + \hat{K}_2\hat{K}_2 + \hat{K}_3\hat{K}_3. \tag{4.142}$$

This is a Casimir operator for the representations of $\mathrm{SU}(2)$ that these operators define. The eigenvalue of $\hat{\boldsymbol{K}}^2$ is mutually conserved with E_f and k. We will use a curly ℓ to label joint eigenstates of $\hat{\boldsymbol{K}}^2$ and $\hat{K}_3$, according to

$$\hat{\boldsymbol{K}}^2\Psi^{(\ell,k)} = \ell\left(\ell+1\right)\Psi^{(\ell,k)}, \quad \hat{K}_3\Psi^{(\ell,k)} = k\Psi^{(\ell,k)}. \tag{4.143}$$

By the definition (4.142), we see that

$$\ell\left(\ell+1\right) \geq 0, \tag{4.144}$$

so there are no permitted values of ℓ in the open interval $(-1, 0)$. Moreover, ℓ must also satisfy

$$\ell\left(\ell+1\right) \geq k^2 \tag{4.145}$$

for any state $\Psi_{\ell,k}$, which for a given ℓ can be satisfied by only finitely many values of k. Thus the irreducible representations of the grand spin algebra are finite-dimensional, and we unambiguously take $\ell \geq 0$.

We also define grand spin raising and lowering operators,

$$\hat{K}_+ = \hat{K}_1 + \mathrm{i}\hat{K}_2 = \mathrm{e}^{\mathrm{i}\phi}\left(\frac{\partial}{\partial\theta} + \mathrm{i}\cot\theta\frac{\partial}{\partial\phi} + \frac{1}{2\sin\theta}\hat{\gamma}^0\right) + \frac{1}{2}\left(\tau_1 + \mathrm{i}\tau_2\right), \quad (4.146)$$

$$\hat{K}_- = \hat{K}_1 - \mathrm{i}\hat{K}_2 = \mathrm{e}^{-\mathrm{i}\phi}\left(-\frac{\partial}{\partial\theta} + \mathrm{i}\cot\theta\frac{\partial}{\partial\phi} + \frac{1}{2\sin\theta}\hat{\gamma}^0\right) + \frac{1}{2}\left(\tau_1 - \mathrm{i}\tau_2\right). \quad (4.147)$$

These satisfy $\left[\hat{K}_+, \hat{K}_-\right] = 2\hat{K}_3$ and $\hat{\boldsymbol{K}}^2 = \hat{K}_3\hat{K}_3 + \frac{1}{2}\left(\hat{K}_+\hat{K}_- + \hat{K}_-\hat{K}_+\right)$. Using these relations we determine conditions on highest and lowest weight states:

$$\hat{K}_+\Psi^{(\ell,k)} = 0 \quad \Rightarrow \quad k^2 + k = \ell^2 + \ell, \quad (4.148)$$

$$\hat{K}_-\Psi^{(\ell,k)} = 0 \quad \Rightarrow \quad k^2 - k = \ell^2 + \ell. \quad (4.149)$$

Thus in the irreducible representation labelled by ℓ, the highest weight state is $k = \ell$ and the lowest weight state is $k = -\ell$. The dimension of the representation is $2\ell + 1$; it consists of the distinct states

$$\Psi^{(\ell,k)}, \quad |k| \leq \ell. \quad (4.150)$$

Making the change of coordinates to $u = \cos\theta$, we find

$$\hat{K}_+ = \mathrm{e}^{\mathrm{i}\phi}\left(-\sqrt{1-u^2}\frac{\partial}{\partial u} + \frac{u}{\sqrt{1-u^2}}\,\mathrm{i}\frac{\partial}{\partial\phi} + \frac{1}{2\sqrt{1-u^2}}\hat{\gamma}^0\right) + \frac{1}{2}\left(\tau_1 + \mathrm{i}\tau_2\right), \quad (4.151)$$

$$\hat{K}_- = \mathrm{e}^{-\mathrm{i}\phi}\left(\sqrt{1-u^2}\frac{\partial}{\partial u} + \frac{u}{\sqrt{1-u^2}}\,\mathrm{i}\frac{\partial}{\partial\phi} + \frac{1}{2\sqrt{1-u^2}}\hat{\gamma}^0\right) + \frac{1}{2}\left(\tau_1 - \mathrm{i}\tau_2\right). \quad (4.152)$$

Now recall from (4.90) that an $n = 1$ eigenspinor of $\hat{K}_3$ $\Psi^{(\ell,k)}(u,\phi)$ is of the form

$$\Psi^{(\ell,k)}(u,\phi) = \mathrm{e}^{\mathrm{i}\left(k-\frac{1}{2}\tau_3\right)\phi}\Theta^{(\ell,k)}(u) = \begin{pmatrix} \mathrm{e}^{\mathrm{i}\left(k-\frac{1}{2}\right)\phi}\Theta^{(\ell,k)}_{1,1}(u) \\ \mathrm{e}^{\mathrm{i}\left(k+\frac{1}{2}\right)\phi}\Theta^{(\ell,k)}_{1,2}(u) \\ \mathrm{e}^{\mathrm{i}\left(k-\frac{1}{2}\right)\phi}\Theta^{(\ell,k)}_{2,1}(u) \\ \mathrm{e}^{\mathrm{i}\left(k+\frac{1}{2}\right)\phi}\Theta^{(\ell,k)}_{2,2}(u) \end{pmatrix}, \tag{4.153}$$

where we now explicitly label the profile functions by the eigenvalues ℓ, k. Then, written out explicitly over the fermion components, we find that

$$\hat{K}_+\Psi^{(\ell,k)}(u,\phi) = \mathrm{e}^{\mathrm{i}\left(k+1-\frac{1}{2}\tau_3\right)\phi} \times \begin{pmatrix} \left(-\sqrt{1-u^2}\,\frac{\mathrm{d}}{\mathrm{d}u} - \left(k-\frac{1}{2}\right)\frac{u}{\sqrt{1-u^2}} + \frac{1}{2\sqrt{1-u^2}}\right)\Theta^{(\ell,k)}_{1,1}(u) + \Theta^{(\ell,k)}_{1,2}(u) \\ \left(-\sqrt{1-u^2}\,\frac{\mathrm{d}}{\mathrm{d}u} - \left(k+\frac{1}{2}\right)\frac{u}{\sqrt{1-u^2}} + \frac{1}{2\sqrt{1-u^2}}\right)\Theta^{(\ell,k)}_{1,2}(u) \\ \left(-\sqrt{1-u^2}\,\frac{\mathrm{d}}{\mathrm{d}u} - \left(k-\frac{1}{2}\right)\frac{u}{\sqrt{1-u^2}} - \frac{1}{2\sqrt{1-u^2}}\right)\Theta^{(\ell,k)}_{2,1}(u) + \Theta^{(\ell,k)}_{2,2}(u) \\ \left(-\sqrt{1-u^2}\,\frac{\mathrm{d}}{\mathrm{d}u} - \left(k+\frac{1}{2}\right)\frac{u}{\sqrt{1-u^2}} - \frac{1}{2\sqrt{1-u^2}}\right)\Theta^{(\ell,k)}_{2,2}(u) \end{pmatrix}, \tag{4.154}$$

$$\hat{K}_-\Psi^{(\ell,k)}(u,\phi) = \mathrm{e}^{\mathrm{i}\left(k-1-\frac{1}{2}\tau_3\right)\phi} \times \begin{pmatrix} \left(\sqrt{1-u^2}\,\frac{\mathrm{d}}{\mathrm{d}u} - \left(k-\frac{1}{2}\right)\frac{u}{\sqrt{1-u^2}} + \frac{1}{2\sqrt{1-u^2}}\right)\Theta^{(\ell,k)}_{1,1}(u) \\ \Theta^{(\ell,k)}_{1,1}(u) + \left(\sqrt{1-u^2}\,\frac{\mathrm{d}}{\mathrm{d}u} - \left(k+\frac{1}{2}\right)\frac{u}{\sqrt{1-u^2}} + \frac{1}{2\sqrt{1-u^2}}\right)\Theta^{(\ell,k)}_{1,2}(u) \\ \left(\sqrt{1-u^2}\,\frac{\mathrm{d}}{\mathrm{d}u} - \left(k-\frac{1}{2}\right)\frac{u}{\sqrt{1-u^2}} - \frac{1}{2\sqrt{1-u^2}}\right)\Theta^{(\ell,k)}_{2,1}(u) \\ \Theta^{(\ell,k)}_{2,1}(u) + \left(\sqrt{1-u^2}\,\frac{\mathrm{d}}{\mathrm{d}u} - \left(k+\frac{1}{2}\right)\frac{u}{\sqrt{1-u^2}} - \frac{1}{2\sqrt{1-u^2}}\right)\Theta^{(\ell,k)}_{2,2}(u) \end{pmatrix}. \tag{4.155}$$

This confirms that the operators $\hat{K}_\pm$ do indeed raise and lower the azimuthal grand spin of $\hat{K}_3$ eigenspinors by ± 1. It also demonstrates that it is particularly easy to solve for some of the component functions of highest- and lowest-weight states. We choose to work with lowest-weight states, rather than highest-weight states which might be more typical, because the lowest-weight condition provides an immediate and simple calculation of $\Theta_{1,1}$, and

our Fuchsian analysis was performed in terms of that component of the spinor. The $\Theta_{1,1}$ component of a lowest weight state $\Psi^{(\ell,-\ell)}$ satisfies

$$\hat{K}_- \Psi^{(\ell,-\ell)} = 0. \tag{4.156}$$

By (4.155),

$$\left(\sqrt{1-u^2}\frac{\mathrm{d}}{\mathrm{d}u} - \left(-\ell - \frac{1}{2}\right)\frac{u}{\sqrt{1-u^2}} + \frac{1}{2\sqrt{1-u^2}}\right)\Theta_{1,1}^{(\ell,-\ell)}(u) = 0 \tag{4.157}$$

$$\Rightarrow \left(1-u^2\right)\frac{\mathrm{d}\Theta_{1,1}^{(\ell,-\ell)}}{\mathrm{d}u} = \left(\left(-\ell - \frac{1}{2}\right)u - \frac{1}{2}\right)\Theta_{1,1}^{(\ell,-\ell)}(u). \tag{4.158}$$

This first-order differential equation is separable and can be quickly solved with partial fractions as follows:

$$\begin{aligned}
\frac{\mathrm{d}\Theta_{1,1}^{(\ell,-\ell)}}{\Theta_{1,1}^{(\ell,-\ell)}} &= \left(\frac{\frac{1}{2}+\frac{\ell}{2}}{u-1} + \frac{+\frac{\ell}{2}}{u+1}\right)\mathrm{d}u \\
\Rightarrow \log\Theta_{1,1}^{(\ell,-\ell)} &= \left(\frac{1}{2}+\frac{\ell}{2}\right)\log(u-1) + \left(\frac{\ell}{2}\right)\log(u+1) + c_0 \\
\Rightarrow \Theta_{1,1}^{(\ell,-\ell)}(u) &= A_0\,(1-u)^{\frac{1}{2}+\frac{\ell}{2}}\,(1+u)^{\frac{\ell}{2}}
\end{aligned} \tag{4.159}$$

for a constant of integration $A_0 \in \mathbb{C}$. By comparison with Table 4.2, we see that this is certainly consistent with the Fuchsian analysis. This function is regular on the sphere just when $\ell \geq 0$. We immediately see further that the energy of this solution is determined by

$$-\lambda = \frac{1}{2} + \ell. \tag{4.160}$$

We might therefore be tempted to claim the following:

Conjecture 4.2 (Conjecture on the spectrum of $n = 1$ grand spin eigenstates)**.** The energy of a stationary state fermion solution $\Psi_{\ell,k}$ of total grand spin $\ell \in$

$\mathbb{N}_0$ is one of the four generic values

$$E_f = \pm_A \frac{1}{2} \pm_B \sqrt{\left(\ell + \frac{1}{2}\right)^2 + g\,(g \pm_A 1)}, \tag{4.161}$$

and the degeneracy of each such energy level is generically $2\ell + 1$, corresponding to the distinct possible values of azimuthal grand spin $k \in \mathbb{Z}$.

To conceptually highlight the role of the total grand spin, we observe that we can rewrite this as

$$E_f = \pm_A \frac{1}{2} \pm_B \sqrt{\ell\,(\ell+1) + \left(g \mp_A \frac{1}{2}\right)^2}. \tag{4.162}$$

After discussing parity in the $n = 1$ case, we will show evidence that all such energy levels admit a single non-trivial solution, and outline a constructive process for determining the specific components of such eigenfermions.

Let us first quickly state one of the other components of the lowest weight eigenstate $\Psi^{(\ell,-\ell)}$. By a similar calculation to (4.157-4.159), we also find

$$\Theta_{2,1}^{(\ell,-\ell)}(u) = B_0\,(1-u)^{\frac{\ell}{2}}\,(1+u)^{\frac{1}{2}+\frac{\ell}{2}}, \quad B_0 \in \mathbb{C}. \tag{4.163}$$

To simplify the derivation of the remaining components, $\Theta_{1,2}^{(\ell,-\ell)}$ and $\Theta_{2,2}^{(\ell,-\ell)}$, we will exploit parity.

4.3.3 Parity in the $n = 1$ model and joint eigenstates

Missing from our discussion until now has been any treatment of the spatial parity of the fermion field. We will now observe that in the absence of back-reaction, the fermion has a discrete parity relative to the background baby Skyrmion, in a similar manner to the fermion of the S^1 model as described in Section 3.3.2. We define the (polar coordinate) parity operation $\hat{P}$ on the fermion field Ψ as follows: for a given spinor field $\Psi = \Psi(t, \theta, \phi)$, $\hat{P}\Psi$ is the

spinor field defined according to

$$\hat{P}\Psi(t,\theta,\phi) = \hat{\gamma}^1\Psi(t,\pi-\theta,\phi-\pi). \tag{4.164}$$

The apparent effect on spacetime variables is to exchange antipodes of the spatial sphere S^2. It is unambiguous that the latitudinal angle θ must be replaced with $\pi-\theta$, but there is an ambiguity regarding whether the azimuthal angle ϕ is replaced with $\phi+\pi$ or $\phi-\pi$. We set the convention that this parity operation is an active transformation, rotating the fermion "forwards" around the azimuthal axis, and therefore take the minus sign in the definition.

In flat Cartesian coordinates, we would expect the intrinsic parity transformation of the spinor to arise via the action of a $\hat{\gamma}^0$ matrix; it is not difficult to see that $\hat{\gamma}^1$ is the appropriate matrix for our curved, polar coordinates. First, the appearance of $\hat{\gamma}^1$ ensures that $\hat{P}$ is an involution:

$$\begin{aligned}
\hat{P}\hat{P}\Psi(t,\theta,\phi) &= \hat{P}\left[\hat{\gamma}^1\Psi(t,\pi-\theta,\phi-\pi)\right] && (4.165)\\
&= \hat{\gamma}^1\hat{\gamma}^1\Psi(t,\pi,\phi-2\pi) && (4.166)\\
&= (-1)\Psi(t,\theta,\phi-2\pi) && (4.167)\\
&= \Psi(t,\theta,\phi), && (4.168)
\end{aligned}$$

as the minus sign from the 2π rotation of the spin-$\frac{1}{2}$ fermion is cancelled by the minus sign from the square of $\hat{\gamma}^1$.

Second, this definition of parity does provide a symmetry of the Lagrangian, guaranteeing that solutions are mapped to solutions. We demonstrate this, with particular care given to the points of spacetime at which the fields are evaluated. In the specific case $n = 1$, the fermionic Lagrangian

(4.74) is expressed in polar coordinates as

$$\begin{aligned}\mathcal{L}_f\big|_{(t,\theta,\phi)} = \overline{\Psi}\big|_{(t,\theta,\phi)} \Bigg[& \hat{\gamma}^0 \left.\frac{\partial \Psi}{\partial t}\right|_{(t,\theta,\phi)} - \hat{\gamma}^1 \left.\left(\frac{\partial \Psi}{\partial \theta} + \frac{1}{2}\cot(\theta)\,\Psi\right)\right|_{(t,\theta,\phi)} \\ & - \hat{\gamma}^2 \left.\frac{1}{\sin\theta}\frac{\partial \Psi}{\partial \phi}\right|_{(t,\theta,\phi)} \\ & - g\left(\tau_1 \sin\theta\cos\phi + \tau_2 \sin\theta \sin\phi + \tau_3 \cos\theta\right) \Psi\big|_{(t,\theta,\phi)} \Bigg] .\end{aligned} \tag{4.169}$$

We must be careful at this point, because the terms on the third line of the above equation (4.169) arise from the coupling with the baby Skyrmion, of the form $\left(\overline{\Psi}\boldsymbol{\tau}\cdot\boldsymbol{\phi}\Psi\right)\big|_{(t,\theta,\phi)}$. We stress that the notion of parity we have defined at (4.164) is a transformation just of the fermion, with respect to a fixed background baby Skyrmion. We will not transform the baby Skyrmion under this operation, and crucially there is *no* independent global transformation on spacetime itself: the fermion $\hat{P}\Psi$ is a new field for the same spacetime and same background baby Skyrmion, whose pointwise behaviour at an event $x^\mu = (t, \theta, \phi)$ is related to how the old field Ψ behaved at the antipodal event $y^\mu = (t, \pi - \theta, \phi - \pi)$.

Let us now substitute $\hat{P}\Psi$ for Ψ in the Lagrangian (4.169). By the chain rule, we find that

$$\left.\frac{\partial \hat{P}\Psi}{\partial x^\nu}\right|_{x^\mu} = \hat{\gamma}^1 \left.\frac{\partial \Psi}{\partial y^\rho}\right|_{y^\mu} \left.\frac{\partial y^\rho}{\partial x^\nu}\right|_{x^\mu} . \tag{4.170}$$

Hence,

$$\left.\frac{\partial \hat{P}\Psi}{\partial t}\right|_{(t,\theta,\phi)} = \hat{\gamma}^1 \left.\frac{\partial \Psi}{\partial t}\right|_{(t,\pi-\theta,\phi-\pi)} , \tag{4.171}$$

$$\left.\frac{\partial \hat{P}\Psi}{\partial \theta}\right|_{(t,\theta,\phi)} = -\hat{\gamma}^1 \left.\frac{\partial \Psi}{\partial \theta}\right|_{(t,\pi-\theta,\phi-\pi)} , \tag{4.172}$$

$$\left.\frac{\partial \hat{P}\Psi}{\partial \phi}\right|_{(t,\theta,\phi)} = \hat{\gamma}^1 \left.\frac{\partial \Psi}{\partial \phi}\right|_{(t,\pi-\theta,\phi-\pi)} . \tag{4.173}$$

Substituting,

$$\begin{aligned}\hat{P}\mathcal{L}_f\big|_{(t,\theta,\phi)} = \overline{\hat{P}\Psi}\Big|_{(t,\theta,\phi)} \Bigg[& \hat{\gamma}^0 \left.\frac{\partial \hat{P}\Psi}{\partial t}\right|_{(t,\theta,\phi)} - \\ & \hat{\gamma}^1 \left(\frac{\partial \hat{P}\Psi}{\partial \theta} + \frac{1}{2}\cot(\theta)\,\hat{P}\Psi\right)\Big|_{(t,\theta,\phi)} \\ & -\hat{\gamma}^2 \left.\frac{1}{\sin\theta}\frac{\partial \hat{P}\Psi}{\partial \phi}\right|_{(t,\theta,\phi)} \\ & -g\left(\tau_1 \sin\theta\cos\phi + \tau_2 \sin\theta\sin\phi + \tau_3\cos\theta\right)\,\hat{P}\Psi\big|_{(t,\theta,\phi)}\Bigg]\end{aligned} \tag{4.174}$$

$$\begin{aligned} = \overline{\Psi}\big|_{(t,\pi-\theta,\phi-\pi)}\,\hat{\gamma}^1 \Bigg[& \hat{\gamma}^0\hat{\gamma}^1 \left.\frac{\partial \Psi}{\partial t}\right|_{(t,\pi-\theta,\phi-\pi)} \\ & -\hat{\gamma}^1 \left(-\hat{\gamma}^1\frac{\partial \Psi}{\partial \theta} + \frac{1}{2}\cot(\theta)\,\hat{\gamma}^1\Psi\right)\Big|_{(t,\pi-\theta,\phi-\pi)} \\ & -\hat{\gamma}^2 \left.\frac{1}{\sin\theta}\hat{\gamma}^1\frac{\partial \Psi}{\partial \phi}\right|_{(t,\pi-\theta,\phi-\pi)} \\ & -g\left(\tau_1 \sin\theta\cos\phi + \tau_2 \sin\theta\sin\phi + \tau_3\cos\theta\right)\,\hat{\gamma}^1\Psi\Big|_{(t,\pi-\theta,\phi-\pi)}\Bigg]. \end{aligned} \tag{4.175}$$

Before combining $\hat{\gamma}$ matrices in this expression, we will make use of the trigonometric identities

$$\cos(\pi-\theta) = -\cos\theta, \quad \sin(\pi-\theta) = \sin\theta, \tag{4.176}$$

$$\cos(\phi-\pi) = -\cos\phi, \quad \sin(\phi-\pi) = -\sin\phi, \tag{4.177}$$

to rewrite all the appearances of trigonometric functions of the polar coordinates as follows,

$$\begin{aligned}\hat{P}\mathcal{L}_f\big|_{(t,\theta,\phi)} = \overline{\Psi}\big|_{(t,\pi-\theta,\phi-\pi)}\,\hat{\gamma}^1 \Bigg[& \hat{\gamma}^0\hat{\gamma}^1\,\frac{\partial\Psi}{\partial t}\bigg|_{(t,\pi-\theta,\phi-\pi)} \\ & - \hat{\gamma}^1\left(-\hat{\gamma}^1\frac{\partial\Psi}{\partial\theta} - \frac{1}{2}\cot(\pi-\theta)\,\hat{\gamma}^1\Psi\right)\bigg|_{(t,\pi-\theta,\phi-\pi)} \\ & - \hat{\gamma}^2\,\frac{1}{\sin(\pi-\theta)}\hat{\gamma}^1\frac{\partial\Psi}{\partial\phi}\bigg|_{(t,\pi-\theta,\phi-\pi)} - g\,(-\tau_1\sin(\pi-\theta)\cos(\phi-\pi) \\ & -\tau_2\sin(\pi-\theta)\sin(\phi-\pi) - \tau_3\cos(\pi-\theta))\,\hat{\gamma}^1\Psi\Big|_{(t,\pi-\theta,\phi-\pi)}\Bigg]. \quad (4.178)\end{aligned}$$

Finally, reducing the combinations of $\hat{\gamma}$ matrices, we are left with

$$\begin{aligned}\hat{P}\mathcal{L}_f\big|_{(t,\theta,\phi)} = \overline{\Psi}\big|_{(t,\pi-\theta,\phi-\pi)} \Bigg[& \hat{\gamma}^0\,\frac{\partial\Psi}{\partial t}\bigg|_{(t,\pi-\theta,\phi-\pi)} \\ & - \hat{\gamma}^1\left(\frac{\partial\Psi}{\partial\theta}\bigg|_{(t,\pi-\theta,\phi-\pi)} + \frac{1}{2}\cot(\pi-\theta)\;\Psi|_{(t,\pi-\theta,\phi-\pi)}\right) \\ & - \hat{\gamma}^2\,\frac{1}{\sin(\pi-\theta)}\frac{\partial\Psi}{\partial\phi}\bigg|_{(t,\pi-\theta,\phi-\pi)} - g\,(\tau_1\sin(\pi-\theta)\cos(\phi-\pi) \\ & +\tau_2\sin(\pi-\theta)\sin(\phi-\pi) + \tau_3\cos(\pi-\theta))\;\Psi|_{(t,\pi-\theta,\phi-\pi)}\Bigg] \quad (4.179) \\ = \mathcal{L}_f\big|_{(t,\pi-\theta,\phi-\pi)}. & \quad (4.180)\end{aligned}$$

Thus the effect of our defined parity operation on the Lagrangian is equivalent to relabelling spacetime points by exchanging spatial antipodes. In particular, the action $\mathcal{S} = \int \mathcal{L}_f\,\mathrm{d}^3x$ is invariant, so the equations of motion from the variational principle are unchanged. If Ψ is a fermion solution, then so is $\hat{P}\Psi$.[2]

[2]Observe that the trigonometric identities for antipodal points in the spin-isospin coupling term were essential to counteract the minus sign arising from the factor of $\left(\hat{\gamma}^1\right)^2$. A mass term for the fermion would be pseudoscalar under this parity transformation, i.e.

$$m_f\,(\overline{\Psi}\Psi)\big|_{x^\mu} \mapsto -m_f\,(\overline{\Psi}\Psi)\big|_{y^\mu}, \quad (4.181)$$

and thus is never permissible in a parity-invariant Lagrangian under our assumptions.

An essentially identical manipulation shows that the parity operator $\hat{P}$ commutes with the fermionic Hamiltonian $\hat{H}_f$ as defined at equation (4.82):

$$\left[\hat{P}, \hat{H}_f\right] = 0. \tag{4.182}$$

It's also straightforward to check that parity commutes with the generalised angular momentum generators $\hat{K}_i$ defined at equations (4.88) and (4.138):

$$\left[\hat{P}, \hat{K}_i\right] = 0. \tag{4.183}$$

Therefore we can simplify our classification of solutions to the Dirac equation by seeking steady state, generalised angular momentum eigenstates of definite parity. As an involution, $\hat{P}$ has eigenvalues ± 1. We refer to the $+1$ eigenspace as the space of even parity states, and the -1 eigenspace as the space of odd parity states, and will record the parity of an eigenstate Ψ^P by the equivalence class of the signature $\sigma_P \in \mathbb{Z}_2$, where

$$\hat{P}\Psi^P = (-1)^{\sigma_P}\, \Psi^P. \tag{4.184}$$

We start by returning to the classification of the profile functions just in terms of the azimuthal grand spin k, as at (4.90),

$$\Psi(\theta, \phi) = \begin{pmatrix} \mathrm{e}^{\mathrm{i}\left(k-\frac{1}{2}\right)\phi}\Theta_{1,1}(\theta) \\ \mathrm{e}^{\mathrm{i}\left(k+\frac{1}{2}\right)\phi}\Theta_{1,2}(\theta) \\ \mathrm{e}^{\mathrm{i}\left(k-\frac{1}{2}\right)\phi}\Theta_{2,1}(\theta) \\ \mathrm{e}^{\mathrm{i}\left(k+\frac{1}{2}\right)\phi}\Theta_{2,2}(\theta) \end{pmatrix}. \tag{4.185}$$

Applying the parity transformation to this,

$$\hat{P}\Psi(\theta,\phi) = \hat{\gamma}^1\Psi(\pi-\theta,\phi-\pi) = \begin{pmatrix} -ie^{i\left(k-\frac{1}{2}\right)(\phi-\pi)}\Theta_{2,1}(\pi-\theta) \\ -ie^{i\left(k+\frac{1}{2}\right)(\phi-\pi)}\Theta_{2,2}(\pi-\theta) \\ -ie^{i\left(k-\frac{1}{2}\right)(\phi-\pi)}\Theta_{1,1}(\pi-\theta) \\ -ie^{i\left(k+\frac{1}{2}\right)(\phi-\pi)}\Theta_{1,2}(\pi-\theta) \end{pmatrix}. \quad (4.186)$$

Now consider

$$e^{i\left(k-\frac{1}{2}\right)(\phi-\pi)} = e^{i\pi\left(\frac{1}{2}-k\right)}e^{i\left(k-\frac{1}{2}\right)\phi} = (-1)^k\, ie^{i\left(k-\frac{1}{2}\right)\phi}, \quad (4.187)$$

$$e^{i\left(k+\frac{1}{2}\right)(\phi-\pi)} = e^{i\pi\left(-\frac{1}{2}-k\right)}e^{i\left(k+\frac{1}{2}\right)\phi} = (-1)^{k+1}\, ie^{i\left(k+\frac{1}{2}\right)\phi}. \quad (4.188)$$

Thus,

$$\hat{P}\Psi(\theta,\phi) = (-1)^k \begin{pmatrix} e^{i\left(k-\frac{1}{2}\right)\phi}\Theta_{2,1}(\pi-\theta) \\ -e^{i\left(k+\frac{1}{2}\right)\phi}\Theta_{2,2}(\pi-\theta) \\ e^{i\left(k-\frac{1}{2}\right)\phi}\Theta_{1,1}(\pi-\theta) \\ -e^{i\left(k+\frac{1}{2}\right)\phi}\Theta_{1,2}(\pi-\theta) \end{pmatrix}. \quad (4.189)$$

If this is a parity eigenstate obeying (4.184), then we obtain the relations

$$\Theta_{1,1}(\theta) = (-1)^{k+\sigma_P}\,\Theta_{2,1}(\pi-\theta), \quad (4.190)$$

$$\Theta_{1,2}(\theta) = (-1)^{k+\sigma_P+1}\,\Theta_{2,2}(\pi-\theta). \quad (4.191)$$

Note that under the change of variables $u = \cos\theta$, the map $\theta \mapsto \pi - \theta$ becomes simply $u \mapsto -u$.

Equipped with this extra classification, let us return to the discussion of lowest-weight eigenstates of angular momentum, as around equations (4.155-4.163). Recall that solving the lowest-weight conditions for $\Theta_{1,1}(u)$

and $\Theta_{2,1}(u)$ gave us

$$\Theta_{1,1}^{(\ell,-\ell)}(u) = A_1 \left(1-u\right)^{\frac{\ell}{2}+\frac{1}{2}} \left(1+u\right)^{\frac{\ell}{2}}, \tag{4.192}$$

$$\Theta_{2,1}^{(\ell,-\ell)}(u) = A_2 \left(1-u\right)^{\frac{\ell}{2}} \left(1+u\right)^{\frac{\ell}{2}+\frac{1}{2}}. \tag{4.193}$$

Therefore the parity eigenstate condition (4.190) tells us

$$A_2 = (-1)^{\ell+\sigma_P} A_1. \tag{4.194}$$

Now we solve for the remaining profile functions of a lowest-weight state using the other components of equation (4.155). For $\Theta_{1,2}$ we have

$$\Theta_{1,1}^{(\ell,-\ell)}(u) + \left(\sqrt{1-u^2}\frac{\mathrm{d}}{\mathrm{d}u} - \frac{\left(-\ell+\frac{1}{2}\right)u}{\sqrt{1-u^2}} + \frac{\frac{1}{2}}{\sqrt{1-u^2}} \right) \Theta_{1,2}^{(\ell,-\ell)}(u) = 0. \tag{4.195}$$

Substituting in our solution (4.192), we obtain the differential equation

$$\frac{\mathrm{d}\Theta_{1,2}^{(\ell,-\ell)}}{\mathrm{d}u} + \frac{\left(\ell-\frac{1}{2}\right)u+\frac{1}{2}}{(1-u^2)}\Theta_{1,2}^{(\ell,-\ell)} = -A_1 \left(1-u\right)^{\frac{\ell}{2}} \left(1+u\right)^{\frac{\ell}{2}-\frac{1}{2}}, \tag{4.196}$$

the general solution of which is

$$\Theta_{1,2}^{(\ell,-\ell)}(u) = \left(1-u\right)^{\frac{\ell}{2}} \left(1+u\right)^{\frac{\ell}{2}-\frac{1}{2}} \left(B_1 - A_1 u\right), \tag{4.197}$$

where we have introduced another constant of integration, B_1. Similarly, the $\Theta_{2,2}$ component of a lowest-weight state is generally

$$\Theta_{2,2}^{(\ell,-\ell)}(u) = \left(1-u\right)^{\frac{\ell}{2}-\frac{1}{2}} \left(1+u\right)^{\frac{\ell}{2}} \left(B_2 - A_2 u\right), \tag{4.198}$$

with B_2 a constant of integration. For a parity eigenstate, by equations (4.191) and (4.194) we find that

$$B_2 = (-1)^{\ell+\sigma_P+1} B_1. \tag{4.199}$$

We observe that these general solutions (4.197-4.198) are well-defined for $\ell \geq 1$, but may fail to be so for $\ell = 0$ unless

$$(B1 - A_1 u) \propto (1+u)\,, \tag{4.200}$$

$$\text{or equivalently } (B1 + A_1 u) \propto (1-u)\,. \tag{4.201}$$

Thus for $\ell = 0$ we must have

$$B_1 = -A_1, \tag{4.202}$$

and thus, up to normalisation, there are just two $\ell = 0$ eigenstates, distinguished by their parity σ_P:

$$\Psi^{(0,0)}_{\sigma_P}(u,\phi) = A_1 \mathrm{e}^{-\frac{\mathrm{i}}{2}\tau_3\phi} \begin{pmatrix} (1-u)^{\frac{1}{2}} \\ -(1+u)^{\frac{1}{2}} \\ (-1)^{\sigma_P}(1+u)^{\frac{1}{2}} \\ (-1)^{\sigma_P}(1-u)^{\frac{1}{2}} \end{pmatrix}, \tag{4.203}$$

where A_1 remains now just as a normalising factor. (We will determine the corresponding energy eigenvalues shortly.)

We can neaten the general solution by simply rewriting

$$B_1 - A_1 u = B - A(1+u), \tag{4.204}$$

for new coefficients A and B. Then our most general expression for a lowest-weight eigenstate so far is a linear combination,

$$\Psi^{(\ell,-\ell)}_{\sigma_P}(u,\phi) = \mathrm{e}^{\left(-\ell-\frac{1}{2}\tau_3\right)\phi}\left[A\begin{pmatrix}(1-u)^{\frac{\ell}{2}+\frac{1}{2}}(1+u)^{\frac{\ell}{2}}\\(-1)(1-u)^{\frac{\ell}{2}}(1+u)^{\frac{\ell}{2}+\frac{1}{2}}\\(-1)^{\ell+\sigma_P}(1-u)^{\frac{\ell}{2}}(1+u)^{\frac{\ell}{2}+\frac{1}{2}}\\(-1)^{\ell+\sigma_P}(1-u)^{\frac{\ell}{2}+\frac{1}{2}}(1+u)^{\frac{\ell}{2}}\end{pmatrix}\right.$$
$$\left.+B\begin{pmatrix}0\\(1-u)^{\frac{\ell}{2}}(1+u)^{\frac{\ell}{2}-\frac{1}{2}}\\0\\(-1)^{\ell+\sigma_P+1}(1-u)^{\frac{\ell}{2}-\frac{1}{2}}(1+u)^{\frac{\ell}{2}}\end{pmatrix}\right]. \tag{4.205}$$

We see that for $\ell = 0$ we must have $B = 0$, which is equivalent to our discussion above. More generally, we will need to solve the Dirac equation to determine the allowed combinations of A and B, which we will do presently. It is not difficult to see immediately, nonetheless, that for general ℓ, a (non-trivial) state with $A = 0$ is not going to solve the Dirac equation, because of the zeroes in half its components. While this decomposition of parity and grand spin eigenstates (into what we might call A-states and B-states) is very useful for collecting the powers of $(1 \pm u)$ in the components, it is not also the eigenbasis for the Hamiltonian $\hat{H}_f$.

Let's proceed to find those combinations which are also Hamiltonian eigenstates. We can do this by substituting the general expression (4.205) into the system of equations (4.105-4.108) for the stationary states, now taking $n = 1$ and $k = -\ell$.

We will explicitly do so just for equation (4.106), as this will be sufficient to completely determine the relationships between E_f, A and B. The terms

in $\Theta_{1,1}$ and $\Theta_{1,2}$ are

$$\begin{aligned}\left(E_f + gu\right)\Theta_{1,2} - g\sqrt{1-u^2}\Theta_{1,1} &= \left(E_f + gu\right)\left[B - A\left(1+u\right)\right]\left(1-u\right)^{\frac{\ell}{2}}\left(1+u\right)^{\frac{\ell}{2}-\frac{1}{2}} \\ &\quad - gA\left(1-u\right)^{\frac{\ell}{2}+1}\left(1+u\right)^{\frac{\ell}{2}+\frac{1}{2}} \qquad (4.206) \\ &= \Big(E_f\left(B-A\right) - gA + \left[E_f(-A) + g(B-A)\right]u\Big) \\ &\quad \times \left(1-u\right)^{\frac{\ell}{2}}\left(1+u\right)^{\frac{\ell}{2}-\frac{1}{2}}. \qquad (4.207)\end{aligned}$$

For the terms involving $\Theta_{2,2}$, first observe the following useful differentiation identity:

$$\begin{aligned} y = C(1-u)^{\alpha}(1+u)^{\beta} \quad &\Rightarrow \quad \ln y = \ln C + \alpha\ln(1-u) + \beta\ln(1+u) \\ &\Rightarrow \quad \frac{1}{y}\frac{\mathrm{d}y}{\mathrm{d}u} = -\frac{\alpha}{1-u} + \frac{\beta}{1+u} \\ &\Rightarrow \quad \frac{\mathrm{d}y}{\mathrm{d}u} = \frac{\beta - \alpha - (\alpha+\beta)\,u}{1-u^2}y. \qquad (4.208)\end{aligned}$$

Thus,

$$\begin{aligned}\sqrt{1-u^2}\frac{\mathrm{d}\Theta_{2,2}}{\mathrm{d}u} &= (-1)^{\ell+\sigma_P+1}B\left[\tfrac{1}{2} - \left(\ell - \tfrac{1}{2}\right)u\right]\left(1-u\right)^{\frac{\ell}{2}-1}\left(1+u\right)^{\frac{\ell}{2}-\frac{1}{2}} \\ &\quad + (-1)^{\ell+\sigma_P}A\left[-\tfrac{1}{2} - \left(\ell + \tfrac{1}{2}\right)u\right]\left(1-u\right)^{\frac{\ell}{2}}\left(1+u\right)^{\frac{\ell}{2}-\frac{1}{2}}, \qquad (4.209)\end{aligned}$$

and

$$\begin{aligned}\frac{\frac{1}{2}u - \ell + \frac{1}{2}}{\sqrt{1-u^2}}\Theta_{2,2} &= \left[\tfrac{1}{2}u - \ell + \tfrac{1}{2}\right](-1)^{\ell+\sigma_P+1}\Big[B\left(1-u\right)^{\frac{\ell}{2}-1}\left(1+u\right)^{\frac{\ell}{2}-\frac{1}{2}} \\ &\quad - A\left(1-u\right)^{\frac{\ell}{2}}\left(1+u\right)^{\frac{\ell}{2}-\frac{1}{2}}\Big]. \qquad (4.210)\end{aligned}$$

Combining equations (4.207) and (4.209-4.210), we can extract an overall factor of $(1-u)^{\frac{\ell}{2}-1}(1+u)^{\frac{\ell}{2}-\frac{1}{2}}$, to obtain

$$E_f\left[(B-A)-Au\right]-g\left[A+(A-B)u\right]+(-1)^{\ell+\sigma_P}\left[(A-B)\ell-A-A(\ell+1)u\right]=0. \tag{4.211}$$

Splitting into the coefficients of 1 and of u, we obtain the system,

$$E_f(B-A)=gA+(-1)^{\ell+\sigma_P+1}\left[(A-B)\ell-A\right], \tag{4.212}$$

$$E_fA=g(B-A)+(-1)^{\ell+\sigma_P+1}A(\ell+1). \tag{4.213}$$

This is in fact the totality of information that is obtained by substituting the general eigenstate given at (4.205) into the Dirac equation(s) in the form (4.105-4.108): explicitly computing the terms in any of the other three equations reproduces equations consistent with and no stronger than (4.212-4.213). This is as we would expect: as there is an as-yet unspecified normalisation condition on A and B, this is the correct number of conditions to put an exactly determined algebraic condition on E_f.

We have observed that for $\ell=0$ we must have $B=0$, so both equations (4.212-4.213) reduce to

$$E_fA=\left[-g+(-1)^{\sigma_P+1}\right]A,$$

$$\text{i.e. } E_f=-g+(-1)^{\sigma_P+1}. \tag{4.214}$$

It is easily checked that these are indeed the correct energy eigenvalues for the $\ell=0$ eigenstates given at (4.203).

We remark that if $A=0$, the system reduces to

$$E_fB=(-1)^{\ell+\sigma_P}\ell B, \tag{4.215}$$

$$0=gB. \tag{4.216}$$

This is consistent with the observation that for non-trivial spin-isospin coupling, i.e. non-zero g, we cannot have a non-trivial state with $A = 0$. On the other hand, if $g = 0$, our lowest-weight solution reduces to a decoupled, isospinless fermion à la Abrikosov [1] in the isospin-down components of the field Ψ, up to the technical point of carefully defining the "grand spin" when there is no spin-isospin coupling. (Compare this result for the energy to the relationship (4.1); and see Abrikosov, or implement the code in Appendix B.2, to confirm that the explicit components of the fermion are equivalent.)

Finally let us consider the non-trivial cases with $\ell \geq 1$. Since $A \neq 0$, we can divide both equations (4.212-4.213) by A, and then eliminate B, to reduce to a quadratic equation for E_f. The solutions give the energy spectrum:

$$E_f = \frac{(-1)^{\ell+\sigma_P+1}}{2} \pm \sqrt{\ell(\ell+1) + \left(g - \frac{(-1)^{\ell+\sigma_P+1}}{2}\right)^2}. \tag{4.217}$$

By comparison with equation (4.162), we see that the sign we called $\pm_A$ is determined to be $(-1)^{\ell+\sigma_P+1}$. The final "quantum number" specifying the eigenstate is the sign $\pm_B$, the choice of upper or lower energy branch, corresponding to the distinct solutions of the quadratic. For notational consistency we'll now also replace the notation $\pm_B$ with $(-1)^{\sigma_B}$. Then we may express our results on the spectrum and energy levels as follows.

Remark 4.3. The energy levels of the fermion are determined by the total grand spin $\ell \geq 0$, parity $\sigma_P \in \mathbb{Z}_2$, and for $\ell > 0$ the branch sign $\sigma_B \in \mathbb{Z}_2$. Given this data, the general energy eigenvalue is

$$E_f = \frac{(-1)^{\ell+\sigma_P+1}}{2} + (-1)^{\sigma_B}\sqrt{\ell(\ell+1) + \left(g - \frac{(-1)^{\ell+\sigma_P+1}}{2}\right)^2}, \tag{4.218}$$

although for consistency when $\ell = 0$ we must choose σ_B odd in that case: the $\ell = 0$ energy levels are just

$$E_f = -g + (-1)^{\sigma_P + 1}. \tag{4.219}$$

The degeneracy of each energy level is the usual factor of $2\ell + 1$ possible values of the eigenvalue k of $\hat{K}_3$ for the irreducible representation of $\mathrm{SU}(2)$. Generically, there are $8\ell + 4$ distinct states of grand spin ℓ, the energy level degeneracy doubled for each choice of σ_P and σ_B. However, for $\ell = 0$ there are only two states, as the only remaining quantum number is the parity sign σ_P.

For a given ℓ, σ_P and σ_B we determine the relationship between the coefficients A and B (up to normalisation) by then substituting the expression for E_f back into equations (4.212-4.213). We observe the ratio(s):

$$\frac{B}{A} = \frac{E_f + g + (-1)^{\ell+\sigma_P+1}(\ell - 1)}{E_f + (-1)^{\ell+\sigma_P+1}\ell} \text{ by (4.212)}, \tag{4.220}$$

$$= \frac{g}{E_f + g - (-1)^{\ell+\sigma_P+1}(\ell + 1)} \text{ by (4.213)}. \tag{4.221}$$

Of course, both expressions above for the ratio $\frac{B}{A}$ must be generally equal, except in degenerate cases such as $g = 0$. In such cases we must correctly normalise the state and then carefully evaluate the limit as we approach the degenerate case to examine how such a state of the spin-isospin system decouples into isospinless fermions. We've already seen that we expect $\ell = 0$ lowest weight states to give a decoupled isospin-down state and a vacuum isospin-up state in the limit $g \to 0$. Similarly, if we take a lowest-weight state for general ℓ to have

$$A = E_f + g - (-1)^{\ell+\sigma_P+1}(\ell + 1), \quad B = g, \tag{4.222}$$

then by (4.221) we expect that this will also lead to a similar decoupled pair of isospin-up vacuum and isospin-down lowest weight state in the limit $g \to 0$. By comparing the form of the raising and lowering grand spin operators $\hat{K}_\pm$ at equations (4.154-4.155), we conjecture that on the other hand, highest-weight grand spin states decouple to isospin-up highest weight isospinless fermions and isospin-down vacuum states. The states of intermediate azimuthal grand spin are not observed so easily by inspection, but we certainly have a constructive process for obtaining them: start with a presentation of a lowest-weight state and then apply the raising operator $\hat{K}_+$ the appropriate number of times. It remains to compute some examples in detail and explicitly see how they might decouple or be otherwise modified in degenerate cases of the relations (4.220-4.221).

4.4 Discussion

We have determined that a spin-isospin coupled Dirac fermion in the field of a background $n = 1$ baby Skyrmion is totally determined by the combined representation theory of $SU(2)$ and spatial parity. This closely matches the results of similar models. The analogous model of the Dirac fermion in the field of a background Skyrmion on $\mathbb{R} \times S^3$ [23, 37] also features a generalised grand spin operator $\boldsymbol{G}$,

$$\boldsymbol{G} = \boldsymbol{L} + \boldsymbol{S} + \boldsymbol{I}, \tag{4.223}$$

the combined contribution of the orbital angular momentum $\boldsymbol{L}$, the spin $\boldsymbol{S} = \frac{1}{2}\boldsymbol{\sigma}$ and the isospin $\boldsymbol{I} = \frac{1}{2}\boldsymbol{\tau}$. It is worth noting that each of these operators has three spatial components on S^3, and acts more similarly to their equivalents on flat Minkowski space $\mathbb{R}^1 \times \mathbb{R}^3$: there is a question of projection onto an axis of rotation, and so spin states can be distinguished by helicity. Thus the total grand spin does not fully determine a state on S^3, since the contribution

to $\boldsymbol{G}$ of positive helicity spin can be cancelled by negative helicity isospin, and vice versa. Indeed, the total grand spin does not alone distinguish an energy level for the fermion solutions on S^3. It must be combined with an additional quantum number corresponding to the degree of the polynomial part of the Fuchsian u-equation.

In our case, at any local point, there is only one axis of spatial rotation. Although our grand spin operators $\hat{K}_i$ give a representation of $\mathrm{SU}(2)$, at each point of S^2, there is only one a one-dimensional subspace of $\mathfrak{su}(2)$ which looks locally like a family of rotation operators. There is no helicity. Our calculation seems more analogous to solving for scalar spherical harmonics on $\mathbb{R}^3$ in the absence of the radial degree of freedom: there is no "principal quantum number", just the analogues of the azimuthal and magnetic numbers l, m of the spherical harmonic $Y^{l,m}$. On the other hand, viewing S^3 as the one-point compactification of $\mathbb{R}^3$, a radial degree of freedom is introduced, so it is natural that there should be an extra quantum number in that case.

Another similar model with which our results seem to broadly agree is the same spin-isospin coupling to baby Skyrmions on flat Minkowski $\mathbb{R} \times \mathbb{R}^2$ [51]. Numerical investigation in that model finds many distinct fermion states when the baby Skyrmion profile function is permitted to vary and is fully coupled to the fermion (rather than being in the background). The fermion in this model is observed to localise near the "boundary" of the baby Skyrmion where the topological charge density is falling off at the greatest rate. In this case there is an azimuthal rotation symmetry generated by an operator essentially identical to our $\hat{K}_3$, but not a full representation of $\mathrm{SU}(2)$ extending this rotation.

Interestingly, Perapechka, Sawado, and Shnir [51] observe that almost all of their fermion states drop out as the coupling constant g goes to zero, leaving just one zero mode in the limit, and the states delocalise as their energy drops. This appears to conflict with our result. From (4.218), when $g = 0$ the

generic energy levels for $\ell > 0$ are

$$E_f = \frac{(-1)^{\ell+\sigma_P+1}}{2} + (-1)^{\sigma_B}\left(\ell + \frac{1}{2}\right). \tag{4.224}$$

At first glance, it appears that there are two zero modes for $\ell = 0$, but we have already seen that for consistency reasons these possibilities are ruled out, and so there are no zero modes at $g = 0$. The fermion on flat Minkowski space in [51] is massive, but in three dimensions where the Dirac representation is irreducible, it is not immediately obvious that the fermion mass would account for the discrepancy.

As an explanation of this disagreement, it may be that our choice of the baby Skyrmion is "too symmetric" or "too weak" for $n = 1$. Scoccola and Bes [59] show that our spherically symmetric baby Skyrmion is appropriate only when a combined parameter αL^4 is sufficiently small, where α is the coupling constant of the Skyrme potential term and L is the radius of the spatial sphere S^2. In the opposite regime that αL^4 is large, the baby Skyrmion localises at one of the poles of the sphere. From the point of view of stereographic projection we can see this as localisation of the soliton at the spatial origin when the radius of the sphere goes to infinity. This is a bifurcation property shared by Skyrmions on S^3 [30, 40]. Even the planar rotational symmetry of a baby Skyrmion is not inviolable: there are choices of baby Skyrme potentials in the flat $(2+1)$-dimensional model where higher-charge, static, energy-minimising baby Skyrmions can have their rotational symmetry broken surprisingly badly. Karliner and Hen [32, 33] demonstrate such as a $B = 5$ baby Skyrmion whose energy density only permits a single discrete reflection symmetry. The same authors also show that a rotating baby Skyrmion on the 2-sphere can dynamically undergo spontaneous symmetry breaking. A rotating $B = 1$ baby Skyrmion can at critical values of angular momentum first break its spherical symmetry to a single axial symmetry, and then break

that remaining symmetry to be left with a general ellipsoidal distribution of topological charge.

A final point of curiosity is the observation that we do not naturally recover the full spectrum of the $\mathbb{R} \times S^2$ Dirac (spin-only) fermion in the limit of our model as g approaches 0. As we mentioned at the beginning of this chapter, and demonstrate with the Maple worksheet in Appendix B.2, the spectrum of the pure Dirac operator is $\mathbb{Z} \setminus \{0\}$, as opposed to $\mathbb{Z} + \frac{1}{2}$. Even in the absence of coupling to the background isovector, the decoupled isospin components of the fermion still seem to "know" that they are isospinors, rather than isoscalars. Perhaps this should be unsurprising: after all, on flat (3+1)-dimensional Minkowski space, the Weyl components of a massless Dirac spinor still obey the Weyl equations, rather than an equation for a scalar field. Nonetheless, even with this interpretation, there is a question of a seemingly "instantaneous" loss of isospin in the limit $g = 0$. Consider that for $g = 0$, we observe two distinct possible candidates for a rotation operator about the polar axis:

$$\hat{K}_3 = -\mathrm{i}\frac{\partial}{\partial\phi} + \frac{1}{2}\tau_3, \quad \hat{L}_3 = -\mathrm{i}\frac{\partial}{\partial\phi}. \tag{4.225}$$

Both $\hat{K}_3$ and $\hat{L}_3$ will commute with the fermionic Hamilton when $g = 0$, although only $\hat{K}_3$ correctly generalises to non-zero g. They clearly also commute with each other. But a "joint eigenstate" would have Fourier mode simultaneously equal to $k \pm \frac{n}{2}$ and m, and so for the case $g = 0$, the fermion would appear to treat the background field as if it suddenly has even winding number n. These issues may point to the inherent weakness of modelling the soliton as living in the background, with a total absence of back-reaction. As with the prescribed background kink in Chapter 3, our appeal to principles of symmetry for background baby Skyrmion required us to construct operations where the fermion underwent both a spacetime transformation

and an internal transformation. This is an undesirable feature of a physical theory of particles: for a quantum field theory, such a symmetry of the S-matrix is typically a violation of the Coleman-Mandula theorem [18].

All these features emphasise the importance of the back-reaction of the fermion onto the baby Skyrmion, and in particular the effect on the soliton's profile function, to the qualitative behaviour of the model, in particular in the context of the zero modes. We discuss some areas of interest for future work in our outlook in Section 5.2.2.

Chapter 5

Conclusion

5.1 Summary

We have classified the spectrum of models of spin-isospin coupling between fermions and topological solitons on the circle S^1 and the sphere S^2. The investigations have been very fruitful, although there is still some outstanding work to be done and we are left with a few further questions in each. The primacy of the bispinors in the kink-fermion model in (1+1)-dimensions leaves us with many open questions to investigate. We stress our belief that the key mechanism for our approach is the internal symmetry shared by the fermion and kink fields. We believe that our argument in Section 4.4 regarding the flaws of the background baby Skyrmion model on S^2 provide further evidence for the importance of a true internal symmetry between fermions and solitons in order to explore their interaction. Fully coupling the kink to the fermion gave rise to a rich mathematical structure which can be investigated with powerful tools from complex analysis.

In each case, the radius of the compact spatial manifold plays a role. On S^1 it affects how the full coupling modifies the energy of fermion solutions; on S^2, the compactification of the sphere seems to alter the nature of fermionic zero modes. The observations by Perapechka, Sawado, and Shnir [51] that fermion modes drop out in the limit of a weak coupling constant in flat space, and by Scoccola and Bes [59] that the radius of the sphere acts in

conjunction with a physical constant in the baby Skyrme model, jointly suggest that we should also include the spherical radius explicitly in our model. It can be inserted into the metric in much the same way we gave the radius ρ of S^1 and will set an energy scale analogously.

5.2 Outlook

We have outlined some avenues of future research in Sections 3.9 and 4.4. We finish by mentioning a few more ideas which are not as directly related to the questions raised in each case, but which we believe would share interesting features.

5.2.1 Fermions and kinks on $\mathbb{R} \times \mathrm{S}^1$

One aspect of the kink-soliton models that we have not addressed in either case is quantisation. However, the fact that the fermion dynamics can be understood in terms of bosonic coordinates in the S^1 model does suggest that quantising the model might be interesting. It is already known in (1+1)-dimensional field theories that there is a duality between bosons and fermions. This was first observed by Coleman [17] as a duality in the renormalisation structures of the quantum sine-Gordon model and the massive Thirring four-fermion model, and was expanded further by Witten [71]. The massive Thirring model contains a Dirac fermion with the Lagrangian

$$\mathcal{L} = \overline{\psi}\left(\mathrm{i}\hbar\partial\!\!\!/ - m\right)\psi - \frac{g}{2}\left(\overline{\psi}\gamma^{\mu}\psi\right)\left(\overline{\psi}\gamma_{\mu}\psi\right). \tag{5.1}$$

The additional four-fermion term is the $\mathrm{U}(1)$ current, and we have already seen that this naturally plays a role in the kink-fermion model. It would be interesting therefore to see the effects of adding such a term to our model.

This will require some quantisation; at the very least, we will likely need to introduce Grassman variables for the Dirac field.

Another interesting modification may be to introduce isospin to the kink-fermion model, as has been considered by Loginov [39]. We believe isospin would fix the parity problem of the model: it would permit a kink-fermion coupling with an internal symmetry without necessitating that the kink be a pseudoscalar. However, if we wish to preserve the shared symmetry, it's not possible to directly introduce Loginov's potential term for the sigma field $\boldsymbol{\phi}$ which admits topological solitons. Similarly, we cannot introduce either a ϕ^4 or sine-Gordon potential term for the scalar field to our current model (i.e. without isospin) without disrupting the shared symmetry.

One possible idea is to give a larger symmetry group to the sigma field than to the fermion, and break the larger symmetry by a potential term for the sigma field while preserving the smaller symmetry of the fermion-soliton coupling term. For example, let $\boldsymbol{\phi} = (\phi_1, \phi_2, \phi_3)$ now be an isospin triplet with $\boldsymbol{\phi} \cdot \boldsymbol{\phi} = 1$, but keep Ψ just in the $\mathrm{SO}(2)$ isospin representation corresponding to the equator $\phi_3 = 0$, and use a potential that also respects rotation about the ϕ_3 axis:

$$\mathcal{L} = \frac{1}{2}\partial_\mu \boldsymbol{\phi} \cdot \partial^\mu \boldsymbol{\phi} + \mathrm{i}\hbar\overline{\Psi}\hat{\partial}\Psi - g\overline{\Psi}\left(\phi_1\tau_1 + \phi_2\tau_2\right)\Psi - V(\phi_3). \tag{5.2}$$

Example potentials which may be interesting:

- $V(\phi_3) = 1 - \phi_3$ gives a single vacuum, which therefore may generalise to higher dimensions with connected boundaries at spatial infinity.
- $V(\phi_3) = 1 - \phi_3^2$ gives distinct vacua $\phi_3 = \pm 1$ and may encourage a true, topologically protected kink in (1+1)d.
- $V(\phi_3) = 1 - \cos\phi_3$ may encourage periodic solutions.

We expect that the bispinor picture would be vastly more complex and not as amenable to an analytic solution. Nonetheless, with any such potential, we would expect the ϕ_3 field to be totally determined by suitable fermion solutions, in such a manner that the appropriate fermionic Noether charge $\overline{\Psi}\hat{\gamma}^3\tau_3\Psi$ localises on rapid changes to the ϕ_3 field.

5.2.2 Fermions and solitons on $\mathbb{R} \times S^2$

As we have mentioned, the obvious next step for the S^2 model is to fully couple the baby Skyrmion field to the fermion. This requires a choice of potential term for the Skyrme field. Since the baby Skyrmion naturally has $SO(3)$ isospin symmetry, we may also be able to do this in such a way as to preserve a subgroup of the joint isospin symmetry between the fermion and the baby Skyrmion.

We are interested in investigating fermions coupled to magnetic skyrmions, particularly to the exactly solvable model of critically coupled magnetic skyrmions introduced by Barton-Singer, Ross, and Schroers [8]. We believe this is a natural subject to investigate for several reasons.

Perapechka and Shnir [52] have already demonstrated that there can be significant effects to the physics of magnetic skyrmions by including fermions. Moreover, Walton [67] has shown that exact solutions for critically coupled magnetic skyrmions exist on a spherical domain. It seems prudent therefore to adapt the analytical and numerical tools we have already developed for baby skyrmions on the sphere to a model of magnetic skyrmions on the sphere.

There are further reasons to suspect that critically coupled magnetic skyrmions may be particularly amenable to the addition of fermions. Schroers [58] has shown that models of critically coupled magnetic skyrmions arise from a gauged non-linear sigma model for suitably chosen gauge fields. In this

framework, the Dzyaloshinskii-Moriya interaction which stabilises the soliton is arbitrary, but a gauge transformation changes this interaction and so leads to a different model of magnetic skyrmions. If the curvature of the gauge connection vanishes, the solutions can be interpreted as Belavin-Polyakov monopoles interacting with impurities. Adam, Queiruga, and Wereszczynski [2] have found supersymmetric extensions of such soliton-impurity models and noted the relationship with the Dzyaloshinskii-Moriya interaction. We are therefore curious whether this unifying framework will lead to a significant role for fermions coupled to magnetic skyrmions.

Appendix A

Spinor transformations on $\mathbb{R} \times S^2$

A.1 Spin connections

We will evaluate the Dirac operator explicitly in the stereographic coordinates (X, Y) of U_S and in polar coordinates. Let us begin in stereographic coordinates. The connection 1-form is

$$\omega^a{}_b = \omega_t{}^a{}_b \mathrm{d}t + \omega_X{}^a{}_b \mathrm{d}X + \omega_Y{}^a{}_b \mathrm{d}Y. \tag{A.1}$$

The 9 *a priori* independent components we wish to solve for are, without loss of generality, the three components each of $\omega^0{}_1, \omega^0{}_2$ and $\omega^1{}_2$. By Cartan's structure equation (4.46)

- $a = 0$

$$\begin{aligned} 0 &= \mathrm{d}\hat{\theta}^0 + \omega^0{}_1 \wedge \hat{\theta}^1 + \omega^0{}_2 \wedge \hat{\theta}^2 \\ &= \left(-\frac{2}{1+R^2}\right)\left(\omega_t{}^0{}_1 \mathrm{d}t \wedge \mathrm{d}X + \omega_Y{}^0{}_1 \mathrm{d}Y \wedge \mathrm{d}X + \omega_t{}^0{}_2 \mathrm{d}t \wedge \mathrm{d}Y + \omega_X{}^0{}_2 \mathrm{d}X \wedge \mathrm{d}Y\right) \end{aligned}$$

This implies $\omega_t{}^0{}_1 = 0 = \omega_t{}^0{}_2$ and $\omega_Y{}^0{}_1 = \omega_X{}^0{}_2$.

- $a = 1$

$$
\begin{aligned}
0 &= d\hat{\theta}^1 + \omega^1{}_0 \wedge \hat{\theta}^0 + \omega^1{}_2 \wedge \hat{\theta}^2 \\
&= d\left(-\frac{2}{1+X^2+Y^2}dX\right) - \omega_X{}^0{}_1 dX \wedge dt \\
&\quad + \left(\omega_t{}^1{}_2 dt + \omega_X{}^1{}_2 dX\right) \wedge \left(-\frac{2}{1+X^2+Y^2}dY\right) \\
&= \frac{4Y}{(1+R^2)^2} dY \wedge dX - \omega_X{}^0{}_1 dX \wedge dt - \frac{2\omega_t{}^1{}_2}{1+R^2} dt \wedge dY - \frac{2\omega_X{}^1{}_2}{1+R^2} dX \wedge dY
\end{aligned}
$$

  This implies $\omega_X{}^0{}_1 = 0 = \omega_t{}^1{}_2$ and $\omega_X{}^1{}_2 = -\frac{2Y}{1+R^2}$.

- $a = 2$

$$
\begin{aligned}
0 &= d\hat{\theta}^2 + \omega^2{}_0 \wedge \hat{\theta}^0 + \omega^2{}_1 \wedge \hat{\theta}^1 \\
&= d\left(-\frac{2}{1+X^2+Y^2}dY\right) - \omega_X{}^0{}_2 dX \wedge dt - \omega_Y{}^0{}_2 dY \wedge dt \\
&\quad - \omega_Y{}^1{}_2 dY \wedge \left(-\frac{2}{1+X^2+Y^2}dX\right) \\
&= \frac{4X}{(1+R^2)^2} dX \wedge dY - \omega_X{}^0{}_2 dX \wedge dt - \omega_Y{}^0{}_2 dY \wedge dt + \frac{2\omega_Y{}^1{}_2}{1+R^2} dY \wedge dX
\end{aligned}
$$

  We finally obtain $\omega_X{}^0{}_2 (= \omega_Y{}^0{}_1) = 0 = \omega_Y{}^0{}_2$ and $\omega_Y{}^1{}_2 = \frac{2X}{1+R^2}$.

Hence the connection 1-form has as its only non-zero contribution

$$\omega^1{}_2 = \frac{2}{1+R^2}\left(X dY - Y dX\right), \tag{A.2}$$

or equivalently

$$\omega^{12} = -\frac{2}{1+R^2}\left(X dY - Y dX\right). \tag{A.3}$$

The components of the spin connection are

$$\Omega_t = 0 \tag{A.4}$$

$$\begin{aligned}\Omega_X &= -\frac{\mathrm{i}}{2}\left(\omega_X{}^{12}\Sigma_{12} + \omega_X{}^{21}\Sigma_{21}\right) \\ &= -\mathrm{i}(\omega_X{}^{12}\Sigma_{12}) \\ &= -\mathrm{i}\left(\frac{2Y}{1+R^2}\right)\frac{1}{2}\gamma^0 \\ &= -\frac{\mathrm{i}Y}{1+R^2}\gamma^0\end{aligned} \tag{A.5}$$

and similarly

$$\begin{aligned}\Omega_Y &= -\frac{\mathrm{i}}{2}(\omega_Y{}^{12}\Sigma_{12} + \omega_Y{}^{21}\Sigma_{21}) \\ &= -\mathrm{i}(\omega_Y{}^{12}\Sigma_{12}) \\ &= -\mathrm{i}\left(-\frac{2X}{1+R^2}\right)\frac{1}{2}\gamma^0 \\ &= \frac{\mathrm{i}X}{1+R^2}\gamma^0.\end{aligned} \tag{A.6}$$

We will work with the Dirac operator on spinors in the form $\not{D} = \gamma^\mu D_\mu$. We have established that in stereographic coordinates,

$$\begin{aligned}\not{D} &= \not{\partial} + \not{\Omega} = \gamma^\mu(\partial_\mu + \Omega_\mu) \\ &= \gamma^\alpha e_\alpha{}^\mu(\partial_\mu + \Omega_\mu) \\ &= \gamma^0(1)\left(\frac{\partial}{\partial t}\right) + \gamma^1\left(-\frac{1+R^2}{2}\right)\left(\frac{\partial}{\partial X} - \frac{\mathrm{i}Y}{1+R^2}\gamma^0\right) \\ &\quad + \gamma^2\left(-\frac{1+R^2}{2}\right)\left(\frac{\partial}{\partial Y} + \frac{\mathrm{i}X}{1+R^2}\gamma^0\right) \\ &= \gamma^0\partial_0 - \gamma^i\left(\frac{(1+R^2)}{2}\frac{\partial}{\partial X^i} - \frac{X^i}{2}\right).\end{aligned} \tag{A.7}$$

Compare this with the expression derived at (11) of Goatham and Krusch [23]: note that in the contribution for the spin connection, there is a relative

factor of $\frac{1}{2}$. This is because on the 2-sphere, contributions to the spatial component of the spin connection only come from the single other spatial component, whereas there are two such contributions from the two other spatial components on the 3-sphere.

In polar coordinates, the connection 1-form is

$$\omega^a{}_b = \omega_t{}^a{}_b \mathrm{d}t + \omega_\theta{}^a{}_b \mathrm{d}\theta + \omega_\phi{}^a{}_b \mathrm{d}\phi. \tag{A.8}$$

(Since there are already a lot of indices to keep track of, we will not use the subscript p to indicate polar coordinates.) Cartan's structure equation gives us the following.

- $a = 0$

$$\begin{aligned} 0 &= \mathrm{d}\hat{\theta}^0 + \omega^0{}_1 \wedge \hat{\theta}^1 + \omega^0{}_2 \wedge \hat{\theta}^2 \\ &= \omega_t{}^0{}_1 \mathrm{d}t \wedge (-\mathrm{d}\theta) + \omega_\phi{}^0{}_1 \mathrm{d}\phi \wedge (-\mathrm{d}\theta) + \omega_t{}^0{}_2 \mathrm{d}t \wedge (-\sin\theta\, \mathrm{d}\phi) \\ &\quad + \omega_\theta{}^0{}_2 \mathrm{d}\theta \wedge (-\sin\theta\, \mathrm{d}\phi) \end{aligned}$$

  This implies $\omega_t{}^0{}_1 = 0 = \omega_t{}^0{}_2$ and $\omega_\phi{}^0{}_1 = \omega_\theta{}^0{}_2 \sin\theta$.

- $a = 1$

$$\begin{aligned} 0 &= \mathrm{d}\hat{\theta}^1 + \omega^1{}_0 \wedge \hat{\theta}^0 + \omega^1{}_2 \wedge \hat{\theta}^2 \\ &= \omega_\theta{}^0{}_1 \mathrm{d}\theta \wedge \mathrm{d}t + \omega_\phi{}^1{}_0 \mathrm{d}\phi \wedge \mathrm{d}t + \omega_t{}^1{}_2 \mathrm{d}t \wedge (-\sin\theta\, \mathrm{d}\phi) \\ &\quad + \omega_\theta{}^1{}_2 \mathrm{d}\theta \wedge (-\sin\theta\, \mathrm{d}\phi) \end{aligned}$$

  Thus $\omega_\theta{}^1{}_0 = 0 = \omega_\theta{}^1{}_2$, and $\omega_\phi{}^1{}_0 = -\omega_t{}^1{}_2 \sin\theta$.

- $a = 2$

  Here,

$$\begin{aligned} d\hat{\theta}^2 &= d\left[-\sin\theta\, d\phi\right] \\ &= -\cos\theta\, d\theta \wedge d\phi \\ &= \cos\theta\, d\phi \wedge d\theta. \end{aligned}$$

  Hence,

$$\begin{aligned} 0 &= d\hat{\theta}^2 + \omega^2{}_0 \wedge \hat{\theta}^0 + \omega^2{}_1 \wedge \hat{\theta}^1 \\ &= \cos\theta\, d\phi \wedge d\theta + \omega_\theta{}^2{}_0 d\theta \wedge dt + \omega_\phi{}^2{}_0 d\phi \wedge dt + \omega_t{}^2{}_1 dt \wedge (-d\theta) \\ &\quad + \omega_\phi{}^2{}_1 d\phi \wedge (-d\theta)\,. \end{aligned}$$

  Thus $\omega_\phi{}^2{}_0 = 0$, $\omega_\phi{}^2{}_1 = \cos\theta$, and $\omega_\theta{}^2{}_0 = -\omega_t{}^2{}_1$.

We've directly established that the components $\omega_t{}^0{}_1$, $\omega_t{}^0{}_2$, $\omega_\theta{}^0{}_1$, $\omega_\theta{}^1{}_2$ and $\omega_\phi{}^0{}_2$ are all zero. Consider next $\omega_t{}^1{}_2$. Combining the above, using the asymmetry of the connection 1-form, and raising and lowering indices with η_{ab}, we establish the following identities.

$$\begin{aligned} \omega_t{}^1{}_2 &= -\omega_\theta{}^2{}_0 = \omega_{\theta 20} = -\omega_{\theta 02} = -\omega_\theta{}^0{}_2 \\ &= \csc\theta\, \omega_\phi{}^0{}_1 = \csc\theta\, \omega_{\phi 01} = -\csc\theta\, \omega_{\phi 10} = \csc\theta\, \omega_\phi{}^1{}_0 \\ &= -\omega_t{}^1{}_2 \\ &= 0. \end{aligned}$$

Thus also $\omega_\phi{}^0{}_1$ and $\omega_\theta{}^0{}_2$ are zero. The only non-zero independent component of the connection 1-form is therefore $\omega_\phi{}^1{}_2 = -\cos\theta$, i.e.,

$$\omega^{12} = \cos\theta\, d\phi, \tag{A.9}$$

and the spin connection in polar coordinates is

$$\Omega_{(p)} = -i\omega_\phi{}^{12}\left(\frac{1}{2}\gamma^0\right)d\phi = -\frac{i}{2}\cos\theta\,\gamma^0 d\phi. \tag{A.10}$$

In polar coordinates, then, the Dirac operator is

$$\begin{aligned}\not{D} &= h_p{}^\mu{}_a\ \gamma^a\left(\partial_\mu + \Omega_{p\,\mu}\right)\\ &= \gamma^0\frac{\partial}{\partial t} - \gamma^1\frac{\partial}{\partial\theta} - \frac{1}{\sin\theta}\gamma^2\left(\frac{\partial}{\partial\phi} - \frac{i}{2}\cos\theta\,\gamma^0\right)\\ &= \gamma^0\frac{\partial}{\partial t} - \gamma^1\left(\frac{\partial}{\partial\theta} + \frac{1}{2}\cot\theta\right) - \gamma^2\frac{1}{\sin\theta}\frac{\partial}{\partial\phi}.\end{aligned} \tag{A.11}$$

A.2 Spinor transition functions

We explicitly compute the spinor transition function from spherical polars to stereographic coordinates on the southern chart. As in section 4.1.3, let us denote these sets of coordinates respectively by

$$x^\mu = (t, \theta, \phi), \tag{A.12}$$

$$\tilde{x}^\mu = (t, X, Y), \tag{A.13}$$

and canonical frames for each set of coordinates respectively

$$e_a{}^\mu = \mathrm{diag}\left(1, -1, -\frac{1}{\sin\theta}\right), \tag{A.14}$$

$$\tilde{f}_a{}^\mu = \mathrm{diag}\left(1, -\frac{1+X^2+Y^2}{2}, -\frac{1+X^2+Y^2}{2}\right) \tag{A.15}$$

We intend to solve the spinor transformation equation (4.36) for S, so we must first express the new (stereographic) coordinates directly in terms of the old (polar) coordinates. Recall that by reference to the usual embedding of

S^2 in $\mathbb{R}^3$, $X = \frac{x}{1-z}$ and $Y = \frac{y}{1-z}$. Therefore,

$$\begin{aligned} X^2 + Y^2 &= \frac{x^2 + y^2}{(1-z)^2}, \\ &= \frac{1 - z^2}{(1-z)^2}, \\ &= \frac{1+z}{1-z}. \end{aligned} \tag{A.16}$$

In spherical polars, $z = \cos\theta$, so

$$X^2 + Y^2 = \frac{1 + \cos\theta}{1 - \cos\theta} = \cot^2\frac{\theta}{2}. \tag{A.17}$$

We also have $\tan\phi = \frac{Y}{X}$; thus, the direct expression of the change is

$$X = \cos\phi \cot\tfrac{\theta}{2}, \quad Y = \sin\phi\cot\tfrac{\theta}{2}. \tag{A.18}$$

The change of basis for the vector indices is therefore given by

$$\frac{\partial \tilde{x}^\mu}{\partial x^\nu} = \frac{\partial(t, X, Y)}{\partial(t, \theta, \phi)} = \begin{pmatrix} 1 & 0 & 0 \\ 0 & -\frac{1}{2}\cos\phi\left(1 + \cot^2\frac{\theta}{2}\right) & -\sin\phi\cot\frac{\theta}{2} \\ 0 & -\frac{1}{2}\sin\phi\left(1 + \cot^2\frac{\theta}{2}\right) & \cos\phi\cot\frac{\theta}{2} \end{pmatrix}. \tag{A.19}$$

In the new basis, the old frame is

$$\begin{aligned} \tilde{e}_a{}^\mu = \frac{\partial \tilde{x}^\mu}{\partial x^\nu} e_a{}^\nu &= \begin{pmatrix} 1 & 0 & 0 \\ 0 & -\frac{1}{2}\cos\phi\left(1 + \cot^2\frac{\theta}{2}\right) & -\sin\phi\cot\frac{\theta}{2} \\ 0 & -\frac{1}{2}\sin\phi\left(1 + \cot^2\frac{\theta}{2}\right) & \cos\phi\cot\frac{\theta}{2} \end{pmatrix} \begin{pmatrix} 1 & 0 & 0 \\ 0 & -1 & 0 \\ 0 & 0 & -\frac{1}{\sin\theta} \end{pmatrix} \\ &= \begin{pmatrix} 1 & 0 & 0 \\ 0 & \frac{1}{2}\cos\phi\left(1 + \cot^2\frac{\theta}{2}\right) & \frac{\sin\phi}{1-\cos\theta} \\ 0 & \frac{1}{2}\sin\phi\left(1 + \cot^2\frac{\theta}{2}\right) & -\frac{\cos\phi}{1-\cos\theta} \end{pmatrix}. \end{aligned} \tag{A.20}$$

Inverting (A.17) above, we see that

$$1 - \cos\theta = 1 - \frac{X^2 + Y^2 - 1}{X^2 + Y^2 + 1} = \frac{2}{1 + X^2 + Y^2}. \tag{A.21}$$

Thus,

$$\tilde{e}_a{}^{\mu} = \begin{pmatrix} 1 & 0 & 0 \\ 0 & -\cos\phi\left(-\frac{1+X^2+Y^2}{2}\right) & -\sin\phi\left(-\frac{1+X^2+Y^2}{2}\right) \\ 0 & -\sin\phi\left(-\frac{1+X^2+Y^2}{2}\right) & \cos\phi\left(-\frac{1+X^2+Y^2}{2}\right) \end{pmatrix}. \tag{A.22}$$

Inspecting this, we read off that the local rotation defined at (4.37) from the old frame to the new frame is

$$\tilde{T}_a{}^b = \begin{pmatrix} 1 & 0 & 0 \\ 0 & -\cos\phi & -\sin\phi \\ 0 & -\sin\phi & \cos\phi \end{pmatrix} \tag{A.23}$$

We obtain the transformation law in the local coordinates (4.38). Noting that $\gamma^0\gamma^1 = \mathrm{i}\gamma^2$ and $\gamma^0\gamma^2 = -\mathrm{i}\gamma^1$, after stripping out the factors of i, we find

$$S^\dagger S = 1, \tag{A.24}$$

$$S^\dagger\gamma^1 S = -\tilde{T}_1{}^2\gamma^2 + \tilde{T}_2{}^2\gamma^1 \qquad = \sin\phi\gamma^2 + \cos\phi\gamma^1, \tag{A.25}$$

$$S^\dagger\gamma^2 S = \tilde{T}_1{}^1\gamma^2 - \tilde{T}_2{}^1\gamma^1 \qquad = -\cos\phi\gamma^2 + \sin\phi\gamma^1. \tag{A.26}$$

(It is not surprising that we determine the spinor transition matrix must be unitary.) The solutions with determinant 1 are

$$S = (\pm)\gamma^1 \mathrm{e}^{\frac{\mathrm{i}}{2}\phi\gamma^0}. \tag{A.27}$$

In the standard representation of the γ matrices which we employ throughout Chapter 4, this has the expression

$$S = (\mp) \begin{pmatrix} 0 & \mathrm{i}e^{-\frac{\mathrm{i}}{2}\phi} \\ \mathrm{i}e^{\frac{\mathrm{i}}{2}\phi} & 0 \end{pmatrix}. \tag{A.28}$$

To specify the direction of the coordinate change, we may label spin transition functions with a subscript to indicate the old and new charts, like so: $S_{(p\to S)}$ for this transition from polar coordinates to the south chart stereographic coordinates.

If instead we change from polar coordinates to the north chart stereographic coordinates, we find

$$\tilde{T}_{(p\to N)a}{}^{b} = \begin{pmatrix} 1 & 0 & 0 \\ 0 & \cos\phi & -\sin\phi \\ 0 & -\sin\phi & -\cos\phi \end{pmatrix}. \tag{A.29}$$

The first column of equations (A.24-A.26) holds in general. Solving for $S_{p\to N}$ of determinant 1, we obtain

$$S_{(p\to N)} = (\pm)\,\gamma^2 e^{-\frac{\mathrm{i}}{2}\phi\gamma^0} = (\pm) \begin{pmatrix} 0 & -e^{\frac{\mathrm{i}}{2}\phi} \\ e^{-\frac{\mathrm{i}}{2}\phi} & 0 \end{pmatrix}. \tag{A.30}$$

Finally, transforming from south to north stereographic coordinates,

$$\tilde{T}_{(S\to N)a}{}^{b} = \begin{pmatrix} 1 & 0 & 0 \\ 0 & -\cos 2\phi & -\sin 2\phi \\ 0 & \sin 2\phi & -\cos 2\phi \end{pmatrix}, \tag{A.31}$$

and the determinant 1 solutions are

$$S_{(S\to N)} = (\pm)\, i\gamma^0 e^{i\gamma^0\phi} = (\pm) \begin{pmatrix} ie^{i\phi} & 0 \\ 0 & -ie^{-i\phi} \end{pmatrix}. \tag{A.32}$$

We observe that these are consistent as transition functions, in the sense that

$$S_{(p\to N)} S^{-1}_{(p\to S)} = (\pm)\, \gamma^2 e^{-i\gamma^0\phi}\gamma^1 = (\pm)\, i\gamma^0 e^{i\gamma^0\phi} = S_{(S\to N)}. \tag{A.33}$$

A.2.1 Spin connection transformation

We will check explicitly that these spinor transition functions are consistent with the spin connections derived in section A.1. Recall the transformation rule for the spin connection, first derived at (4.43),

$$\tilde{\Omega}_\nu = \frac{\partial x^\mu}{\partial \tilde{x}^\nu} \left(S \left[\partial_\mu S^{-1} \right] + S\Omega_\mu S^{-1} \right) \tag{A.34}$$

After (A.10), the only non-zero component of the spin connection for polar coordinates is

$$\Omega_\phi = -\frac{i}{2} \cos\theta\, \gamma^0. \tag{A.35}$$

The non-trivial components of the spin connection in southern stereographic coordinates are, therefore,

$$\tilde{\Omega}_X = \frac{\partial \phi}{\partial X} \left(S \frac{\partial S^{-1}}{\partial \phi} + S\Omega_\phi S^{-1} \right) \tag{A.36}$$

$$\tilde{\Omega}_Y = \frac{\partial \phi}{\partial Y} \left(S \frac{\partial S^{-1}}{\partial \phi} + S\Omega_\phi S^{-1} \right), \tag{A.37}$$

where S is the spinor transition function $S_{(p\to S)} = \gamma^1 e^{\frac{i}{2}\phi\gamma^0}$, arbitrarily fixing the sign. Some quick calculations show that the common factor is

$$\begin{aligned} S\frac{\partial S^{-1}}{\partial \phi} + S\Omega_\phi S^{-1} &= \frac{i}{2}\gamma^0\,(1+\cos\theta) \\ &= i\gamma^0 \frac{X^2+Y^2}{1+X^2+Y^2}. \end{aligned} \tag{A.38}$$

Then writing $\phi = \arctan\frac{Y}{X}$, we quickly find

$$\tilde{\Omega}_X = \left(-\frac{Y}{X^2+Y^2}\right) i\gamma^0 \frac{X^2+Y^2}{1+X^2+Y^2}, \tag{A.39}$$

$$\tilde{\Omega}_Y = \left(\frac{X}{X^2+Y^2}\right) i\gamma^0 \frac{X^2+Y^2}{1+X^2+Y^2}, \tag{A.40}$$

which exactly matches what we found at (A.5) and (A.6).

Appendix B

Maple code for deriving the master $\Theta(u)$ equation and performing Fuchsian analysis

This appendix contains the code for Maple worksheets which perform much of the laborious algebra for the S^2 system(s) in Chapter 4. Section B.1 is a worksheet for our spin-isospin coupled model, while Section B.2 is a worksheet which works out details of a Dirac fermion in the absence of isospin. For the ease of cross-referencing with the material in Chapter 4, the worksheet in section B.1 has been split into subsections – however, all the code in this section should be run as a single continuous Maple worksheet.

B.1 Code for spin-isospin coupling

B.1.1 The master equation

```
> EquationI := 0 = (E[f]-g*u)*Theta[1,1](u) - g*sqrt(1-u
  ^2)*Theta[1,2](u) - a*(-1*sqrt(1-u^2)*diff(Theta[2,1](u
  ),u)+u/(2*sqrt(1-u^2))*Theta[2,1](u)+(k-n/2)/sqrt(1-u
  ^2)*Theta[2,1](u));
```

```
EquationII := 0 = (E[f]+g*u)*Theta[1,2](u) - g*sqrt(1-u^2)
   *Theta[1,1](u) - a*(-1*sqrt(1-u^2)*diff(Theta[2,2](u),u
   )+u/(2*sqrt(1-u^2))*Theta[2,2](u) + (k+n/2)/sqrt(1-u^2)
   *Theta[2,2](u));
EquationIII := 0 = (-E[f]-g*u)*Theta[2,1](u) - g*sqrt(1-u
   ^2)*Theta[2,2](u) - a*(-1*sqrt(1-u^2)*diff(Theta[1,1](u
   ),u)+u/(2*sqrt(1-u^2))*Theta[1,1](u) + (-k+n/2)/sqrt(1-
   u^2)*Theta[1,1](u));
EquationIV := 0 = (-E[f]+g*u)*Theta[2,2](u) - g*sqrt(1-u
   ^2)*Theta[2,1](u) - a*(-1*sqrt(1-u^2)*diff(Theta[1,2](u
   ),u)+u/(2*sqrt(1-u^2))*Theta[1,2](u) + (-k-n/2)/sqrt(1-
   u^2)*Theta[1,2](u));

> Eq2a := isolate(EquationII, Theta[1,2](u));

> Eq1a := isolate(EquationI, Theta[1,1](u));

> Eq3a := isolate(EquationIII, Theta[2,1](u));

> Eq4a := isolate(EquationIV, Theta[2,2](u));

> ProtoE2 := simplify(subs[eval](Eq2a, Eq4a) assuming(-1<u
   , u<1)) assuming(-1<u,u<1):

> LongE2 := simplify(subs[eval](Eq3a, ProtoE2) assuming
   (-1<u, u<1)) assuming(-1<u,u<1):

> LongE2a := denom(rhs(LongE2))*lhs(LongE2) = denom(rhs(
   LongE2))*rhs(LongE2);

> ProtoE1 := simplify(subs[eval](Eq3a, Eq1a) assuming(-1<u
   ,u<1)) assuming(-1<u,u<1):
```

```
> LongE1 := simplify(subs[eval](Eq2a, ProtoE1) assuming
  (-1<u,u<1)) assuming(-1<u,u<1):

> LongE1a := denom(rhs(LongE1))*lhs(LongE1) = denom(rhs(
  LongE1))*rhs(LongE1);

> # At this point, things will be more human-readable if
  we start condensing these expressions into coefficient
  functions.

> LongE1b := collect(lhs(LongE1a)/4-rhs(LongE1a)/4=0,\\{
  diff(Theta[1,1](u),u$2),diff(Theta[1,1](u),u),Theta
  [1,1](u),Theta[2,2](u)\\})

> A1 := simplify(subs([diff(Theta[1,1](u),u$2) = 1, diff(
  Theta[1,1](u),u)=0,Theta[1,1](u)=0,Theta[2,2](u)=0],lhs
  (LongE1b)));
B1 := simplify(subs([diff(Theta[1,1](u),u$2) = 0, diff(
  Theta[1,1](u),u)=1,Theta[1,1](u)=0,Theta[2,2](u)=0],lhs
  (LongE1b)));
C1 := simplify(subs([diff(Theta[1,1](u),u$2) = 0, diff(
  Theta[1,1](u),u)=0,Theta[1,1](u)=1,Theta[2,2](u)=0],lhs
  (LongE1b)));
D1 := simplify(subs([diff(Theta[1,1](u),u$2) = 0, diff(
  Theta[1,1](u),u)=0,Theta[1,1](u)=0,Theta[2,2](u)=1],lhs
  (LongE1b)));

> LongE2b := collect(lhs(LongE2a)/4-rhs(LongE2a)/4=0,\\{
  diff(Theta[2,2](u),u$2),diff(Theta[2,2](u),u),Theta
  [2,2](u),Theta[1,1](u)\\})
```

```
> A2 := simplify(subs([diff(Theta[2,2](u),u$2) = 1, diff(
   Theta[2,2](u),u)=0,Theta[2,2](u)=0,Theta[1,1](u)=0],lhs
   (LongE2b)));
B2 := simplify(subs([diff(Theta[2,2](u),u$2) = 0, diff(
   Theta[2,2](u),u)=1,Theta[2,2](u)=0,Theta[1,1](u)=0],lhs
   (LongE2b)));
C2 := simplify(subs([diff(Theta[2,2](u),u$2) = 0, diff(
   Theta[2,2](u),u)=0,Theta[2,2](u)=1,Theta[1,1](u)=0],lhs
   (LongE2b)));
D2 := simplify(subs([diff(Theta[2,2](u),u$2) = 0, diff(
   Theta[2,2](u),u)=0,Theta[2,2](u)=0,Theta[1,1](u)=1],lhs
   (LongE2b)));

> GeneralE1 := A1*diff(Theta[1, 1](u), u, u) + B1*diff(
   Theta[1,1](u), u) + C1*Theta[1, 1](u) = D1*Theta[2, 2](
   u):
GeneralE2 := A2*diff(Theta[2, 2](u), u, u) + B2*diff(Theta
   [2, 2](u), u) + C2*Theta[2, 2](u) = D2*Theta[1, 1](u):
GeneralSystem := [GeneralE1, GeneralE2]:
GeneralSystem[1];
GeneralSystem[2];

> simplify(C1 - subs(k=-k,C2));

> simplify(A1-A2);

> simplify(B1-B2);

> simplify(D1-D2);

> A3 := simplify(subs(m=0, A1/D1));
B3 := simplify(subs(m=0, B1/D1));
```

```
C3 := simplify(subs(m=0, C1/D1));

> LongEq4 := Theta[2,2](u) = A3*diff(Theta[1,1](u),u,u) +
   B3*diff(Theta[1,1](u),u) + C3*Theta[1,1](u):

> LongEq5 := subs[eval](LongEq4,GeneralSystem[2]):

> GeneralMasslessDE := collect(lhs(LongEq5)-rhs(LongEq5)
   =0,\\{diff(Theta[1,1](u),u$4),diff(Theta[1,1](u),u$3),
   diff(Theta[1,1](u),u$2),diff(Theta[1,1](u),u),Theta
   [1,1](u)\\}):

> # Now let's sort out the prefactor and put this equation
    into normal form.

> Prefactor:= simplify(subs([diff(Theta[1,1](u),u$4)=1,
   diff(Theta[1,1](u),u$3)=0,diff(Theta[1,1](u),u$2)=0,
   diff(Theta[1,1](u),u)=0,Theta[1,1](u)=0],lhs(
   GeneralMasslessDE)));

> NormalFormFactor := a*denom(Prefactor)^3*(u-1)*(u+1);

> GeneralMasslessDENormalForm := collect(simplify(lhs(
   GeneralMasslessDE)*NormalFormFactor=0),\\{diff(Theta
   [1,1](u),u$4),diff(Theta[1,1](u),u$3),diff(Theta[1,1](u
   ),u$2),diff(Theta[1,1](u),u),Theta[1,1](u)\\});

> # These expressions are complicated, but we have
   succesfully isolated them. Just might need to be
   careful about the apparent roots involving E[f] and g.
```

B.1.2 Fuchsian analysis

```
> # Let's look at neatly isolating the coefficient
   functions.

> GeneralSystem[1]

> subs([diff(Theta[1,1](u),u$2)=1,diff(Theta[1,1](u),u)=0,
   Theta[1,1](u)=0],GeneralSystem[1]);
subs([diff(Theta[1,1](u),u$2)=0,diff(Theta[1,1](u),u)=1,
   Theta[1,1](u)=0],GeneralSystem[1]);
subs([diff(Theta[1,1](u),u$2)=0,diff(Theta[1,1](u),u)=0,
   Theta[1,1](u)=1],GeneralSystem[1]);

> # That approach seems to work.

> R1 := simplify(subs([diff(Theta[1,1](u),u$4)=1,diff(
   Theta[1,1](u),u$3)=0,diff(Theta[1,1](u),u$2)=0,diff(
   Theta[1,1](u),u)=0,Theta[1,1](u)=0],lhs(
   GeneralMasslessDENormalForm)));

> R2 := simplify(subs([diff(Theta[1,1](u),u$4)=0,diff(
   Theta[1,1](u),u$3)=1,diff(Theta[1,1](u),u$2)=0,diff(
   Theta[1,1](u),u)=0,Theta[1,1](u)=0],lhs(
   GeneralMasslessDENormalForm)));

> R3 := simplify(subs([diff(Theta[1,1](u),u$4)=0,diff(
   Theta[1,1](u),u$3)=0,diff(Theta[1,1](u),u$2)=1,diff(
   Theta[1,1](u),u)=0,Theta[1,1](u)=0],lhs(
   GeneralMasslessDENormalForm)));

> R4 := simplify(subs([diff(Theta[1,1](u),u$4)=0,diff(
   Theta[1,1](u),u$3)=0,diff(Theta[1,1](u),u$2)=0,diff(
   Theta[1,1](u),u)=1,Theta[1,1](u)=0],lhs(
   GeneralMasslessDENormalForm)));
```

```
> R5 := simplify(subs([diff(Theta[1,1](u),u$4)=0,diff(
   Theta[1,1](u),u$3)=0,diff(Theta[1,1](u),u$2)=0,diff(
   Theta[1,1](u),u)=0,Theta[1,1](u)=1],lhs(
   GeneralMasslessDENormalForm)));

> # First, let's see if the Fuchs relations are satisfied
   if we just ignore the parameter-dependent pole(s).

> # Check the regularity of the pole at infinity.

> Rv1 := simplify(v^8*subs(u=1/v, R1)):
Rv2 := simplify(12*v^7*subs(u=1/v,R1) - v^6*subs(u=1/v,R2)
   ):
Rv3 := simplify(subs(u=1/v, 36*v^6*R1 - 6*v^5*R2 + v^4*R3)
   ):
Rv4 := simplify(subs(u=1/v, 24*v^5*R1 - 6*v^4*R2 + 2*v^3*
   R3 - v^2*R4)):
Rv5 := simplify(subs(u=1/v, R5)):

> # In terms of v = 1/u, the DE is
Rv1*diff(Theta[1,1](v),v$4) + Rv2*diff(Theta[1,1](v),v$3)
   + Rv3*diff(Theta[1,1](v),v$2) + Rv2*diff(Theta[1,1](v),
   v) + Rv1*Theta[1,1](v) = 0;

> # Isolate the exponent.

> pInf := simplify(Rv2/Rv1*v):
qInf :=simplify(Rv3/Rv1*v^2):
rInf := simplify(Rv4/Rv1*v^3):
sInf := simplify(Rv5/Rv1*v^4):
pInf0 := simplify(subs(v=0, pInf));
qInf0 := simplify(subs(v=0, qInf));
```

```
rInf0 := simplify(subs(v=0, rInf));
sInf0 := simplify(subs(v=0, sInf));
IndicialEquationInf := lambda*(lambda-1)*(lambda-2)*(
   lambda-3) + pInf0*lambda*(lambda-1)*(lambda-2) + qInf0*
   lambda*(lambda-1) + rInf0*lambda + sInf0 = 0;
ExponentsAtInf := [solve( IndicialEquationInf, lambda)];

> # Check the poles.

> # At the north pole:
pNorth := simplify(R2/R1*(u-1)):
qNorth := simplify(R3/R1*(u-1)^2):
rNorth := simplify(R4/R1*(u-1)^3):
sNorth := simplify(R5/R1*(u-1)^4):
pNorth0 := simplify(subs(u=1, pNorth));
qNorth0 := simplify(subs(u=1, qNorth));
rNorth0 := simplify(subs(u=1, rNorth));
sNorth0 := simplify(subs(u=1, sNorth));
IndicialEquationNorth := mu*(mu-1)*(mu-2)*(mu-3) + pNorth0
   *mu*(mu-1)*(mu-2) + qNorth0*mu*(mu-1) + rNorth0*mu +
   sNorth0 = 0;
ExponentsAtNorth := [solve( IndicialEquationNorth, mu)];

> # At the south pole:
pSouth := simplify(R2/R1*(u+1)):
qSouth := simplify(R3/R1*(u+1)^2):
rSouth := simplify(R4/R1*(u+1)^3):
sSouth := simplify(R5/R1*(u+1)^4):
pSouth0 := simplify(subs(u=-1, pSouth));
qSouth0 := simplify(subs(u=-1, qSouth));
```

```
rSouth0 := simplify(subs(u=-1, rSouth));
sSouth0 := simplify(subs(u=-1, sSouth));
IndicialEquationSouth := nu*(nu-1)*(nu-2)*(nu-3) + pSouth0
   *nu*(nu-1)*(nu-2) + qSouth0*nu*(nu-1) + rSouth0*nu +
   sSouth0 = 0;
ExponentsAtSouth := [solve( IndicialEquationSouth, nu)];

> simplify(add(i, i=ExponentsAtInf) + add(j, j=
   ExponentsAtNorth) + add(l, l=ExponentsAtSouth));

> # This doesn't satisfy the Fuchs relation yet. We should
    be careful of the parameter-dependent pole(s).

> # Now let's look at that coalescent pole for the general
    n.

> solve((g*n - E[f])*u + E[f]*n - g=0,u)

> # Consider perhaps that at large n, this looks rather
   like the other apparent parameter pole, u = -E[f]/g.
   But proceed generally.

> pCoalescent := simplify(R2/R1*(u+(n*E[f] - g)/(g*n - E[f
   ])));
qCoalescent := simplify(R3/R1*(u+(n*E[f] - g)/(g*n - E[f])
   )^2):
rCoalescent := simplify(R4/R1*(u+(n*E[f] - g)/(g*n - E[f])
   )^3):
sCoalescent := simplify(R5/R1*(u+(n*E[f] - g)/(g*n - E[f])
   )^4):
pCoalescent0 := simplify(subs(u=-(n*E[f] - g)/(g*n - E[f])
   ,pCoalescent));
```

```
qCoalescent0 := simplify(subs(u=-(n*E[f] - g)/(g*n - E[f])
    ,qCoalescent));
rCoalescent0 := simplify(subs(u=-(n*E[f] - g)/(g*n - E[f])
    ,rCoalescent));
sCoalescent0 := simplify(subs(u=-(n*E[f] - g)/(g*n - E[f])
    ,sCoalescent));
IndicialEquationCoalescent := kappa*(kappa-1)*(kappa-2)*(
    kappa-3) + pCoalescent0*kappa*(kappa-1)*(kappa-2) +
    qCoalescent0*kappa*(kappa-1) + rCoalescent0*kappa +
    sCoalescent0 = 0;
ExponentsAtCoalescent := [solve(
    IndicialEquationCoalescent,kappa)];

> simplify(add(i, i=ExponentsAtInf) + add(i, i=
    ExponentsAtNorth) + add(i, i=ExponentsAtSouth) + add(i,
     i=ExponentsAtCoalescent))

> # This satisfies the Fuchs relation for general n: the
    order of the DE is m=4 and the number of finite
    singularities is now p=3, and m*(m-1)*(p-1)/2 = 12.
```

B.1.3 Fuchsian analysis for $n = 1$

```
> # Observe that if n=1, the more complex parameter-
    dependent pole coalesces to u=-1.

> # So let's look at that special case.

> simplify(subs(n=1,GeneralMasslessDE))

> MasslessN1DE := simplify(a*subs(n=1,
    GeneralMasslessDENormalForm)/(g*u+E[f])^2);
```

```
> # Take the same approach as before. Isolate the
   coefficient functions; check the regularity of the pole
    at infinity; derive the exponents and check the Fuchs
   relation.

> N1R1 := simplify(subs([diff(Theta[1,1](u),u$4)=1,diff(
   Theta[1,1](u),u$3)=0,diff(Theta[1,1](u),u$2)=0,diff(
   Theta[1,1](u),u)=0,Theta[1,1](u)=0],lhs(MasslessN1DE)))
   ;
N1R2 := simplify(subs([diff(Theta[1,1](u),u$4)=0,diff(
   Theta[1,1](u),u$3)=1,diff(Theta[1,1](u),u$2)=0,diff(
   Theta[1,1](u),u)=0,Theta[1,1](u)=0],lhs(MasslessN1DE)))
   ;
N1R3 := simplify(subs([diff(Theta[1,1](u),u$4)=0,diff(
   Theta[1,1](u),u$3)=0,diff(Theta[1,1](u),u$2)=1,diff(
   Theta[1,1](u),u)=0,Theta[1,1](u)=0],lhs(MasslessN1DE)))
   ;
N1R4 := simplify(subs([diff(Theta[1,1](u),u$4)=0,diff(
   Theta[1,1](u),u$3)=0,diff(Theta[1,1](u),u$2)=0,diff(
   Theta[1,1](u),u)=1,Theta[1,1](u)=0],lhs(MasslessN1DE)))
   ;
N1R5 := simplify(subs([diff(Theta[1,1](u),u$4)=0,diff(
   Theta[1,1](u),u$3)=0,diff(Theta[1,1](u),u$2)=0,diff(
   Theta[1,1](u),u)=0,Theta[1,1](u)=1],lhs(MasslessN1DE)))
   ;

> # Check the regularity of the pole at infinity.

> N1Rv1 := simplify(v^8*subs(u=1/v, N1R1)):
```

```
N1Rv2 := simplify(12*v^7*subs(u=1/v,N1R1) - v^6*subs(u=1/v
    ,N1R2)):
N1Rv3 := simplify(subs(u=1/v, 36*v^6*N1R1 - 6*v^5*N1R2 + v
    ^4*N1R3)):
N1Rv4 := simplify(subs(u=1/v, 24*v^5*N1R1 - 6*v^4*N1R2 +
    2*v^3*N1R3 - v^2*N1R4)):
N1Rv5 := simplify(subs(u=1/v, N1R5)):

> # In terms of v = 1/u, the DE is
N1Rv1*diff(Theta[1,1](v),v$4) + N1Rv2*diff(Theta[1,1](v),
    v$3) + N1Rv3*diff(Theta[1,1](v),v$2) + N1Rv2*diff(Theta
    [1,1](v),v) + N1Rv1*Theta[1,1](v) = 0;

> # Isolate the exponent.

> pInfN1 := simplify(N1Rv2/N1Rv1*v):
qInfN1 :=simplify(N1Rv3/N1Rv1*v^2):
rInfN1 := simplify(N1Rv4/N1Rv1*v^3):
sInfN1 := simplify(N1Rv5/N1Rv1*v^4):
pInf0N1 := simplify(subs(v=0, pInfN1));
qInf0N1 := simplify(subs(v=0, qInfN1));
rInf0N1 := simplify(subs(v=0, rInfN1));
sInf0N1 := simplify(subs(v=0, sInfN1));
IndicialEquationInfN1 := lambda*(lambda-1)*(lambda-2)*(
    lambda-3) + pInf0N1*lambda*(lambda-1)*(lambda-2) +
    qInf0N1*lambda*(lambda-1) + rInf0N1*lambda + sInf0N1 =
    0;
ExponentsAtInfN1 := [solve( IndicialEquationInfN1, lambda)
    ];

> # At the north pole:
```

```
pNorthN1 := simplify(N1R2/N1R1*(u-1)):
qNorthN1 := simplify(N1R3/N1R1*(u-1)^2):
rNorthN1 := simplify(N1R4/N1R1*(u-1)^3):
sNorthN1 := simplify(N1R5/N1R1*(u-1)^4):
pNorth0N1 := simplify(subs(u=1, pNorthN1));
qNorth0N1 := simplify(subs(u=1, qNorthN1));
rNorth0N1 := simplify(subs(u=1, rNorthN1));
sNorth0N1 := simplify(subs(u=1, sNorthN1));
IndicialEquationNorthN1 := mu*(mu-1)*(mu-2)*(mu-3) +
   pNorth0N1*mu*(mu-1)*(mu-2) + qNorth0N1*mu*(mu-1) +
   rNorth0N1*mu + sNorth0N1 = 0;
ExponentsAtNorthN1 := [solve( IndicialEquationNorthN1, mu)
   ];

> # At the south pole:
pSouthN1 := simplify(N1R2/N1R1*(u+1)):
qSouthN1 := simplify(N1R3/N1R1*(u+1)^2):
rSouthN1 := simplify(N1R4/N1R1*(u+1)^3):
sSouthN1 := simplify(N1R5/N1R1*(u+1)^4):
pSouth0N1 := simplify(subs(u=-1, pSouthN1));
qSouth0N1 := simplify(subs(u=-1, qSouthN1));
rSouth0N1 := simplify(subs(u=-1, rSouthN1));
sSouth0N1 := simplify(subs(u=-1, sSouthN1));
IndicialEquationSouthN1 := nu*(nu-1)*(nu-2)*(nu-3) +
   pSouth0N1*nu*(nu-1)*(nu-2) + qSouth0N1*nu*(nu-1) +
   rSouth0N1*nu + sSouth0N1 = 0;
ExponentsAtSouthN1 := [solve( IndicialEquationSouthN1, nu)
   ];
```

```
> simplify(add(i, i=ExponentsAtInfN1) + add(j, j=
  ExponentsAtNorthN1) + add(l, l=ExponentsAtSouthN1));

> # The Fuchs relation remains satisfied considering only
  the poles at 1,-1 and infinity when n=1: the order of
  the DE is still m=4, while now the number of finite
  poles is now p=2, and m*(m-1)*(p-1)/2 = 6.
```

B.1.4 The energy levels

```
> EnergyLevelsN1 := [solve(IndicialEquationInfN1,E[f])];

> subs(lambda=-l-1/2,EnergyLevelsN1);

> simplify(%)
```

B.2 Code for the pure Dirac fermion on $\mathbb{R} \times S^2$ without isospin

```
> # The Fuchsian analysis can be quickly performed using
  the components of the Dirac equation.

> Equation1 := E[f]*Theta[1](u) = a*(-sqrt(1-u^2)*diff(
  Theta[2](u),u)+u/(2*sqrt(1-u^2))*Theta[2](u) + m/sqrt
  (1-u^2)*Theta[2](u));

> Equation2 := E[f]*Theta[2](u) = a*(sqrt(1-u^2)*diff(
  Theta[1](u),u)-u/(2*sqrt(1-u^2))*Theta[1](u) + m/sqrt
  (1-u^2)*Theta[1](u));

> MEq1 := simplify(E[f]*subs(isolate(Equation2,Theta[2](u)
  ),Equation1) assuming(-1<u,u<1)) assuming(-1<u,u<1);
```

```
> R1 := simplify((u^2-1)*subs([diff(Theta[1](u),u$2)=1,
   diff(Theta[1](u),u)=0,Theta[1](u)=0],rhs(MEq1)-lhs(MEq1
   )));
R2 := simplify((u^2-1)*subs([diff(Theta[1](u),u$2)=0,diff(
   Theta[1](u),u)=1,Theta[1](u)=0],rhs(MEq1)-lhs(MEq1)));
R3 := simplify((u^2-1)*subs([diff(Theta[1](u),u$2)=0,diff(
   Theta[1](u),u)=0,Theta[1](u)=1],rhs(MEq1)-lhs(MEq1)));

> PureMasslessDE := R1*diff(Theta[1](u),u$2) + R2*diff(
   Theta[1](u),u) + R3*Theta[1](u)=0;

> # Check the pole at infinity.

> Rv1 := simplify(v^4*subs(u=1/v,R1)):

> Rv2 := simplify(2*v^3*subs(u=1/v,R1)-v^2*subs(u=1/v,R2))
   :

> Rv3 := simplify(subs(u=1/v,R3)):

> # In terms of v = 1/u, the differential equation is

> Rv1*diff(Theta[1](v),v$2) + Rv2*diff(Theta[1](v),v) +
   Rv3*Theta[1](v) = 0;

> # Multiplying by v^2, we can see that v=0 is also a
   regular singular point.

> # Let's work out the exponents.

> # About the north pole, u=1:

> pNorth := simplify(R2/R1*(u-1));
qNorth := simplify(R3/R1*(u-1)^2);
pNorth0 := subs(u=1,pNorth);
```

```
qNorth0 := subs(u=1,qNorth);
IndicialEquationNorth := mu*(mu-1) + pNorth0*mu + qNorth0
   = 0;
solve(IndicialEquationNorth,mu);

> # About the south pole, u=-1:

> pSouth := simplify(R2/R1*(u+1));
qSouth := simplify(R3/R1*(u+1)^2);
pSouth0 := subs(u=-1,pSouth);
qSouth0 := subs(u=-1,qSouth);
IndicialEquationSouth := nu*(nu-1) + pSouth0*nu + qSouth0
   = 0;
solve(IndicialEquationSouth,nu);

> # About complex infinity, v=0:

> pInf := simplify(Rv2/Rv1*v);
qInf := simplify(Rv3/Rv1*v^2);
pInf0 := subs(v=0,pInf);
qInf0 := subs(v=0,qInf);
IndicialEquationInf := kappa*(kappa-1) + pInf0*kappa +
   qInf0 = 0;
solve(IndicialEquationInf,kappa);

> # The Fuchs relation is satisfied.
```

```
> # Observe that the contribution from the exponents at
   the north and south poles will always be |m|. If we
   assume that for a lowest- or highest-weight state,
   there is no polynomial contribution, then -kappa = |m|.
    Since kappa = 1/2 +/- E[f]/a we have E[f]/a = +/-(
   kappa - 1/2) = +/- (|m| + 1/2). This illustrates the
   Lichnerowicz-Weitzenboeck theorem.

> # We will work out our SU(2) operators to confirm this
   assertion.

>

> # We set up our gamma matrix representation so we can
   quickly build operators and evaluate their application.
with(LinearAlgebra):

> g0 := Matrix([[1,0],[0,-1]]); g1 := Matrix([[0,-I],[-I
   ,0]]); g2 := Matrix([[0,-1],[1,0]]);

> F := Vector(<F1(u,phi),F2(u,phi)>);

> HamF := I*g0.(g1.(-sqrt(1-u^2)*diff(F,u) + u/(2*sqrt(1-u
   ^2))*F) + g2.(1/sqrt(1-u^2)*diff(F,phi)));

> L3F := -I*diff(F,phi);

> LPlusF := exp(I*phi)*(-sqrt(1-u^2)*diff(F,u) + I*u/sqrt
   (1-u^2)*diff(F,phi) + 1/(2*sqrt(1-u^2))*g0.F);

> LMinusF := exp(-I*phi)*(sqrt(1-u^2)*diff(F,u) + I*u/sqrt
   (1-u^2)*diff(F,phi) + 1/(2*sqrt(1-u^2))*g0.F);

> # Check the SU(2) commutation relations.
```

```
> LPLMF := simplify(subs([F1(u,phi) = LMinusF[1],F2(u,phi)
   =LMinusF[2]],LPlusF)):

> LMLPF := simplify(subs([F1(u,phi) = LPlusF[1],F2(u,phi)=
   LPlusF[2]],LMinusF)):

> simplify(LPLMF - LMLPF - 2*L3F);

> L3LPF := simplify(subs([F1(u,phi) = LPlusF[1],F2(u,phi)=
   LPlusF[2]],L3F)):

> LPL3F := simplify(subs([F1(u,phi) = L3F[1],F2(u,phi)=L3F
   [2]],LPlusF)):

> simplify(L3LPF - LPL3F - LPlusF);

> L3LMF := simplify(subs([F1(u,phi) = LMinusF[1],F2(u,phi)
   =LMinusF[2]],L3F)):

> LML3F := simplify(subs([F1(u,phi) = L3F[1],F2(u,phi)=L3F
   [2]],LMinusF)):

> simplify(L3LMF - LML3F + LMinusF);

> # This confirms that we have an SU(2) rep. We should
   also check that the SU(2) operators commute with the
   Hamiltonian.

> HamLPF := simplify(subs([F1(u,phi) = LPlusF[1],F2(u,phi)
   =LPlusF[2]],HamF)):

> LPHamF := simplify(subs([F1(u,phi) = HamF[1],F2(u,phi)=
   HamF[2]],LPlusF)):
```

```
> HamLMF := simplify(subs([F1(u,phi) = LMinusF[1],F2(u,phi
  )=LMinusF[2]],HamF)):

> LMHamF := simplify(subs([F1(u,phi) = HamF[1],F2(u,phi)=
  HamF[2]],LMinusF)):

> HamL3F := simplify(subs([F1(u,phi) = L3F[1],F2(u,phi)=
  L3F[2]],HamF)):

> L3HamF := simplify(subs([F1(u,phi) = HamF[1],F2(u,phi)=
  HamF[2]],L3F)):

> simplify(HamLPF - LPHamF);

> simplify(HamLMF - LMHamF);

> simplify(HamL3F - L3HamF);

> # They do. Finally we construct the Casimir operator.

> LSquaredF := simplify(subs([F1(u,phi) = L3F[1],F2(u,phi)
  =L3F[2]],L3F) + (1/2)*(LPLMF + LMLPF));

> HamSquaredF := simplify(subs([F1(u,phi) = HamF[1],F2(u,
  phi) = HamF[2]],HamF));

> simplify(HamSquaredF - LSquaredF);

> # So H^2 = L^2 + 1/4; i.e., on a joint eigenstate of
  energy E[f] and total angular momentum l, E[f]^2 = l*(l
  +1) + 1/4 = (l + 1/2)^2.

> # Thus indeed the energy eigenvalues are non-zero
  integers.
```

```
> # Finally let us solve for highest and lowest weight
   states, to check our assertion that their polynomial
   parts are trivial.

> HighestWeightCondition := simplify(subs(phi=0,simplify(
   subs([F1(u,phi) = exp(I*l*phi)*Theta[1](u),F2(u,phi)=
   exp(I*l*phi)*Theta[2](u)],LPlusF=0))));

> LowestWeightCondition := simplify(subs(phi=0,simplify(
   subs([F1(u,phi) = exp(I*(-l)*phi)*Theta[1](u),F2(u,phi)
   =exp(I*(-l)*phi)*Theta[2](u)],LMinusF=0))));

> HighestWeight1 := subs(_C1=A,dsolve(lhs(
   HighestWeightCondition)[1]=0,Theta[1](u)));

> LowestWeight1 := subs(_C1=A,dsolve(lhs(
   LowestWeightCondition)[1]=0,Theta[1](u)));

> # This proves our assertion.

> # Finally let us look at the degeneracy of such a state,
    as a condition on the coefficients of the components
   of a lowest weight state.

> HighestWeight2 := subs(_C1=B,dsolve(lhs(
   HighestWeightCondition)[2]=0,Theta[2](u))):

> LowestWeight2 := subs(_C1=B,dsolve(lhs(
   LowestWeightCondition)[2]=0,Theta[2](u))):

> DiracEquation := E[f]*F = HamF;
```

```
> LowestWeightDiracEquation := simplify(subs[eval]([F1(u,
   phi) = exp(I*(-l)*phi)*rhs(LowestWeight1),F2(u,phi) =
   exp(I*(-l)*phi)*rhs(LowestWeight2)],DiracEquation))
   assuming(-1<u,u<1):

> CoeffEq1 := simplify(subs(phi=0,lhs(
   LowestWeightDiracEquation)[1] = rhs(
   LowestWeightDiracEquation)[1])):

> CoeffEq2 := simplify(subs(phi=0,lhs(
   LowestWeightDiracEquation)[2] = rhs(
   LowestWeightDiracEquation)[2])):

> UpperBranch := subs(E[f]=l+1/2,[CoeffEq1,CoeffEq2]):

> LowerBranch := subs(E[f]=-1*(l+1/2),[CoeffEq1,CoeffEq2])
   :

> solve(UpperBranch,A) assuming(-1<u,u<1);

> solve(LowerBranch,A) assuming(-1<u,u<1);

> # We observe that the distinct branches account for the
   two possible parities of a solution; each has
   degeneracy 1.
```

Bibliography

[1] A. A. Abrikosov Jr. "Dirac operator on the Riemann sphere". Dec. 2002. URL: https://arxiv.org/abs/hep-th/0212134 (visited on 05/29/2022). Unpublished.

[2] C. Adam, Jose M. Queiruga, and A. Wereszczynski. "BPS soliton-impurity models and supersymmetry". In: *Journal of High Energy Physics* 2019.7 (2019). DOI: 10.1007/jhep07(2019)164.

[3] C. Adam et al. "Relativistic Moduli Space for Kink Collisions". In: (2021). DOI: https://doi.org/10.48550/arXiv.2111.06790.

[4] C. Adam et al. "Spectral Walls in Soliton Collisions". In: (2019). DOI: https://doi.org/10.48550/arXiv.1903.12100.

[5] Christoph Adam et al. "A new consistent neutron star equation of state from a generalized Skyrme model". In: *Physics Letters B* 811 (Dec. 2020), p. 135928. DOI: 10.1016/j.physletb.2020.135928.

[6] A. Alonso-Izquierdo. "Asymmetric kink scattering in a two-component scalar field theory model". In: *Communications in Nonlinear Science and Numerical Simulation* 75 (Aug. 2019), pp. 200–219. DOI: 10.1016/j.cnsns.2019.04.001.

[7] Marco Barsanti and Gianni Tallarita. "Baby-Skyrmions dressed by fermions, an analytic sector". In: (June 4, 2021). arXiv: 2106.02410 [hep-th].

[8] Bruno Barton-Singer, Calum Ross, and Bernd J. Schroers. "Magnetic Skyrmions at Critical Coupling". In: *Communications in Mathematical*

Physics 375.3 (2020), pp. 2259–2280. DOI: 10.1007/s00220-019-03676-1.

[9] Dionisio Bazeia, João G. F. Campos, and Azadeh Mohammadi. "Resonance mediated by fermions in kink-antikink collisions". In: (Aug. 28, 2022). arXiv: 2208.13261 [hep-th].

[10] Alexei N Bogdanov and DA Yablonskii. "Thermodynamically stable "vortices" in magnetically ordered crystals. The mixed state of magnets". In: *Zh. Eksp. Teor. Fiz* 95.1 (Jan. 1989), p. 178. URL: https://www.researchgate.net/profile/A-Bogdanov-2/publication/210269779_Thermodynamically_stable_vortices_in_magnetically_ordered_crystals_The_mixed_state_of_magnets (visited on 04/22/2023).

[11] E. B. Bogomol'nyi. "Stability of classical solutions". In: *Soviet Journal of Nuclear Physics* 24.4 (1976), pp. 449–454.

[12] C.G. Callan and J.A. Harvey. "Anomalies and fermion zero modes on strings and domain walls". In: *Nuclear Physics B* 250.1-4 (Jan. 1985), pp. 427–436. DOI: 10.1016/0550-3213(85)90489-4.

[13] João G. F. Campos and Azadeh Mohammadi. "Fermions on wobbling kinks: normal versus quasinormal modes". In: *Journal of High Energy Physics* 2021.9 (Sept. 2021). DOI: 10.1007/jhep09(2021)103. arXiv: 2106.04712 [hep-th].

[14] Shi Chen, Kenji Fukushima, and Zebin Qiu. "Skyrmions in a magnetic field and π^0 domain wall formation in dense nuclear matter". In: *Physical Review D* 105.1 (Jan. 2022), p. l011502. DOI: 10.1103/physrevd.105.l011502.

[15] Ivan C. Christov et al. "Kink-Antikink Collisions and Multi-Bounce Resonance Windows in Higher-Order Field Theories". In: (2020). DOI: https://doi.org/10.48550/arXiv.2005.00154.

[16] K. Colanero and M.-C. Chu. "A dynamical chiral bag model". In: *Physical Review C* 65.4 (2002), p. 045203. DOI: 10.1103/physrevc.65.045203.

[17] Sidney Coleman. "Quantum sine-Gordon equation as the massive Thirring model". In: *Physical Review D* 11.8 (Apr. 1975), pp. 2088–2097. DOI: https://doi.org/10.1103/PhysRevD.11.2088.

[18] Sidney Coleman and Jeffrey Mandula. "All Possible Symmetries of the *S* Matrix". In: *Physical Review* 159.5 (5 July 1967), pp. 1251–1256. DOI: 10.1103/physrev.159.1251. URL: https://link.aps.org/doi/10.1103/PhysRev.159.1251.

[19] David Cortés-Ortuño et al. "Thermal stability and topological protection of skyrmions in nanotracks". In: *Scientific Reports* 7.1 (June 22, 2017). DOI: 10.1038/s41598-017-03391-8.

[20] Paul Adrien Maurice Dirac. "Quantised singularities in the electromagnetic field". In: *Proceedings of the Royal Society London*. Vol. 133. 821. The Royal Society, 1931, pp. 60–72. DOI: 10.1098/rspa.1931.0130.

[21] Tevian Dray. "The relationship between monopole harmonics and spin-weighted spherical harmonics". In: *Journal of Mathematical Physics* 26.5 (1985), pp. 1030–1033. DOI: 10.1063/1.526533.

[22] David Foster et al. "Two-dimensional skyrmion bags in liquid crystals and ferromagnets". In: *Nature Physics* 15.7 (2019), pp. 655–659. DOI: 10.1038/s41567-019-0476-x.

[23] Stephen W. Goatham and Steffen Krusch. "Fermions, Skyrmions and the 3-sphere". In: *Journal of Physics A: Mathematical and Theoretical* 43.3 (2010), p. 035402. DOI: 10.1088/1751-8113/43/3/035402.

[24] Siamak Sadat Gousheh, Azadeh Mohammadi, and Leila Shahkarami. "Casimir energy for a coupled fermion-kink system and its stability".

In: *Physical Review D* 87.4 (2013), p. 045017. DOI: 10.1103/physrevd.87.045017.

[25] Chris Halcrow and Derek Harland. "Nucleon-nucleon potential from instanton holonomies". In: (2022). DOI: 10.48550/ARXIV.2208.04863.

[26] Seamus Heaney. *Death of a Naturalist*. Faber and Faber, 1966. ISBN: 0571066658.

[27] G.'t Hooft. "Magnetic monopoles in unified gauge theories". In: *Nuclear Physics B* 79.2 (Sept. 1974), pp. 276–284. DOI: https://doi.org/10.1016/0550-3213(74)90486-6.

[28] Atsushi Hosaka and Hiroshi Toki. "Chiral bag model for the nucleon". In: *Physics Reports* 277.2-3 (1996), pp. 65–188. DOI: 10.1016/s0370-1573(96)00013-0.

[29] Edward L. Ince. *Ordinary Differential Equations*. Dover Publications, Incorporated, 2012. ISBN: 9780486158211.

[30] M de Innocentis and R S Ward. "Skyrmions on the 2-sphere". In: *Nonlinearity* 14.3 (Apr. 2001), pp. 663–671. DOI: 10.1088/0951-7715/14/3/312. URL: https://doi.org/10.1088/0951-7715/14/3/312.

[31] R. Jackiw and P. Rossi. "Zero modes of the vortex-fermion system". In: *Nuclear Physics B* 190.4 (Dec. 1981), pp. 681–691. DOI: 10.1016/0550-3213(81)90044-4.

[32] Marek Karliner and Itay Hen. "Review of Rotational Symmetry Breaking in Baby Skyrme Models". In: (2009). URL: https://arxiv.org/abs/0901.1489.

[33] Marek Karliner and Itay Hen. "Rotational Symmetry Breaking in Baby Skyrme Models". In: *The Multifaceted Skyrmion*. Ed. by Gerald E Brown and Manique Rho. WORLD SCIENTIFIC, Jan. 2010. Chap. 11, pp. 179–213. DOI: 10.1142/9789814280709_0008. eprint: https://www.worldscientific.

com/doi/pdf/10.1142/9789814280709_0008. URL: https://www.worldscientific.com/doi/abs/10.1142/9789814280709_0008.

[34] Noah Kent et al. "Creation and observation of Hopfions in magnetic multilayer systems". In: *Nature Communications* 12.1 (Mar. 2021). DOI: https://doi.org/10.1038/s41467-021-21846-5.

[35] Robion C. Kirby. *The Topology of 4-Manifolds*. Springer, 1991. ISBN: 9783540511489.

[36] Steffen Krusch. "S^3 Skyrmions and the Rational Map Ansatz". In: *Nonlinearity* 13.6 (Oct. 2000), pp. 2163–2185. DOI: 10.1088/0951-7715/13/6/315.

[37] Steffen Krusch. "Fermions coupled to skyrmions on S^3". In: *Journal of Physics A: Mathematical and General* 36.29 (2003), pp. 8141–8163. DOI: 10.1088/0305-4470/36/29/318.

[38] André Lichnerowicz. "Spineurs harmoniques". French. In: *Comptes rendus hebdomadaires des séances de l'Académie des sciences de Paris* (257 1963), pp. 7–9.

[39] A. Yu. Loginov. "Scattering of fermionic isodoublets on the sine-Gordon kink". In: *The European Physical Journal C* 82.8 (Aug. 2022). DOI: https://doi.org/10.1140/epjc/s10052-022-10649-7.

[40] N. S. Manton. "Geometry of Skyrmions". In: *Communications in Mathematical Physics* 111.3 (Sept. 1987), pp. 469–478. DOI: 10.1007/BF01238909.

[41] N. S. Manton and B. J. Schroers. "Bundles over Moduli Spaces and the Quantization of BPS Monopoles". In: *Annals of Physics* 225.2 (1993), pp. 290–338. DOI: 10.1006/aphy.1993.1060.

[42] N. S. Manton et al. "Kink Moduli Spaces – Collective Coordinates Reconsidered". In: (2020). DOI: https://doi.org/10.48550/arXiv.2008.01026.

[43] Nicholas Manton and Paul Sutcliffe. *Topological Solitons (Cambridge Monographs on Mathematical Physics)*. Cambridge University Press, 2004, p. 506. ISBN: 9780521838368.

[44] Jack McKenna. *What is the argument of the quarter period $iK'(k)$ when $|k| = 1$, i.e. $k = e^{i\alpha}$? (Is it $\frac{\pi-\alpha}{2}$?)* Mathematics Stack Exchange. (version: 2022-06-20). June 20, 2022. URL: https://math.stackexchange.com/q/4476699 (visited on 09/15/2022).

[45] M.-L. Michelsohn. *Spin Geometry*. Ed. by H. Blaine Lawson. Princeton Mathematical Series 38. Princeton University Press, 1990, p. 427. ISBN: 0691085420.

[46] John Willard Milnor and James D. Stasheff. *Characteristic classes*. Princeton University Press, 1974, p. 330. ISBN: 9780691081229.

[47] Naoto Nagaosa and Yoshinori Tokura. "Topological properties and dynamics of magnetic skyrmions". In: *Nature Nanotechnology* 8.12 (Dec. 2013), pp. 899–911. DOI: https://doi.org/10.1038/nnano.2013.243.

[48] Mikio Nakahara. *Geometry, topology, and physics*. Institute of Physics Publishing, 2003, p. 573. ISBN: 0750306068.

[49] Carlos Naya et al. "Skyrmions and Hopfions in 3D Frustrated Magnets". In: (2021). DOI: 10.48550/ARXIV.2111.06385.

[50] Richard S. Palais. "The principle of symmetric criticality". In: *Communications in Mathematical Physics* 69.1 (Oct. 1979), pp. 19–30. DOI: 10.1007/BF01941322.

[51] I. Perapechka, Nobuyuki Sawado, and Ya. Shnir. "Soliton solutions of the fermion-Skyrmion system in (2+1) dimensions". In: *Journal of High Energy Physics* 2018.10 (2018), p. 81. DOI: 10.1007/jhep10(2018)081.

[52] Ilya Perapechka and Yakov Shnir. "Fermion exchange interaction between magnetic Skyrmions". In: *Physical Review D* 99.12 (2019), p. 125001. DOI: 10.1103/physrevd.99.125001.

[53] B. M. A. G. Piette, B. J. Schroers, and W. J. Zakrzewski. "Multisolitons in a Two-dimensional Skyrme Model". In: arXiv, 1994. DOI: https://doi.org/10.48550/arXiv.hep-th/9406160.

[54] Alexander Markovich Polyakov. "Particle Spectrum in Quantum Field Theory". In: *JETP Letters* 20 (1974). Ed. by J. C. Taylor, pp. 194–195. URL: http://jetpletters.ru/ps/1789/article_27297.shtml (visited on 05/11/2022).

[55] M. K. Prasad and Charles M. Sommerfield. "Exact Classical Solution for the 't Hooft Monopole and the Julia-Zee Dyon". In: *Physical Review Letters* 35.12 (Sept. 1975), pp. 760–762. DOI: 10.1103/PhysRevLett.35.760.

[56] W. P. Reinhardt and P. L. Walker. *NIST Digital Library of Mathematical Functions*. Ed. by F. W. J. Olver et al. http://dlmf.nist.gov/, Release 1.1.6 of 2022-06-30. http://dlmf.nist.gov/22. URL: http://dlmf.nist.gov/ (visited on 09/15/2022).

[57] Calum Ross and Bernd J. Schroers. "Magnetic zero-modes, vortices and Cartan geometry". In: *Letters in Mathematical Physics* 108 (2017), pp. 949–983. DOI: 10.1007/s11005-017-1023-2.

[58] Bernd Schroers. "Gauged sigma models and magnetic Skyrmions". In: *SciPost Physics* 7.3 (Sept. 2019). DOI: doi:10.21468/SciPostPhys.7.3.030.

[59] Norberto N. Scoccola and Daniel R Bes. "Two dimensional skyrmions on the sphere". In: *Journal of High Energy Physics* 1998.09 (1998). URL: https://arxiv.org/abs/hep-th/9708146 (visited on 09/05/2022).

[60] S. D. Seddon et al. "Real-space observation of ferroelectrically induced magnetic spin crystal in SrRuO3". In: *Nature Communications* 12.1 (Mar. 2021). DOI: https://doi.org/10.1038/s41467-021-22165-5.

[61] Leila Shahkarami and Siamak Sadat Gousheh. "Exact solutions of a fermion-soliton system in two dimensions". In: *Journal of High Energy Physics* 2011.6 (2011), p. 116. DOI: 10.1007/jhep06(2011)116.

[62] Leila Shahkarami, Azadeh Mohammadi, and Siamak Sadat Gousheh. "Casimir energy for a coupled fermion-soliton system". In: *Journal of High Energy Physics* 2011.11 (2011), p. 140. DOI: 10.1007/jhep11(2011)140.

[63] T. H. R. Skyrme. "A Non-Linear Field Theory". In: *Proceedings of the Royal Society of London. Series A, Mathematical and Physical Sciences* 260.1300 (1961), pp. 127–138. ISSN: 00804630. URL: http://www.jstor.org/stable/2413845.

[64] T. H. R. Skyrme. "Particle states of a quantized meson field". In: *Proceedings of the Royal Society of London. Series A. Mathematical and Physical Sciences* 262.1309 (July 1961), pp. 237–245. DOI: https://doi.org/10.1098/rspa.1961.0115.

[65] T.H.R. Skyrme. "A unified field theory of mesons and baryons". In: *Nuclear Physics* 31 (Mar. 1962), pp. 556–569. DOI: https://doi.org/10.1016/0029-5582(62)90775-7.

[66] Niels R. Walet and Tom Weidig. "Full 2D Numerical Study of the Quantum Hall Skyrme Crystal". In: (2001). DOI: https://doi.org/10.48550/arXiv.cond-mat/0106157.

[67] Edward Walton. "On the geometry of magnetic Skyrmions on thin films". In: *Journal of Geometry and Physics* 156 (2020), p. 103802. DOI: 10.1016/j.geomphys.2020.103802.

[68] E. T. Whittaker and G. N. Watson. *A Course of Modern Analysis*. 4th ed. Cambridge University Press, 1963.

[69] Edward Witten. "Current algebra, baryons, and quark confinement". In: *Nuclear Physics B* 223.2 (Aug. 1983), pp. 433–444. DOI: https://doi.org/10.1016/0550-3213(83)90064-0.

[70] Edward Witten. "Global aspects of current algebra". In: *Nuclear Physics B* 223.2 (Aug. 1983), pp. 422–432. DOI: https://doi.org/10.1016/0550-3213(83)90063-9.

[71] Edward Witten. "Non-abelian bosonization in two dimensions". In: *Communications in Mathematical Physics* 92.4 (Dec. 1984), pp. 455–472. DOI: https://doi.org/10.1007/BF01215276.

[72] Tai Tsun Wu and Chen Ning Yang. "Concept of nonintegrable phase factors and global formulation of gauge fields". In: *Physical Review D* 12.12 (1975), pp. 3845–3857. DOI: 10.1103/physrevd.12.3845.